Molecular analysis of ovarian resorption induced by hydric stress in *Blattella germanica*

Alba Herráiz Yebes

DOCTORAL THESIS UPF / 2013

THESIS DIRECTORS

Dr. Xavier Bellés and Dr. Maria Dolors Piulachs

INSTITUT DE BIOLOGIA EVOLUTIVA (CSIC-Universitat Pompeu Fabra)

Agradecimientos

En primer lugar, quiero dar las gracias a mis dos directores, Xavier y Dolors, por haberme dado la oportunidad de hacer esta tesis, por haberme enseñado y acompañado durante todo el proceso, y por haber confiado en mí (a veces más que yo). También por haberme hecho sentir arropada desde el día en que llegué; saber que podía contar con vosotros para lo que fuera hizo más llevadero estar lejos de casa.

También doy las gracias a todo el P64, pasado y presente, especialmente a Paula, Mercedes, Érica y Jesús, con los que he pasado más tiempo y de los que he aprendido muchísimo, tanto de Ciencia como de otras muchas cosas. No me olvido de los demás, Eva, Olga, Jia-Hsin, Raúl, Carlos, Naswha, Aníbal, Moysés, Carol y Guillem. De todos ellos me llevo un gran recuerdo. A Raúl y a Aníbal quiero agradecerles, además de los buenos ratos, el trabajo bioinformático, sin el cual esta tesis no habría sido posible.

A Cristina Olivella le agradezco su pasión y dedicación, el que siempre me haya echado un cable cuando lo he necesitado y todas las risas que hemos compartido.

También a los compañeros de otros laboratorios les agradezco su amabilidad y ayuda, y especialmente a Neus y Cristina Manjón les doy las gracias por haber hecho divertidísimas mis largas estancias en lupas.

A Jose Luis Maestro quiero agradecerle su buen talante, sus ganas de colaborar, sus sugerencias siempre acertadas y, sobre todo, su bondad intrínseca, que es muy reconfortante.

Al equipo de administración, Anna, Rita, Emiliano y Blanca, les agradezco su calidez personal y su impecable eficiencia, que tanto han ayudado en los momentos buenos y en los no tan buenos.

Doy las gracias a José Manuel Fortuño por toda la ayuda con el microscopio de barrido, y por el entusiasmo demostrado.

Agradezco a Joan Cerdá y François Chauvigné que me enseñaran a trabajar con oocitos de *Xenopus*, y que me iniciaran en el curioso mundo de las acuaporinas.

También quisiera recordar aquí a los alumnos de prácticas Jelle, Elena y Laura, de los que aprendí mucho y a los que espero haber enseñado algo.

Agradezco a Casi300 haber hecho de un piso compartido un verdadero hogar, y la paciencia infinita que han tenido conmigo durante todo el proceso de escribir esta tesis. A Javi además le agradezco la ayuda que me sigue prestando en la distancia, y haberse convertido en un gran amigo.

A todos los amigos les agradezco el apoyo e interés, y sobre todo, el que siempre hayan estado ahí, para aguantarme al teléfono los que

están lejos o para tomarse unas cañas los que están cerca, cuando lo he necesitado.

Quiero dar las gracias a mis padres por haberme instado a seguir mi camino, por haber apoyado todas las decisiones que he tomado, y por hacerme saber que si me equivoco, siempre puedo volver a empezar. También les agradezco los sabios consejos en momentos difíciles. A mi Germanito le agradezco todas las risas y todas las conversaciones serias, y espero ser un buen ejemplo para él.

Agradezco a toda mi familia (tíos, primos, consortes…) que se hayan preocupado e interesado por este proyecto. Especialmente a mi tío Toni que ha seguido más de cerca mis altibajos. A él le debo la gran frase "La tesis es un estado de ánimo. Y no siempre es bueno". Quiero recordar especialmente a mi yaya y a mi abu, que aunque no sabían qué era exactamente lo que hacía, siempre se sintieron orgullosas de mí, y sé que les habría encantado verme llegar hasta aquí.

Por último, quiero dar las gracias a Edu por haber estado a mi lado durante este tiempo, por hacerme explicarle exactamente en qué consiste lo que hago, por no dejarme tirar la toalla cuando estuve tentada, por sentirse orgulloso de mí, y, resumiendo, por hacerme sentir que este trabajo es precioso e importante no sólo para los científicos.

A todos, muchas gracias.

Abstract

In the present thesis we studied the effects of hydric stress in the ovary of the cockroach *Blattella germanica*. At morphological level, we described ovarian resorption induced by water deprivation. At a molecular level, we looked for markers differentially expressed under hydric stress. First, we focused on aquaporins given their role as water channel proteins. We cloned, sequenced and functionally characterised an aquaporin that transports water and urea. Then, we obtained a library of microRNAs (small non-coding RNAs that regulate gene expression post transcriptionally) present in the ovary under stress conditions. We analysed the differential expression of 13 of them and we observed that the majority were overexpressed under hydric stress. We selected miR-34-5p to perform a deeper study, including a study of their potential target mRNAs. Among the possible targets, we studied the function of Windei, a factor that resulted necessary for the trimethylation of lysine 9 in histone H3 and for chorion formation. Finally, we selected CARMER (an arginine methyltransferase) as hydric stress marker candidate. We assessed that it is overexpressed in response to hydric stress and that it is necessary for the dimethylation of arginine 17 in histone H3.

Resumen

En esta tesis estudiamos los efectos del estrés hídrico en el ovario de la cucaracha *Blattella germanica*. A nivel morfológico describimos el proceso de reabsorción ovárica tras la privación de agua. A nivel molecular buscamos marcadores diferencialmente expresados en respuesta a este estrés. Primero nos centramos en las acuaporinas por su papel como proteínas que forman un canal transportador de agua. Clonamos, secuenciamos y caracterizamos funcionalmente una acuaporina que transporta agua y urea. Después obtuvimos una biblioteca de microRNAs (RNAs cortos no codificantes que regulan la expresión génica post-transcripcionalmente) presentes en el ovario en situación de estrés. Analizamos la expresión diferencial de 13 de ellos y observamos que la mayoría se sobreexpresaban en situación de estrés. Elegimos miR-34-5p para hacer un estudio más profundo, incluyendo un análisis de sus potenciales mRNA diana. De entre ellos, estudiamos la función de Windei y comprobamos que dicho factor es necesario para la trimetilación de la lisina 9 en la histona H3 y para la formación del corion. Por último, seleccionamos CARMER (una arginina methyltransferasa) como candidato a marcador de estrés hídrico. Comprobamos que CARMER se sobreexpresa en respuesta a estrés y que es necesario para la dimetilación de la arginina 17 en la histona H3.

Preface

The predoctoral fellowship awarded to the author of this PhD thesis was received from the International Laboratory on Global Change (LINCGlobal), an institution founded by the Spanish National Research Council (CSIC) and the Pontifical Catholic University of Chile (PUC). LINCGlobal is a multidisciplinary institution that aims to understand, predict and develop strategies to respond to the impact of Global Change on ecosystems. In this context, *Global Change* refers to the series of changes derived from the human activity in the fundamental processes that define the functioning of the biosphere. It includes the transformation of the Earth´s land surface and the derived effects on climate, biogeochemical cycles, and biodiversity.

Changes in temperature, increase of UV radiation and lack of water are predictable consequences of global change that can be reproduced in the laboratory, allowing us to study its effects in selected organisms in a controlled environment. During the last 30 years, the group that received the candidate has been working on a number of aspects related to development and reproduction in a well-known insect model: the German cockroach, *Blattella germanica*, using molecular tools. Therefore, a great deal of information has been gathered on genomics and molecular physiology of this species. The first idea was, then, to start a research program using this model to study the early effects of water deprivation, and to identify molecular markers of this kind of

stress that might serve as indicators of incipient water shortage in insects living in areas in danger of desertification.

Briefly, the present work aims at laying the first foundations for the above research project. We have focused on the effects of water stress on ovarian maturation because it is a sensitive process, and the first one that the female aborts when facing adverse environmental conditions. Our approach has been to remove drinking water from the rearing jars of experimental animals, and then analyse the resulting effects upon ovarian maturation, at both morphological and molecular levels.

Abbreviations

20E	20-hydroxyecdysone
AQP	Aquaporin
ar/R	Aromatic/arginine
ATF7IP	Activating transcription factor 7 interacting-protein
BIB	Big Brain
BLAST	Basic Local Alignment Search Tool
BME	β-mercaptoethanol
cDNA	Complementary DNA
cRNA	Capped RNA
DAPI	4',6-diamidino-2-phenylindole
DEPC	Diethylpyrocarbonate
DNase	Deoxyribonuclease
DRIP	*Drosophila* Integral Protein
dsRNA	double strand RNA
EC	Early chorion
EST	Expressed sequence tag
FE	Follicular epithelium
GO	Gene Ontology
H3K9me3	Trimethylation of lysine 9 in histone H3
H3R17me2a	Asymmetric dimethylation of arginine 17 in histone H3
HKMT	Histone lysine methyltransferase
LBO	Length of basal oocyte
LC	Late chorion
MBS	Modified Barth's saline
MC	Mid chorion

MIP	Membrane Integral Protein
miRNA	MicroRNA
ncRNA	Non-coding RNA
NPA	Asparagine-proline-alanine
nt	Nucleotide
ORF	Open reading frame
PBS	Phosphate buffered saline
PRIP	*Pyrocoelia rufa* Integral Protein
PRMT	Protein arginine methyltransferase
PTM	Post translational modification
qRT-PCR	Quantitative real time PCR
RACE	Rapid amplification of cDNA ends
RISC	RNA-induced silencing complex
RNAi	RNA interference
RNase	Ribonuclease
RF	Resorbed follicles
SD	Standard deviation
SDS	Sodium dodecyl sulfate
s.e.m	Standard error of the mean
SEM	Scanning electron microscopy
TM	Transmembrane
TRICT	Tetramethylrhodamine isothiocyanate
UTR	Untranslated region

Contents

1. INTRODUCTION AND OBJECTIVES

1.1. Introduction

Water is the main component of living beings, and fresh water availability is indispensable for life. Water scarcity is a Global Change predictable consequence that can be reproduced in the laboratory, allowing us to study its effects in model organisms.

The German cockroach, *Blattella germanica*, is a hemimetabolous insect well adapted to xeric environments (Appel, 1995). It is easy to grow and handle, and its physiology and reproduction has been studied in our laboratory for more than 30 years. These reasons make it a good model to study the effects of hydric stress under laboratory conditions.

Biotic and abiotic stresses affect reproduction on several insects, for example, by inducing the degeneration of the ovaries in a process known as resorption (Clifton and Noriega, 2011; Guo et al., 2011; Medeiros et al., 2011). We have focused our interest in the study of the effects of hydric stress in the ovary, as it is one of the first affected organs upon different stresses. The approach will consist in describing the morphologic effects of hydric stress in the ovary and then looking for candidate molecular markers of this kind of stress.

a) *B. germanica* ovary

B. germanica has panoistic ovaries, the most primitive ovary type. In panoistic ovaries all germ cells are oocytes and each ovarian

follicle is composed by a developing oocyte surrounded by a monolayer of follicular cells. This ovary type differs from the more modified meroistic type, in which cells from germinal lineage become either oocytes or nurse cells (cells that provide the oocyte with the RNA, proteins and ribosomes necessary for the future embryo). The meroistic type can be further divided into telotrophic meroistic, in which nurse cells remain in the apical region of the ovariole and reach the oocyte through a nutritive cord, and polytrophic meroistic, in which nurse cells and oocyte form a cluster of interconnected cells surrounded by the follicular epithelium (Büning, 1994).

The ovariole is the functional unit of the insect ovary, and it is composed by a vitellarium, which holds the developing follicles, and a germarium, where the germ and somatic stem cells are placed (Figure 1.1). Each ovariole also has a terminal filament that fixes the ovariole to the body wall, and a pedicle that connects all the ovarioles and lead into the oviduct, which communicates both ovaries (Klowden, 2008). *B. germanica* has around 20 ovarioles per ovary and only the basal oocyte of each one matures, is fertilized and is oviposited at the end of the corresponding gonadotrophic cycle.

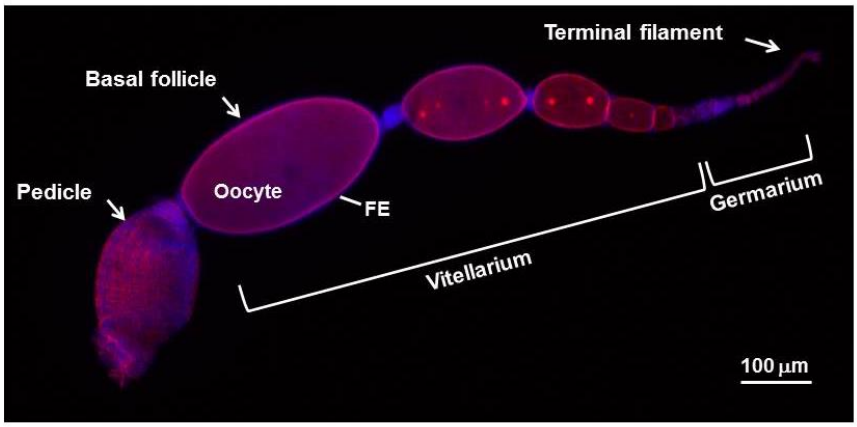

Figure 1.1: *B. germanica* ovariole. In the picture are shown the pedicle, the vitellarium holding the developing follicles, the germarium, and the terminal filament. Each follicle is composed by an oocyte surrounded by a follicular epithelium (FE).

The first gonadotrophic cycle starts on the last (sixth) nymphal instar and lasts the first 8 days of the adult stage. It can be divided into pre-vitellogenesis, vitellogenesis and choriogenesis. In the pre-vitellogenic stage, the follicular cells divide mitotically and increase its number up to 10 fold (from ca. 700 cells in the first day of the last nymphal instar to a maximum of 7,200 cells at the onset of vitellogenesis). Pre-vitellogenesis lasts until day 3 of adult life, when follicular cells arrest cytokinesis and become binucleated (Ciudad, 2008; Irles et al., 2009). During vitellogenesis, the oocyte grows exponentially due to the incorporation of vitellogenin, which is synthesized in the fat body in response to juvenile hormone, being thereafter internalized in the oocyte by receptor-mediated endocytosis (Ciudad et al., 2006; Comas et al., 2001). Internalization is possible because follicular cells shrink and leave intracellular spaces among them, a phenomenon known as *patency*,

which is also under juvenile hormone control (Davey and Huebner, 1974; Pascual et al., 1992) (Figure 1.2A, B). Choriogenesis takes place on day 7, when follicular cells, under the action of the hormone 20-hydroxyecdysone, secrete chorion proteins. The resulting chorion is a multilayer envelope for the egg that sustains and protects it (Belles et al., 1993). The gonadotrophic cycle ends with the oviposition and the formation of an eggcase or ootheca, with proteins secreted by the colleterial glands (Figure 1.2C), where the oviposited eggs are packed. The female carries the ootheca adhered to the genital atrium until the nymphs hatch, a period that in our laboratory conditions lasts around 18 days (Irles et al., 2009).

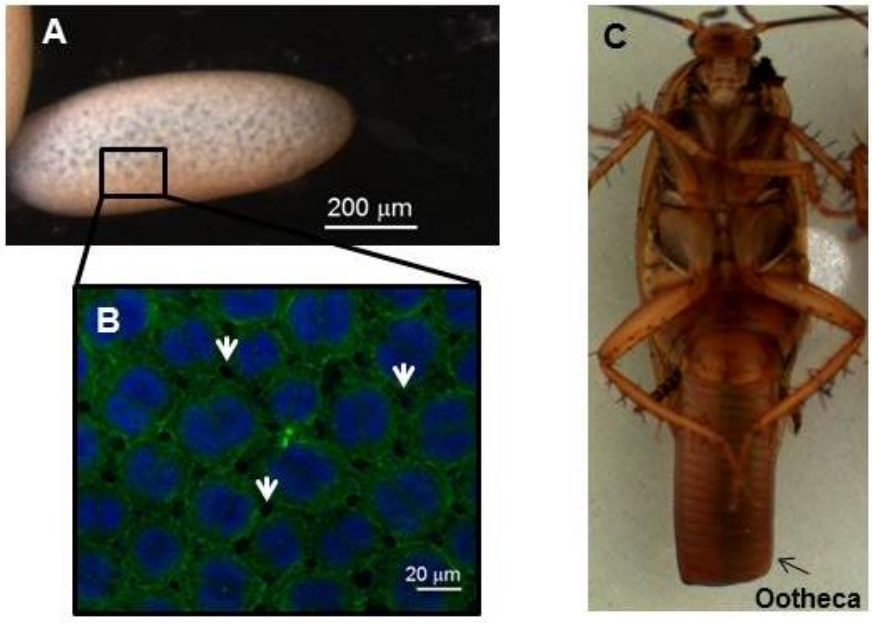

Figure 1.2: Vitellogenic basal follicle and female carrying the ootheca. A) Ovarian basal follicle of a 5-day-old female. **B)** Follicular epithelium from the basal follicle in "A" showing patency (arrows). Blue: nuclei. Green: actins. **C)** Female carrying the ootheca.

b) Candidate markers of hydric stress

Our long-term objective was to find general molecular markers of hydric stress, and we followed the approach of considering candidates with functions highly conserved through evolution and related to manage the homeostatic equilibrium. Our first approach was to investigate aquaporins (AQPs), membrane water channels that are present in species belonging to all life kingdoms (King et al., 2004). Afterwards we explored the role of microRNAs (miRNAs), which are highly conserved small non-coding RNAs that regulate gene expression post transcriptionally (Belles et al., 2011). The idea of analyse regulators of gene expression at mRNA level directed us to the study of transcriptional regulators, like histone modifiers, which affect transcription by helping to establish an "open" or "closed" chromatin status (Berger, 2007).

- Aquaporins

AQPs are membrane proteins that form water channels, allowing water -and other small solutes- transport through the cell membrane. They share a conserved molecular structure containing six transmembrane domains (TM1-TM6) connected by five loops (A-E), and cytoplasmic N- and C- termini. All AQPs also contain two canonical Asp-Pro-Ala (NPA) motifs. In the cell membrane, AQPs fold into right-handed α-barrels, with a central transmembrane channel surrounded by the six full-length transmembrane domains and the two NPA-containing loops, B and E. This tridimensional

structure is known as “the hourglass model” (reviewed by Campbell et al., 2000) (Figure 1.3).

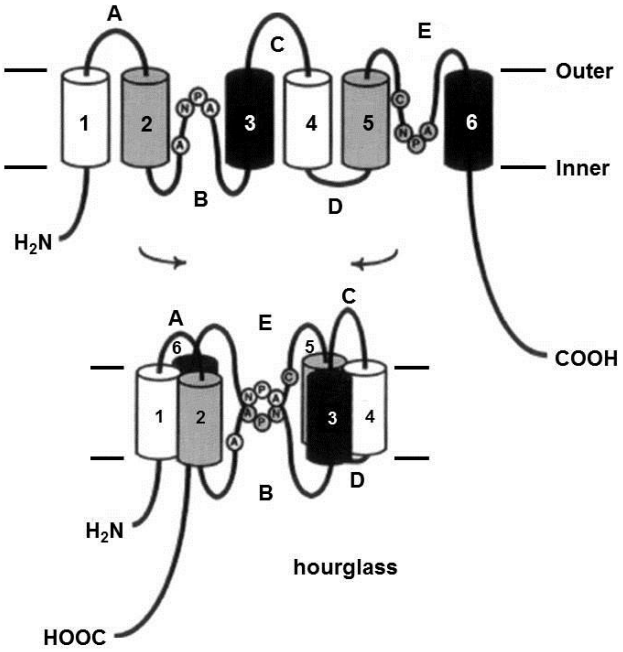

Figure 1.3: Secondary structure of AQPs, including the six transmembrane domains (1-6), the five connecting loops (A-E), the N- and C- cytosolic termini, and the two NPA motifs. In the membrane each AQP is folded into an “hourglass” conformation (down). Modified from Jung et al. (1994).

Changes in AQPs expression upon hydric stress have been reported mainly in plants in drought tolerance studies (Mahdieh et al., 2008; Zhou et al., 2012). In insects, changes in AQPs expression have been reported in species that lose high amounts of water during its life cycle, like the sleeping chironomid *Polypedilum vanderplanki*, a dipteran whose larvae desiccate in drought conditions and rehydrate when water is available (Kikawada et al., 2008); or during the acquisition of freeze tolerance in the goldenrod gall fly (*Eurosta*

solidaginis), when it needs to rapidly lose water and accumulate glycerol (Philip and Lee, 2010).

- MicroRNAs

MiRNAs are highly conserved small non-coding RNAs that regulate gene expression at post-transcriptional level. In the last decade, miRNAs have arisen as key regulators of many processes like embryogenesis, development, differentiation, growth, metamorphosis, and apoptosis (reviewed by Belles et al., 2012). They have also been described to modify their expression upon a variety of stresses (Freitak et al., 2012; Lee et al., 2012) and its aberrant expression is used as a marker of different cancers (reviewed by Allegra et al., 2012).

MiRNA biogenesis occurs through several steps (Figure 1.4). They are transcribed within the nucleus by RNA polymerase II to primary transcripts (pri-miRNAs), long transcripts that could contain several miRNAs. The pri-miRNAs are processed within the nucleus by the enzyme Drosha, releasing hairpin precursor miRNAs, which are exported to the cytoplasm by the protein exportin-5. In the cytoplasm, the RNase Dicer cleaves the hairpin and produce a RNA:RNA duplex of about 22 nt. One of the duplex strands is degraded, while the other, the mature miRNA, is loaded into the RNA-induced silencing complex (RISC). Then the mature miRNA guides the RISC complex to the target mRNA. Usually the RISC complex binds to the 3'-untranslated region (3'-UTR) and blocks mRNA translation when pairing is not perfect, or cleaves the

mRNA if pairing is perfect (Ambros, 2004; Bartel, 2004). However, some works have shown that miRNAs can also activate translation when bind to the 5'-UTR of the target mRNAs (Vasudevan et al., 2007).

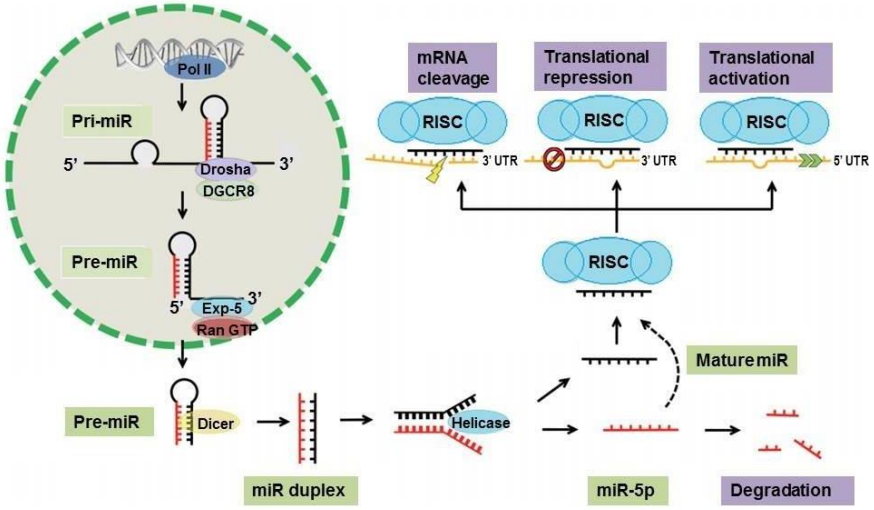

Figure 1.4: MiRNAs biogenesis and mode of action. MiRNAs are transcribed within the nucleus by RNA polymerase II into primary transcripts, which are processed by Drosha/DGCR8. The resulting hairpin precursors are exported by exportin-5 to the cytoplasm, where are cleaved by Dicer into miRNA duplexes. Then, one of the strands of the duplex is degraded, and the other, the mature miRNA, is loaded into the RISC complex to guide it to the target mRNAs. Once bound to the target mRNA, the RISC complex can cleave it, block its transcription, or less usually, activate its transcription. Modified from Li and Yang (2013).

- Histone modifiers

Chromatin is the complex association between DNA and histone and non-histone proteins within the nucleus of eukaryotic cells. The basic unit of chromatin is the nucleosome, a disc-shaped histone core (composed by two molecules of each histone H2A, H2B, H3,

and H4) where DNA is wrapped around (Figure 1.5A). Each nucleosome is separated from the next one by a DNA linker region; the resultant structure is called “beads on a string” and represents the first level of DNA packing (Figure 1.5B). A second level is produced when nucleosomes pack together into a compact chromatin fibre, in a process that involves a fifth histone protein, histone H1. The highest level of packing is found in the chromosomes, especially during mitosis (Figure 1.5C) (Alberts et al., 2002).

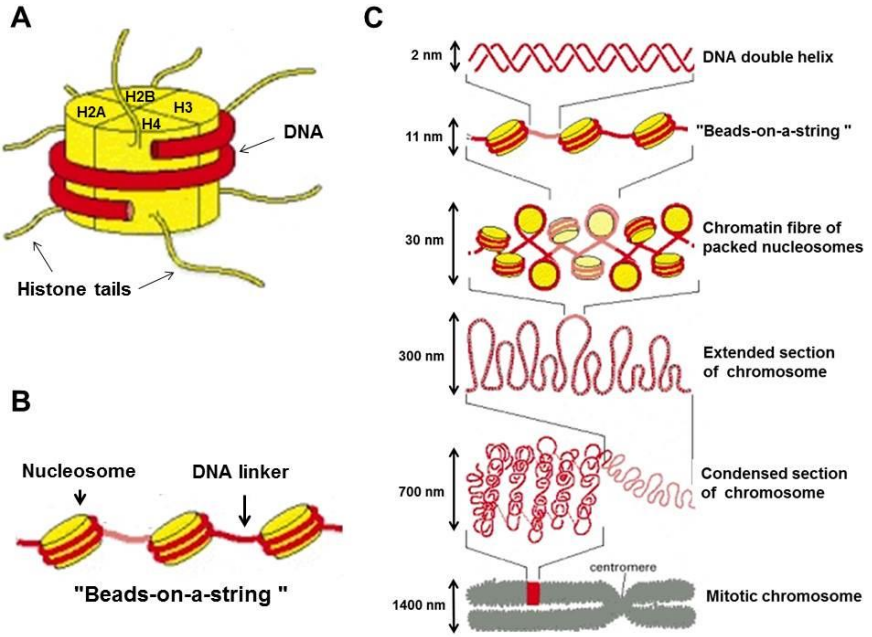

Figure 1.5: Chromatin organization. A) Nucleosome: DNA wrapped around a histone octamer. **B)** “Beads-on-a-string” conformation: nucleosomes separated by DNA linker. **C)** Chromatin condensation levels. From the “beads-on-a-string” conformation, nucleosomes place one on top of the other and package together in a 30 nm fibre. Then, the fibre is condensed forming a chromosome, which present extended and condensed sections. The higher level of condensation is found during mitosis. Modified from Alberts et al. (2002).

DNA and histone proteins experience modifications that alter the chromatin structure and compaction. These modifications play key roles in the regulation of transcription, as it is affected by the degree of chromatin compaction, which determines the DNA accessibility for the transcriptional machinery (Figure 1.6). DNA is methylated in cytosine residues and this generally prevents transcription, while histone post translational modifications (PTMs) –which can be acetylation, phosphorylation, methylation, ubiquitination or ADP-ribosylation- are related with both transcriptional repression and activation (Berger, 2007).

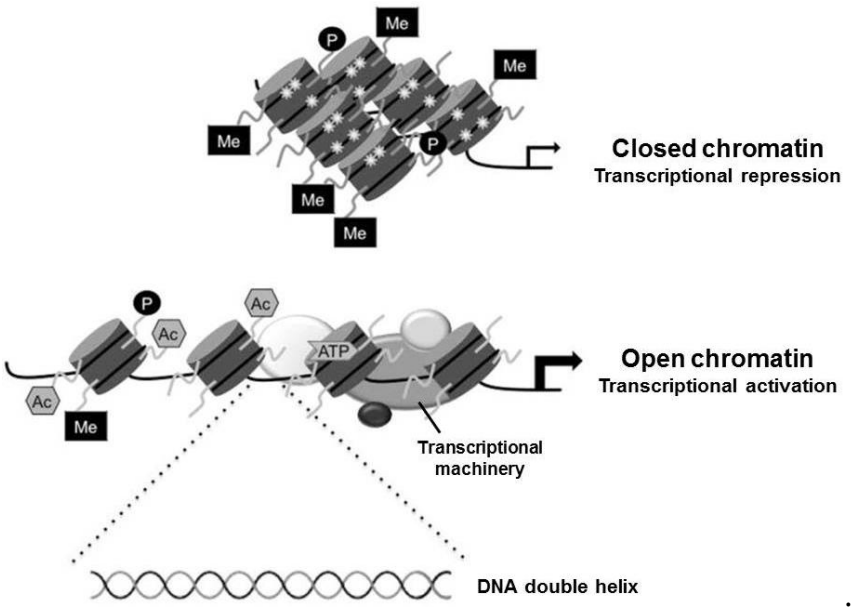

Figure 1.6: Epigenetic control of gene transcription. Transcription is repressed in highly compacted chromatin (top), where DNA is methylated (starbursts) and histone tails are typically deacetylated but present modifications such as methylation (Me) or phosphorylation (P). On the contrary, transcription is active in regions with an open chromatin structure (bottom), as DNA is accessible for the transcription machinery. In transcriptionally active regions DNA is often scarcely methylated, and histone tails are widely acetylated (Ac). Modified from Zhang et al. (2009).

Several works relate changes in histone post translational modifications with stress responses (Chervona and Costa, 2012; Desrosiers and Tanguay, 1988; Tikoo et al., 2001); while others suggest that overexpression of genes encoding histone modifiers confers stress resistance (Alcendor et al., 2007; List et al., 2009), thus the study of histone modifiers could be highly valuable in the context of hydric stress.

1.2. Objectives of the Thesis

The main objective of the present thesis was to establish the basis for the study of hydric stress effects in the German cockroach *Blattella germanica*. Having this purpose in mind, and the long-term objective of finding reliable molecular markers of hydric stress, we planned the following specific objectives:

1. To describe the morphologic changes experienced by the ovary under hydric stress.
2. To assess the occurrence of AQPs in the ovary and characterise them in structural and functional terms.
3. To analyse the miRNAs differentially expressed in ovaries under hydric stress.
4. To select miRNAs overexpressed under hydric stress and study them in deep, including the study of putative targets.
5. To identify genes which respond to hydric stress and analyse them in structural and functional terms.

1.3. References

Alberts, B., Johnson, A. Lewis, J., Raff, M., Roberts, K. and Walter, P.. (2002). DNA and Chromosomes. In *Molecular Biology of the Cell. 4th edition*, pp 191-234. New York: Garland science.

Alcendor, R. R., Gao, S., Zhai, P., Zablocki, D., Holle, E., Yu, X., Tian, B., Wagner, T., Vatner, S. F. and Sadoshima, J. (2007). Sirt1 regulates aging and resistance to oxidative stress in the heart. *Circ Res* **100**, 1512-21.

Allegra, A., Alonci, A., Campo, S., Penna, G., Petrungaro, A., Gerace, D. and Musolino, C. (2012). Circulating microRNAs: new biomarkers in diagnosis, prognosis and treatment of cancer (review). *Int J Oncol* **41**, 1897-912.

Ambros, V. (2004). The functions of animal microRNAs. *Nature* **431**, 350-5.

Appel, A. G. (1995). *Blattella* and related species. In *Understanding and controlling the German cockroach*, (eds. M. K. Rust J. M. Owens and D. A. Reierson), pp. 1-20. New York: Oxford University Press.

Bartel, D. P. (2004). MicroRNAs: genomics, biogenesis, mechanism, and function. *Cell* **116**, 281-97.

Belles, X., Cassier, P., Cerda, X., Pascual, N., Andre, M., Rosso, Y. and Piulachs, M. D. (1993). Induction of choriogenesis by 20-hydroxyecdysone in the German cockroach. *Tissue Cell* **25**, 195-204.

Belles, X., Cristino, A. S., Tanaka, E. D., Rubio, M. and Piulachs, M. D. (2012). Insect MicroRNAs: From Molecular Mechanisms to Biological Roles. In *Insect Molecular Biology and Biochemistry*, (ed. L. I. Gilbert), pp 30-56. Amsterdam: Elsevier-Academic Press.

Berger, S. L. (2007). The complex language of chromatin regulation during transcription. *Nature* **447**, 407-12.

Büning, J. (1994). The Insect Ovary. Ultrastructure, previtellogenic growth and evolution. Cambridge: Chapman & Hall.

Campbell, E. M., Ball, A., Hoppler, S. and Bowman, A. S. (2008). Invertebrate aquaporins: a review. *J Comp Physiol B* **178**, 935-55.

Ciudad, L. (2008). Mecanismos reguladores de la maduración ovárica en *Blattella germanica* (L.) (Dictyoptera, Blattellidae). PhD Thesis. *Departamento de Fisiologia. Facultad de Biología*. Barcelona: Universidad de Barcelona.

Ciudad, L., Piulachs, M. D. and Belles, X. (2006). Systemic RNAi of the cockroach vitellogenin receptor results in a phenotype similar to that of the *Drosophila* yolkless mutant. *FEBS J* **273**, 325-35.

Clifton, M. E. and Noriega, F. G. (2011). Nutrient limitation results in juvenile hormone-mediated resorption of previtellogenic ovarian follicles in mosquitoes. *J Insect Physiol* **57**, 1274-81.

Comas, D., Piulachs, M. D. and Belles, X. (2001). Induction of vitellogenin gene transcription in vitro by juvenile hormone in *Blattella germanica*. *Mol Cell Endocrinol* **183**, 93-100.

Chervona, Y. and Costa, M. (2012). The control of histone methylation and gene expression by oxidative stress, hypoxia, and metals. *Free Radic Biol Med* **53**, 1041-7.

Davey, K. G. and Huebner, E. (1974). The response of the follicle cells of *Rhodnius prolixus* to juvenile hormone and antigonadotropin in vitro. *Can J Zool* **52**, 1407-12.

Desrosiers, R. and Tanguay, R. M. (1988). Methylation of *Drosophila* histones at proline, lysine, and arginine residues during heat shock. *J Biol Chem* **263**, 4686-92.

Freitak, D., Knorr, E., Vogel, H. and Vilcinskas, A. (2012). Gender- and stressor-specific microRNA expression in *Tribolium castaneum*. *Biol Lett* **8**, 860-3.

Guo, J. Y., Dong, S. Z., Ye, G. Y., Li, K., Zhu, J. Y., Fang, Q. and Hu, C. (2011). Oosorption in the endoparasitoid, *Pteromalus puparum*. *J Insect Sci* **11**, 90.

Irles, P., Belles, X. and Piulachs, M. D. (2009). Identifying genes related to choriogenesis in insect panoistic ovaries by Suppression Subtractive Hybridization. *BMC Genomics* **10**, 206.

Jung, J. S., Preston, G. M., Smith, B. L., Guggino, W. B. and Agre, P. (1994). Molecular structure of the water channel through aquaporin CHIP. The hourglass model. *J Biol Chem* **269**, 14648-54.

Kikawada, T., Saito, A., Kanamori, Y., Fujita, M., Snigorska, K., Watanabe, M. and Okuda, T. (2008). Dehydration-inducible changes in expression of two aquaporins in the sleeping chironomid, *Polypedilum vanderplanki*. *Biochim Biophys Acta* **1778**, 514-20.

King, L. S., Kozono, D. and Agre, P. (2004). From structure to disease: the evolving tale of aquaporin biology. *Nat Rev Mol Cell Biol* **5**, 687-98.

Klowden, M. J. (2008). Reproductive Systems. In *Physiological Systems in Insects*, pp 198-255. San Diego: Elsevier-Academic Press.

Lee, Y. J., Johnson, K. R. and Hallenbeck, J. M. (2012). Global protein conjugation by ubiquitin-like-modifiers during ischemic stress is regulated by microRNAs and confers robust tolerance to ischemia. *PLoS One* **7**, e47787.

Li, H. and Yang, B. B. (2013). Friend or foe: the role of microRNA in chemotherapy resistance. *Acta Pharmacol Sin* **34**, 870-9.

List, O., Togawa, T., Tsuda, M., Matsuo, T., Elard, L. and Aigaki, T. (2009). Overexpression of grappa encoding a histone methyltransferase enhances stress resistance in *Drosophila*. *Hereditas* **146**, 19-28.

Mahdieh, M., Mostajeran, A., Horie, T. and Katsuhara, M. (2008). Drought stress alters water relations and expression of PIP-type aquaporin genes in *Nicotiana tabacum* plants. *Plant Cell Physiol* **49**, 801-13.

Medeiros, M. N., Ramos, I. B., Oliveira, D. M., da Silva, R. C., Gomes, F. M., Medeiros, L. N., Kurtenbach, E., Chiarini, L. B., Masuda, H., de Souza, W. et al. (2011). Microscopic and molecular characterization of ovarian follicle atresia in *Rhodnius prolixus* Stahl under immune challenge. *J Insect Physiol* **57**, 945-53.

Pascual, N., Cerdá, X., Benito, B., Tomás, J., Piulachs, M. D. and Belles, X. (1992). Ovarian ecdysteroid levels and basal oöcyte development during maturation in the cockroach *Blattella germanica* (L.). *J Insect Physiol* **38**, 339-348.

Philip, B. N. and Lee, R. E., Jr. (2010). Changes in abundance of aquaporin-like proteins occurs concomitantly with seasonal acquisition of freeze tolerance in the goldenrod gall fly, *Eurosta solidaginis*. *J Insect Physiol* **56**, 679-85.

Tikoo, K., Lau, S. S. and Monks, T. J. (2001). Histone H3 phosphorylation is coupled to poly-(ADP-ribosylation) during reactive oxygen species-induced cell death in renal proximal tubular epithelial cells. *Mol Pharmacol* **60**, 394-402.

Vasudevan, S., Tong, Y. and Steitz, J. A. (2007). Switching from repression to activation: microRNAs can up-regulate translation. *Science* **318**, 1931-4.

Zhang, D., Yu, Z. Y., Cruz, P., Kong, Q., Li, S. and Kone, B. C. (2009). Epigenetics and the control of epithelial sodium channel expression in collecting duct. *Kidney Int* **75**, 260-7.

Zhou, S., Hu, W., Deng, X., Ma, Z., Chen, L., Huang, C., Wang, C., Wang, J., He, Y., Yang, G. et al. (2012). Overexpression of the wheat aquaporin gene, TaAQP7, enhances drought tolerance in transgenic tobacco. *PLoS One* **7**, e52439.

2. PHENOTYPE OF *BLATTELLA GERMANICA* OVARIES SUBJECTED TO HYDRIC STRESS

Phenotype of *Blattella germanica* ovaries subjected to hydric stress

Alba Herraiz, Xavier Belles, Maria-Dolors Piulachs

Institut de Biologia Evolutiva (CSIC-Universitat Pompeu Fabra), and LINCGlobal, Passeig Marítim de la Barceloneta 37-49. 08003 Barcelona, Spain.

2.1. Abstract

When insect females face environmental stresses, one of the first organs affected is the ovary, which suffers degenerating processes. This allows recycling nutrients and energy that help the female resist until conditions are more favourable for reproduction.

Here, we show that hydric stress provoked by drinking water deprivation, prevents reproduction in females of the German cockroach *Blattella germanica*, although the effects in the ovaries depend on when the stress is induced and how long is it. After a series of preliminary experiments, we found that if drinking water removal takes place on the third day of adult life, the basal ovarian follicles undergo resorption that becomes evident 48 h later. Females submitted to this treatment undertake a process of caspase activation and cell death that culminates in follicles resorption.

2.2. Introduction

Stress can be defined as a state in which homeostasis is compromised, and it triggers a variety of adaptive responses of the organism to restore it (Chrousos, 2009). Agents that cause stress can be either biotic, as fungal or bacterial infections, or abiotic, as UV radiation, heat, dehydration, etc. In response to stress, cells experience rapid changes to adapt their metabolism and protect themselves against damage (Kroemer et al., 2010). However, if damage is too severe for recovery, cells usually die by apoptosis

(programmed cell death) or necrosis (uncontrolled death) (Benoit, 2011).

Stress conditions can affect reproduction, as organisms have to balance the energy requirements for reproduction and survival, in order to optimise fitness (Barrett et al., 2009). Females from several insect species undertake ovarian resorption when subjected to certain environmental stresses, like starvation (Guo et al., 2011), absence of mating (de Souza et al., 2007; Kotaki, 2003), host deprivation (Asplen and Byrne, 2006; Bodin et al., 2009) or infection (Medeiros et al., 2011). Ovarian resorption allows resources invested in ovaries to be reallocated into somatic functions that increase lifespan and thus future reproductive potential (Barrett et al., 2009).

In this chapter, we explore the consequences of hydric stress on the ovary of the German cockroach, *Blattella germanica*, by studying the occurrence of ovarian resorption under such stress.

B. germanica is a hemimetabolous insect with panoistic ovaries, the less modified type of insect ovaries. Each ovary has around 20 ovarioles, and only the basal follicle of each ovariole matures and is oviposited in each gonadotrophic cycle. In the adult period, oogenesis is divided into 3 stages: pre-vitellogenesis (from the imaginal moult until day 3 of adult life), vitellogenesis (days 4 to 6), and choriogenesis (from day 7 until oviposition). The whole gonadotrophic cycle lasts around 8 days, and at the end of it the

eggs are oviposited in a special structure known as ootheca that is carried by the female attached to the genital atrium until nymphs hatching.

In the present chapter we report that hydric stress affects reproduction on *B. germanica* females, as ovaries from individuals subjected to water deprivation either do not develop or are resorbed, and finally die.

2.3. Material and Methods

a) Insects

Female specimens of *B. germanica* (L.) were used in all experiments. They were obtained from a colony reared in the dark at 29±1°C and 60–70% relative humidity and fed with Panlab dog chow and water *ad libitum*. Freshly ecdysed adult females were selected from the colony and used at appropriate ages. All dissections were carried out on carbon dioxide-anaesthetized specimens.

b) Hydric stress induction

Control insects received food and water *ad libitum*. Experimental individuals were water-deprived at different times (detailed explanation is reported in Results section) and received food *ad libitum*. Control and experimental individuals were then dissected at

selected ages, were morphologically examined and the length of the basal oocyte (LBO) was measured.

c) Ovaries staining and visualization

Images of ovaries from control and stressed 5-day-old females were obtained with an AxioCam MRc5 camera adapted to a stereomicroscope (SteREO Discovery.V8, Carl Zeiss MicroImaging). Control females from day 0, 2, 3, 4, 5, 6 and 7, and stressed females from day 4, 5, 6 and 7, were injected with 1 µl of a 1:100 dilution of FAM-FLIVO (ImmunoChemistry Technologies, Bloomington, MN, USA), an in vivo activated-caspase marker. Ovaries from injected females were dissected 1 h later in Ringer's solution and the individualised ovarioles were fixed during 20 min in 4% paraformaldehyde in PBS (0.2 M, pH 6.8) at room temperature. For F-actin visualisation, samples were incubated with Phalloidin–tetramethylrhodamine B isothiocyanate (TRITC; 5 µg/ml; Sigma) during 20 min and rinsed with PBS 0.2 M for 3×10 min. Subsequently, samples were incubated with DAPI (1µg/ml; Sigma) during 5 min, for nucleic acid staining, and rinsed with PBS 0.2 M for 3×10 min. The stained and rinsed ovarioles were mounted in Mowiol (Calbiochem, Madison, WI, USA) and were observed by an AxioCam MRm camera adapted to an epifluorescence microscopy AxioImager.Z1 (ApoTome System, Carl Zeiss MicroImaging). Images were analysed with the AxioVision 4.8 software (Zeiss).

2.4. Results

a) Effects of hydric stress on *B. germanica* adult females

In order to identify the critical moment in which water stress causes clear damage in ovaries, adult *B. germanica* females were subjected to the following water deprivation conditions (Figure 2.1): 1) water deprivation from day 0, day 1, day 3, or day 4 since the imaginal moult; 2) 10 h with water and 14 h without it, every day since the imaginal moult; 3) water deprivation from day 0 to day 3, and then water provision from day 3. Survival, oocyte maturation and oviposition time were recorded in treated and control females.

Individuals that were water-deprived from day 0 (n=10) and 1 (n=10), died between 8 and 11 days after moulting to the adult stage, without oviposit. We dissected a 5-day-old female of each experiment, and we found that oocytes did not grow.

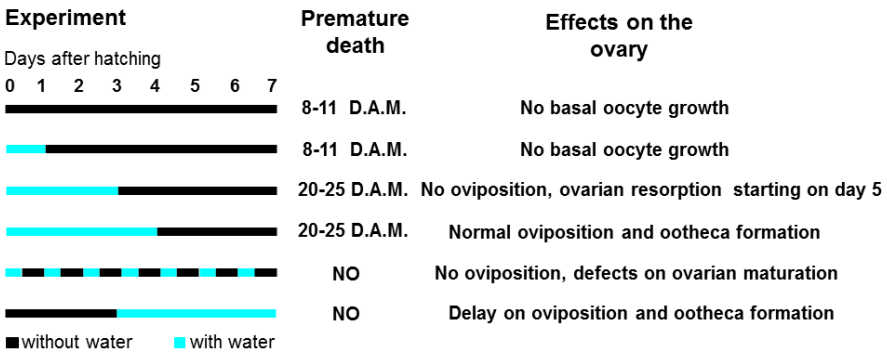

Figure 2.1: Effects of water deprivation at different times on *B. germanica* females. D.A.M.: days after moult.

Those females that were water-deprived from day 3 (n=10) did not oviposit either. Observing the ovary in these females at day 5, we found partial resorption of basal ovarian follicles (about 20%), while at day 9 and 10 all of them were resorbed. Those females that were water-deprived from day 4 oviposited at the same time than control females and formed a proper ootheca (n=10). All females from these 2 last experiments died between 20 and 25 days after moulting to the adult stage.

Females subjected to 14 h without water every day (n=15) survived as long as control females, but they showed defects on basal oocyte maturation and oviposition: Only 3 individuals oviposited and formed the ootheca properly, and 2 females dissected at day 10 of the adult stage showed no basal follicle growth.

Females that were water-deprived from day 0 to day 3, and water-provided from day 3 (n=10) survived as long as control females, and presented a delay on oviposition, which took place from day 10, two days later than in control females.

As ovarian resorption was clearer in the females water-deprived from day 3, we chose this treatment to work with.

b) Resorption of basal ovarian follicles in stressed females

As indicated above, 3-day-old adult females were water-deprived and ovaries were dissected at days 4, 5, 6, 7 and 8 of adult life.

Ovaries from control specimens were dissected at the same ages. No clear changes in basal ovarian follicle morphology were observed 24 h after water deprivation (day 4). However, differences between control and water-deprived specimens were well apparent from day 5 on (48 h after water removal), and a great diversity of phenotypes was observed. At this age, the basal ovarian follicles in control females are between 1.30 and 1.68 mm long, are white and opaque, and have an elliptical shape (Figure 2.2A). We can divide the phenotypes found in basal follicles from water-deprived females in three categories: 1) basal follicles indistinguishable from those of control females (Figure 2.2B), 2) basal follicles looking like those from young control females (not shown), and 3) resorbed basal follicles. We considered as resorbed those basal follicles rounded (Figure 2.2C, arrow), fragile (Figure 2.2D, 2.2E (asterisk) and 2.2I), transparent and/or brown coloured (Figure 2.2E, arrow), amorphous (Figure 2.2G) and significantly smaller than control ones (Figure 2.2F (arrow) and 2.2H). It is worth noting that the majority of the resorbed follicles presented more than one of these features, as some of the follicles showed in figure 2.2C, which are fragile, transparent and small.

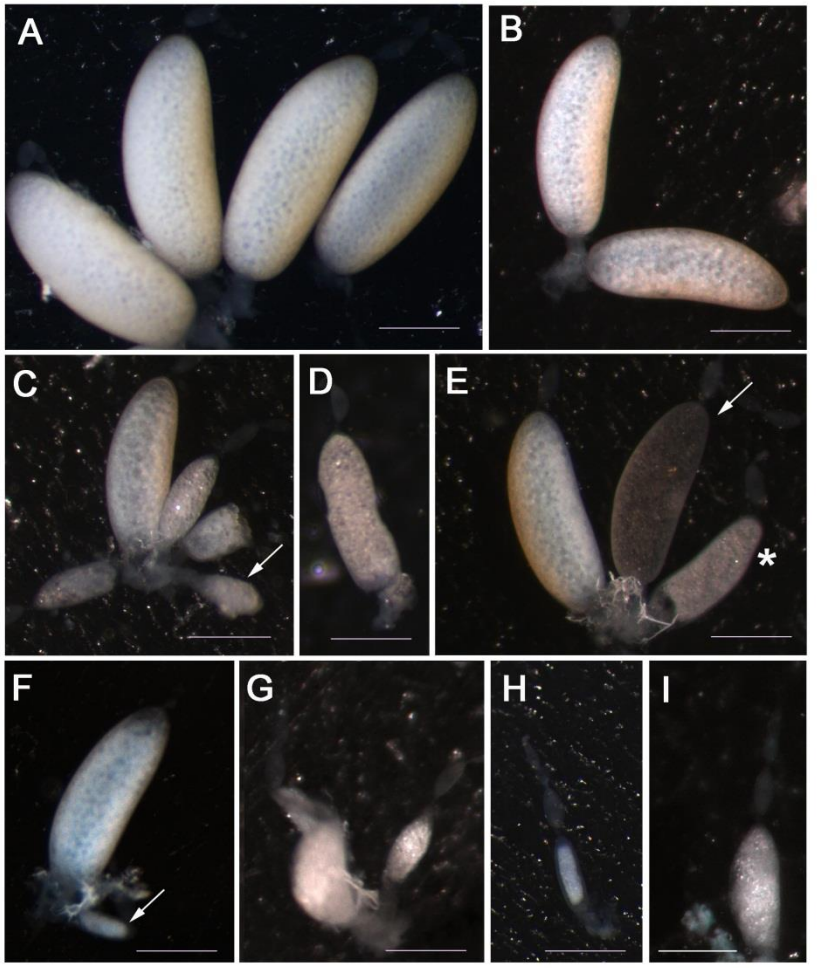

Figure 2.2: Ovarioles from 5-day-old females. A) Control female. B-I) Females subjected to 48 h of water deprivation. Arrow in C indicates a rounded follicle. Arrow in F indicates a small follicle. Arrow in E indicates a brown and transparent follicle. Asterisk in E indicates a fragile follicle. Scale bar: 500 µm.

The percentage of stressed females (water-deprived at day 3) presenting small basal follicles that looked like those from younger control females increased until day 7 (Table 2.1, Small). The percentage of stressed females presenting resorbed follicles and the percentage of resorbed follicles per female also increased with the

time of exposure to hydric stress; we have distinguished 2 categories: females presenting up to 50% resorbed follicles (Table 2.1, < 50% RF) and females presenting more than 90% resorbed follicles (Table 2.1, > 90% RF). Control females usually oviposit at the end of day 7, but stressed females never oviposited.

Table 2.1: Percentages of females water-deprived on day 3 showing the different phenotypes found. Age: age of the female in days. Normal: females with ovaries showing normal phenoptype. Small: females with ovaries showing the appearance and size of follicles from younger control females < 50% RF: females with ovaries showing up to 50% of their follicles resorbed (RF meaning *resorbed follicle*). > 90% RF: females with ovaries showing more than 90% of follicles resorbed. N: sample size.

Age	Normal	Small	< 50% RF	> 90% RF	N
4	87.5%	12.5%	0%	0%	8
5	35%	10%	20%	35%	20
6	11.43%	11.43%	14.40%	37.14%	35
7	13.3%	20%	23.3%	43.3%	30
8	0%	12.5%	8.3%	79.2%	24

c) Cell death in ovaries from control females

Prior to analyse cell death in ovaries from water-stressed females, we wanted to assess the pattern of cell death in the follicular epithelium in normal conditions during the first gonadotrophic cycle in the adult, measuring active caspases. For this purpose we injected females with ages from day 0 to day 7 with FLIVO and observed

the ovaries under the microscope 1 h later (Figure 2.3). At the pre-vitellogenesis stage (days 0 to 2), when follicular cells are dividing mitotically (Figure 2.3A''), we did not detect any caspase activation (Figure 2.3A and data not shown). At day 3, when cytokinesis stops and the follicular epithelium reorganizes (Figure 2.3B'-B'''), a slight activated caspase labelling appeared on the cytoplasm of follicular cells (Figure 2.3B). At day 4 the epithelium is reorganized, and the follicular cells become binucleated, with the nuclei showing a characteristic "bean shape" (Figure 2.3C'-C'''); we found labelling for caspase activation in the nuclei of follicular cells at this age (Figure 2.3C). Caspase labelling became stronger at day 5 (Figure 2.3D), when follicular cells let spaces among them (patency) to allow proteins, like vitellogenin and lipophorin, reach the oocyte. The surface of the oocyte presents specific receptors that allow proteins to be incorporated by receptor-mediated endocytosis (Ciudad et al., 2007; Ciudad et al., 2006). In 6-day-old females the signal of activated caspases decreased (Figure 2.3E) and it disappeared in 7-day-old females (Figure 2.3F). At this age, follicular cells close the intercellular spaces and the nuclei lose the "bean shape" (Figure 2.3F'-F'''). At the end of the cycle, during choriogenesis, the actins change the distribution and invade the cytoplasm, forming bundles that cover completely the cells (Figure 2.3G'). At this moment we detected again slight activated caspase labelling on the cytoplasm (Figure 2.3G).

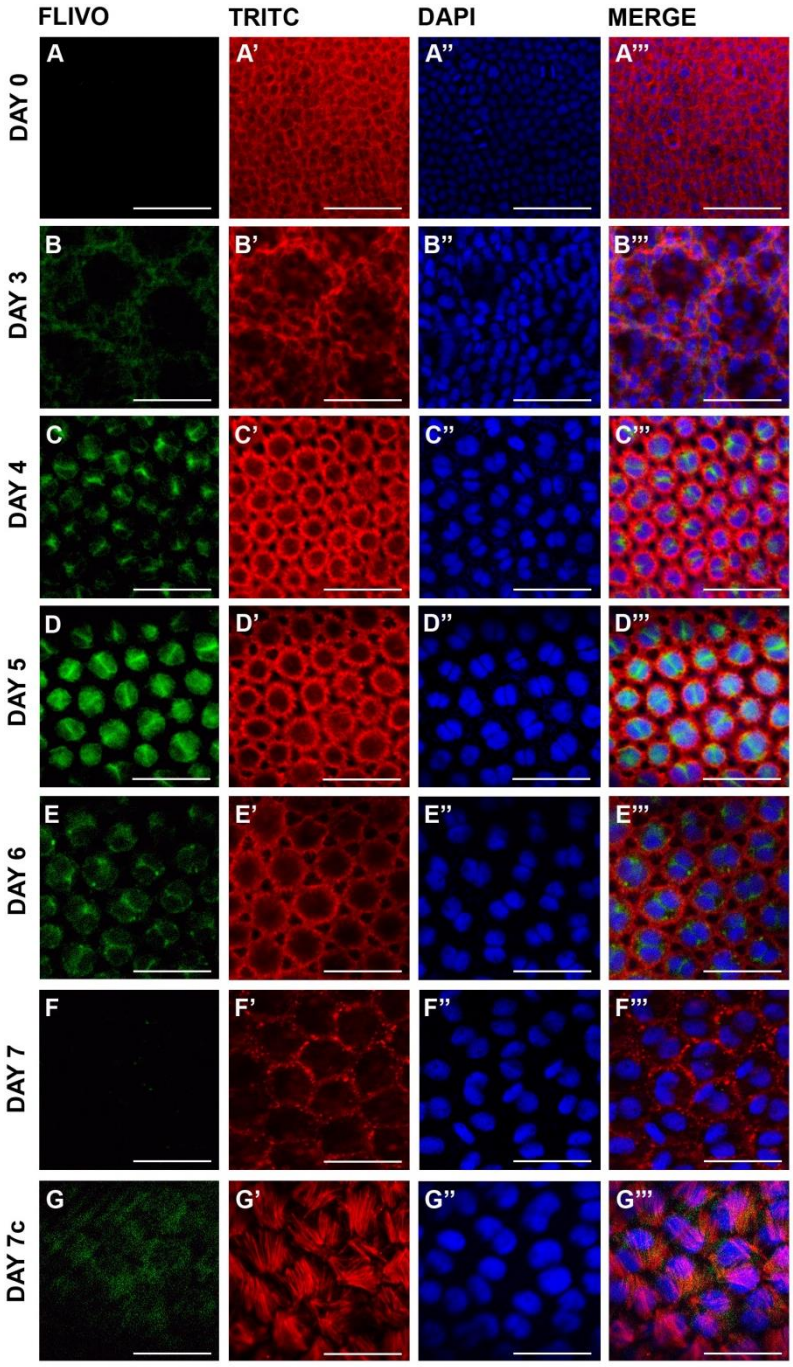

Figure 2.3: Follicular epithelium from adult *B. germanica* females along the first gonadotrophic cycle. Female age is indicated on the left (day). DAY 7c: chorionated follicle from day 7. FLIVO: activated caspase marker; TRITC: actin marker; DAPI: nucleic acid marker. Scale bar: 50 μm.

d) Cell death in ovaries from water-stressed females

In order to analyse ovarian cell death caused by hydric stress, females that were water-deprived on day 3 were injected at day 4, 5, 6 or 7 with FLIVO, and ovaries were observed 1 h later.

After 24 h of hydric stress, basal ovarian follicles showed the same morphology and size than controls. However, we observed more intense active caspase staining in the nuclei of follicular cells from stressed females (Figure 2.4A). We also observed places where actin and nucleus staining was undetectable, which can be a sign of cellular disintegration (Figure 2.4A'-A''').

As stated in section "b" of Results, we found three different phenotypes in ovarian basal follicles from stressed females from day 5 on (from 48 h of stress on) when examined under the stereomicroscope: 1) identical to control ovarian follicles, 2) like basal follicles of control younger females, and 3) resorbed. Within the group 1, in follicles from 5-day-old females we detected fewer nuclei with active caspases than in controls (Figure 2.4B). Moreover, actins and nuclei were undetectable in some cells, which, in addition, were the only ones that showed caspases staining (Figure 2.4B-B'''). At days 6 and 7 we did not observe differences relative to caspase activation, or to actin and nuclei staining between control and water-stressed basal follicles (Figure 2.4C-C''', and data not shown).

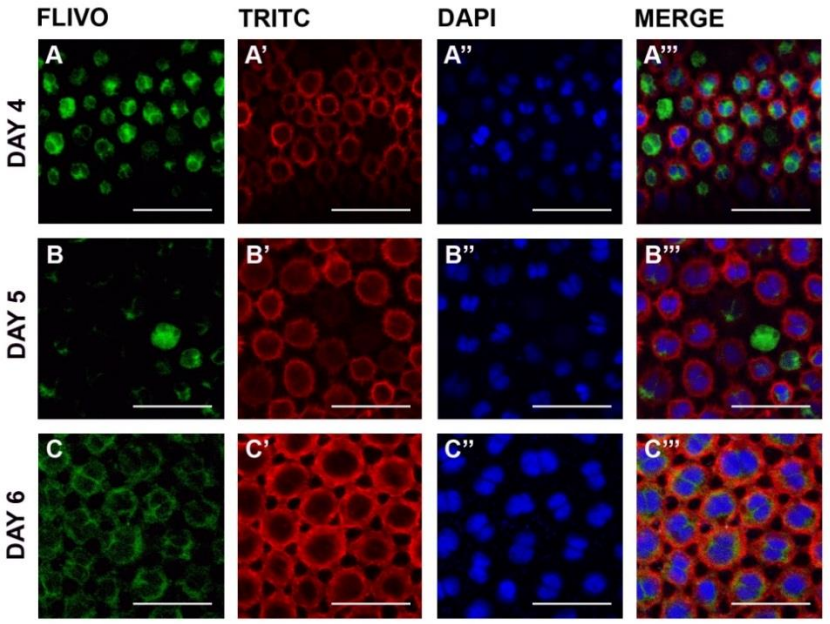

Figure 2.4: Follicular epithelium from adult *B. germanica* stressed females (water-deprived on day 3). Images correspond to ovarian follicles that appeared identical to controls when analysed with the stereomicroscope. See controls in Figure 2.3. Ages are indicated on the left (day). FLIVO: activated caspase marker; TRITC: actin marker; DAPI: nucleic acid marker. Scale bar: 50 μm.

Basal ovarian follicles from group 2 (similar to basal follicles from control younger females) presented higher caspase activation than control follicles with the same length. Figure 2.5A-A''' shows a follicular epithelium from an ovarian follicle belonging to a 6-day-old stressed female, which has the length and appearance of a follicle from a 3-day-old control female. It presents high activated caspase staining in the cytoplasm of the follicular cells, which is in contrast with 3-day-old controls, in which activated caspases staining is very faint, as shown before (Figure 2.3B).

Finally, among the resorbed follicles (group 3) we observed different degrees of degeneration. Basal follicles showing the most severe phenotype exhibited intense active caspase staining in the cytoplasm of follicular cells, high cytoskeleton disorganization and chromatin condensation (Figure 2.5B-B’’’).

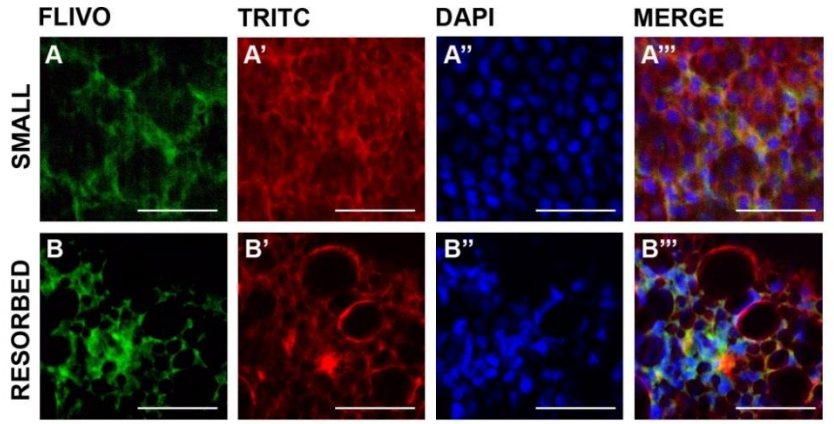

Figure 2.5: Follicular epithelium from 6-day-old *B. germanica* stressed females (water-deprived on day 3). A-A’’’): Ovarian follicle with the length of one from a 3-day-old control female. **B-B’’’)**: Ovarian follicle showing resorption. FLIVO: activated caspase marker; TRITC: actin marker; DAPI: nucleic acid marker. Scale bar: 50 μm.

2.5. Discussion

In the present chapter we have described the effects of the lack of water on survival and oogenesis in adult females of the cockroach *B. germanica*.

According to our results, water deprivation affects survival and oogenesis in different ways depending on when it takes place. If drinking water was removed shortly after the imaginal moult (day 0 or 1) ovarian basal follicles never matured. Moreover, the individuals died within few days. Basal follicles neither matured when water was alternatively supplied and suppressed along the gonadotrophic cycle, although survival under these treatment remained unaffected. When water was suppressed from the imaginal moult to day 3 and then re-supplied, basal follicle maturation and oviposition took place but delayed with respect to control females, and the treatments did not influence survival. From these results, we can conclude that a proper water supply is essential for the onset of oogenesis.

When water was suppressed at day 3 or 4 of the adult stage, individuals survived significantly longer than when it was suppressed shortly after moult. In these two experiments the effects on the ovary were different: when water was suppressed on day 3, ovaries degenerated and females never oviposited, while when it was suppressed on day 4, oogenesis and oviposition were as in controls. Interestingly, in *Drosophila melanogaster* it has been described that diverse stimuli triggers degeneration of egg chambers at two specific stages, region 2 within the germarium, and stage 8 during mid-oogenesis (reviewed by McCall, 2004). Based in our results, we hypothesize that *B. germanica* would also have a sort of checkpoint at the beginning of vitellogenesis, where the decision of

going on with oogenesis or stop it and reinvest the resources in other functions should be taken.

Ovarian resorption has been found in several insects triggered by different circumstances as poor nutrition, virginity, infectious diseases and host deprivation (Bodin et al., 2009; Guo et al., 2011; Kotaki, 2003; Medeiros et al., 2011). Here we show that hydric stress is also a factor that can induce ovarian resorption; when hydric stress was started on day 3 of the adult life, females undertook it. Early symptoms of stress were not evident, and ovaries from control and stressed females appeared indistinguishable under the stereomicroscope until 48 h after water deprivation. However, we found more intense activated caspase staining on follicular cells 24 h after stress induction than on follicular cells from control females from the same age, which suggests that cell death processes are triggered shortly after water deprivation.

From 48 h after the induction of the hydric stress we found a variety of phenotypes relative to the severity of resorption; the strongest phenotype was characterized by collapsed follicles exhibiting high activated caspase staining, disorganized cytoskeleton and chromatin condensation, which are classical features of cell death (Elmore, 2007). Phenotype variability has been also observed in resorbed ovarian follicles in the mosquito *Culex pipiens pallens*: some follicles maintained their structure but thickened the follicular epithelium, whereas in others the structure of the nurse cells

disappeared, some of them lost volume and shrank, and, in the most severe cases, the follicle was only composed by surviving epithelial cells, some of which showed a condensed chromatin-like structure within the nucleus (Uchida et al., 2004).

We also found basal follicles that looked like those from control younger females, as if they had stopped maturation at a certain point. However, these follicles presented the activated caspase staining higher than controls with the corresponding size, thus suggesting that they were degenerating rather than maturing at a slower rate than controls.

Which kind of cell death takes place in resorbing follicles is not clear. Here we show that activated caspases are present in follicular cells of stressed females 24 and 48 h after stress induction, while its presence becomes less abundant after that moment. In addition, the percentage of resorbed follicles increases with the time of exposure to hydric stress. It is probable that more than one type of cell death took place in the resorbing follicles. In different models it has been described that several injurious stimuli can induce apoptosis at low doses, but these same stimuli can result in necrosis at higher doses (Elmore, 2007). In fact, a recent study conducted in the hemipteran insect *Dipetalogaster maxima* indicates that apoptosis, autophagy and necrosis are involved on follicular atresia induced by starvation (Aguirre et al., 2013).

Caspases not only control apoptosis, but also execute non apoptotic functions involved in proliferation, differentiation, cell shape, and cell migration (reviewed by Miura, 2012). We found activated caspase staining in follicular cells of healthy basal follicles from day 4 to day 6, peaking at day 5. This correlates with the measurements of the patency index made by Pascual et al. (1992), suggesting that this caspase activation is involved in the control of the shrinkage of follicular cells in this stage. On the other hand, the activation found in healthy chorionated follicles is presumably related with apoptotic processes, as the follicular epithelium degrades concomitant with choriogenesis (Irles et al., 2009).

In the present chapter we have reported that hydric stress prevents reproduction in the German cockroach *B. germanica*, triggering ovarian basal follicle resorption when induced at the onset of vitellogenesis. The description of the phenotypic effects experienced by the ovaries upon such stress paves the way for further molecular analysis.

2.6. References

Aguirre, S. A., Pons, P., Settembrini, B. P., Arroyo, D. and Canavoso, L. E. (2013). Cell death mechanisms during follicular atresia in *Dipetalogaster maxima*, a vector of Chagas' disease (Hemiptera: Reduviidae). *J Insect Physiol* **59**, 532-41.

Asplen, M. K. and Byrne, D. N. (2006). Quantification and ultrastructure of oosorption in *Eretmocerus eremicus* (Hymenoptera: Aphelinidae). *J Morphol* **267**, 1066-74.

Barrett, E. L., Moore, A. J. and Moore, P. J. (2009). Diet and social conditions during sexual maturation have unpredictable influences on female life history trade-offs. *J Evol Biol* **22**, 571-81.

Benoit, J. (2011). Stress Tolerance of Bed Bugs: A Review of Factors That Cause Trauma to *Cimex lectularius* and *C. Hemipterus*. *Insects* **2**, 151-172.

Bodin, A., Jaloux, B., Delbecque, J. P., Vannier, F., Monge, J. P. and Mondy, N. (2009). Reproduction in a variable environment: How does *Eupelmus vuilleti*, a parasitoid wasp, adjust oogenesis to host availability? *J Insect Physiol* **55**, 643-8.

Chrousos, G. P. (2009). Stress and disorders of the stress system. *Nat Rev Endocrinol* **5**, 374-81.

Ciudad, L., Belles, X. and Piulachs, M. D. (2007). Structural and RNAi characterization of the German cockroach lipophorin receptor, and the evolutionary relationships of lipoprotein receptors. *BMC Mol Biol* **8**, 53.

Ciudad, L., Piulachs, M. D. and Belles, X. (2006). Systemic RNAi of the cockroach vitellogenin receptor results in a phenotype similar to that of the Drosophila yolkless mutant. *FEBS J* **273**, 325-35.

de Souza, E. A., Neves, C. A., de Oliveira Campos, L. A., Zanuncio, J. C. and Serrao, J. E. (2007). Effect of mating delay

on the ovary of *Melipona quadrifasciata anthidioides* (Hymenoptera: Apidae) queens. *Micron* **38**, 471-7.

Elmore, S. (2007). Apoptosis: a review of programmed cell death. *Toxicol Pathol* **35**, 495-516.

Guo, J. Y., Dong, S. Z., Ye, G. Y., Li, K., Zhu, J. Y., Fang, Q. and Hu, C. (2011). Oosorption in the endoparasitoid, *Pteromalus puparum*. *J Insect Sci* **11**, 90.

Irles, P., Belles, X. and Piulachs, M. D. (2009). Identifying genes related to choriogenesis in insect panoistic ovaries by Suppression Subtractive Hybridization. *BMC Genomics* **10**, 206.

Kotaki, T. (2003). Oosorption in the stink bug, *Plautia crossota stali:* induction and vitellogenin dynamics. *J Insect Physiol* **49**, 105-13.

Kroemer, G., Marino, G. and Levine, B. (2010). Autophagy and the integrated stress response. *Mol Cell* **40**, 280-93.

McCall, K. (2004). Eggs over easy: cell death in the *Drosophila* ovary. *Dev Biol* **274**, 3-14.

Medeiros, M. N., Ramos, I. B., Oliveira, D. M., da Silva, R. C., Gomes, F. M., Medeiros, L. N., Kurtenbach, E., Chiarini, L. B., Masuda, H., de Souza, W. et al. (2011). Microscopic and molecular characterization of ovarian follicle atresia in *Rhodnius prolixus* Stahl under immune challenge. *J Insect Physiol* **57**, 945-53.

Miura, M. (2012). Apoptotic and nonapoptotic caspase functions in animal development. *Cold Spring Harb Perspect Biol* **4** a008664.

Pascual, N., Cerdá, X., Benito, B., Tomás, J., Piulachs, M. D. and Belles, X. (1992). Ovarian ecdysteroid levels and basal oocytedevelopment during maturation in the cockroach *Blattella germanica* (L.). *J Insect Physiol* **38**, 339-348.

Uchida, K., Nishizuka, M., Ohmori, D., Ueno, T., Eshita, Y. and Fukunaga, A. (2004). Follicular epithelial cell apoptosis of atretic

follicles within developing ovaries of the mosquito *Culex pipiens pallens*. *J Insect Physiol* **50**, 903-12.

3. IDENTIFICATION AND FUNCTIONAL CHARACTERIZATION OF AN OVARIAN AQUAPORIN FROM THE COCKROACH *BLATTELLA GERMANICA* L. (DICTYOPTERA, BLATTELLIDAE)

Identification and functional characterization of an ovarian aquaporin from the cockroach *Blattella germanica* (L.) (Dictyoptera, Blattellidae)

Alba Herraiz*, François Chauvigné**, Joan Cerdà**, Xavier Belles*, Maria-Dolors Piulachs*

* Institut de Biologia Evolutiva (CSIC-UPF), and LINCGlobal, Passeig Marítim de la Barceloneta 37-49. 08003 Barcelona, Spain.

** Laboratory of Institut de Recerca i Tecnologia Agroalimentàries (IRTA)-Institut de Ciències del Mar (CSIC), Passeig Marítim de la Barceloneta 37-49. 08003 Barcelona, Spain.

Herraiz A., Chauvigné F, Cerdà J, Belles X, Piulachs MD. Identification and functional characterization of an ovarian aquaporin from the cockroach *Blattella germanica* (L.) (Dictyoptera, Blattellidae).

J Exp Biol. 2011 Nov 1; 214(Pt 21): 3630-8.
DOI: 10.1242/jeb.057406

3.1. Abstract

Aquaporins (AQPs) are membrane proteins that form water channels, allowing rapid movement of water across cell membranes. AQPs have been reported in species of all life kingdoms and in almost all tissues, but little is known about them in insects. Our purpose was to explore the occurrence of AQPs in the ovary of the phylogenetically basal insect *Blattella germanica* (L.) and to study their possible role in fluid homeostasis during oogenesis. We isolated an ovarian AQP from *B. germanica* (BgAQP) that has a deduced amino acid sequence showing six potential transmembrane domains, two NPA motifs, and an ar/R constriction region, which are typical features of the AQP family. Phylogenetic analyses indicated that BgAQP belongs to the PRIP group of insect AQPs, previously suggested to be water-specific. However, ectopic expression of BgAQP in *Xenopus laevis* (Daudin) oocytes demonstrated that this AQP transports water and modest amounts of urea, but not glycerol, which suggests that PRIP group of insect AQPs may have heterogeneous solute preferences. BgAQP was shown to be highly expressed in the ovary, followed by the fat body and muscle tissues, but water-stress did not modify significantly the ovarian expression levels. RNA interference (RNAi) reduced BgAQP mRNA levels in the ovary but the oocytes developed normally. The absence of an apparent ovarian phenotype after BgAQP RNAi suggests that other functionally redundant AQPs that were not silenced in our experiments might exist in the ovary of *B. germanica*.

3.2. Introduction

Aquaporins (AQPs) are membrane proteins that facilitate water transport, which have been identified from species belonging to all life kingdoms, including unicellular (archaea, bacteria, yeast and protozoa) and multicellular (plants and animals) organisms (King et al., 2004; Maurel et al., 2008). They belong to the Major Intrinsic Proteins (MIP) superfamily that share a common structure comprising 6 transmembrane domains (TM1-TM6) connected by five loops (A-E), and cytoplasmic N- and C- termini. AQPs contain two canonical Asp-Pro-Ala (NPA) motifs located in steric contiguity with the aromatic/arginine (ar/R) constriction region involved in proton exclusion and channel selectivity (de Groot et al., 2003; Murata et al., 2000). The ar/R constriction site is defined by four residue positions (56, 180, 189, and 195; human AQP1 numbering), which in water-selective AQPs are Phe^{56}, His^{180}, Cys^{189} and Arg^{195} (human AQP1) (de Groot et al., 2003). The AQP polypeptide chain is formed by two closely related halves that may have arisen by gene duplication (Zardoya, 2005). In the cell membrane, each AQP is folded into a right-handed α-barrel, with a central transmembrane channel surrounded by the six full-length transmembrane helices and the two NPA-containing loops, B and E. This conformation in the plasma membrane is known as the hourglass model (Jung et al., 1994). Some AQPs, known as aquaglyceroporins, transport other non-charged solutes such as glycerol and urea in addition to water (Gomes et al., 2009; Rojek et al., 2008; Törnroth-Horsefield et al., 2010). The amino acids

forming the ar/R constriction (His is replaced by the smaller amino acid Gly in aquaglyceroporins) (Beitz et al., 2006), and five other residues (P1-P5) located on the side-chains at the neighbourhood of the ar/R constriction (Froger et al., 1998), are responsible for the substrate selectivity. The transport function of many AQPs can be inhibited by mercurial sulfhydryl-reactive compounds, such as $HgCl_2$, which block the water pore (Hirano et al., 2010; Preston et al., 1993).

While there is considerable data on mammalian AQPs, studies on insect AQPs are much limited. Phylogenetic analysis based on 18 insect genomes revealed the presence of AQP orthologs in all of them (Campbell et al., 2008). However, only 15 AQPs from insects have been characterized in terms of substrate selectivity (Campbell et al., 2008; Goto et al., 2011; Kataoka et al., 2009a; Kataoka et al., 2009b; Liu et al., 2011; Philip et al., 2011). The first insect AQP functionally characterized was AQPcic, from the filter chamber of *Cicadella viridis* (L.), and was shown to be water-selective (Le Caherec et al., 1996). Since then, water-transporting AQPs have also been isolated from *Aedes aegypti* (L.) (Duchesne et al., 2003), *Rhodnius prolixus* Stahl (Echevarria et al., 2001), *Drosophila melanogaster* Meigen (Kaufmann et al., 2005), *Polypedilum vanderplanki* Hinton (Kikawada et al., 2008), *Acyrthosiphon pisum* (Harris) (Shakesby et al., 2009), *Bombyx mori* L. (Kataoka et al., 2009a), *Grapholita molesta* (Busck) (Kataoka et al., 2009b), *Eurosta solidaginis* Fitch (Philip et al., 2011), *Anopheles gambiae* Giles (Liu et al., 2011) and *Belgica antarctica* Jacobs (Goto et al.,

2011). Only two insect AQPs were shown to transport glycerol and urea in addition to water: AQP-Bom2 and AQP-Gra2, from *B. mori* and *G. molesta*, respectively (Kataoka et al., 2009a; Kataoka et al., 2009b). Finally, *D. melanogaster* Big Brain AQP transports monovalent cations in the epidermal precursor regions of developing larvae (Yanochko and Yool, 2002).

Our aim was to investigate the presence of AQPs in the ovary of the cockroach *Blattella germanica* (L.) (Dictyoptera, Blattellidae) and their possible role in water homeostasis during oogenesis and vitellogenesis. *B. germanica* has panoistic ovaries, which is the less modified insect ovarian type (Büning, 1994). During oocyte maturation, basal oocytes increase in size due to the incorporation of vitellogenin, other yolk precursors and water (Belles et al., 1987; Ciudad et al., 2006; Martín et al., 1995; Telfer, 2009). Moreover, although *B. germanica* is well adapted to xeric environments (Appel, 1995), water-stress readily leads to oocyte resorption. These circumstances make *B. germanica* a good model to study ovarian AQPs. Finally, insect AQPs that have been described so far were from holometabolans or from phylogenetically distal hemimetabolans (hemipterans and phthirapterans, within the paraneopterans), and therefore *B. germanica*, which is a phylogenetically basal insect within the polyneopterans, is of evolutionary interest.

3.3. Material and methods

a) Insects

Female specimens of *B. germanica* (L.) were used in all experiments. They were obtained from a colony reared in the dark at 29±1°C and 60–70% relative humidity in non aseptic environment. Under these conditions, the cockroach fat body and ovary harbour the endosymbiont bacteroid *Blattabacterium cuenoti* (Giorgi and Nordin, 1994; Lopez-Sanchez et al., 2009). Sixth instar nymphs or freshly ecdysed adult females were selected from the colony and used at appropriate ages. All dissections and tissue sampling were carried out on carbon dioxide-anaesthetized specimens. Tissues used in the experiments were as follows: entire ovary, fat body abdominal lobes, levator and depressor muscles of tibia, digestive tract from the pharynx to the rectum (Malphigian tubules excluded), isolated Malpighian tubules, and colleterial glands. After the dissection, the tissues were frozen on liquid nitrogen and stored at -80ºC until use.

b) Cloning and sequencing

The sequence of a partial cDNA encoding a putative *B. germanica* AQP (544 bp) was obtained from an EST library available in GenBank (Accession number: FG128078.1). This fragment was amplified from cDNA synthesized from 3-day-old adult ovaries using specific oligonucleotide primers and conventional PCR. The

resulting fragment was cloned into pSTBlue-1 vector (Novagen Madrid, Spain) and sequenced. To clone the full-length cDNA, 5'- and 3'-RACE (Invitrogen, Paisley, UK) were used according to the manufacturer's instructions. The PCR products were analyzed by agarose gel electrophoresis, cloned into pSTBlue-1 vector and sequenced. The sequence, that showed to be an AQP homologue, was named BgAQP (Accession number FR744897).

c) Comparison of sequences and phylogenetic analysis

Putative insect AQP sequences were retrieved from GenBank. Protein sequences were aligned with that obtained for *B. germanica*, using CLUSTALX (v 1.83). Poorly aligned positions and divergent regions were removed by using GBLOCKS 0.91b (http://molevol.ibmb.csic.es/Gblocks_server/) (Castresana, 2000). The resulting alignment was analyzed by the PHYML 3.0 program (Guindon and Gascuel, 2003) based on the maximum-likelihood principle with the LG amino acid substitution model. The data was bootstrapped for 100 replicates using PHYML. The sequences used in the phylogenetic analysis were as follows. XP_002429480.1 (*Pediculus humanus* L.), AAL09065.1 (PrAQP1, *Pyrocoelia rufa* Olivier), FJ489680 (*Es*AQP1, *E. solidaginis*), NP_610686.1 (DmPRIP, *D. melanogaster*), XP_001865728.1 (*Culex quinquefasciatus* Say), XP_001656932.1 (AaAQP2, *A. aegypti*), BAF62090.1 (PvAQP1, *P. vanderplanki*), AB602340 (BaAQP1, *B. antarctica*), XP_319585.4 (AgAQP1, *A. gambiae*), NP_001153661.1 (*B. mori*), XP_968342.1 (TcPRIP, *T. castaneum*

(Herbst)), XP_001607929.1 (NvPRIP, *N. vitripennis* (Walker)), XP_394391.1 (*A. mellifera*), XP_972862.1 (TcDRIP, *Tribolium castaneum*), Q23808.1 (AQPcic, *C. viridis*), BAG72254.1 (*Coptotermes formosanus* Shiraki), XP_002425393.1 (*P. humanus*), ABW96354.1 (*Bemisia tabaci* (Gennadius)), XP_624531.1 (AmDRIP, *Apis mellifera* L.), (NvDRIP, *Nasonia vitripennis*), AAA81324.1 (DmDRIP, *D. melanogaster*), AAA96783.1 (BfWC1, *Haematobia irritans* (L.)), ABV60346.1 (*Ll*AQP, *Lutzomyia longipalpis* (Lutz & Neiva)), XP_319584.4 (*A. gambiae*), AF218314.1 (AaAQP1, *A. aegypti*), XP_001865732.1 (*C. quinquefasciatus*), BAD69569.1 (AQP-Bom1, *B. mori*), BAH47554.1 (AQP-Gra1, *G. molesta*), NP_001139376.1 (*A. pisum*), NP_001139377.1 (*A. pisum*), XP_396705.2 (AmBIB, *A. mellifera*), XP_001604170.1 (NvBIB *N. vitripennis*), XP_314890.4 (*A. gambiae*), XP_001649747.1 (AaAQP3, *A. aegypti*), XP_001866597.1 (*C. quinquefasciatus*), XP_314891.4 (*A. gambiae*), AAF52844.1 (DmBIB, *D. melanogaster*), XP_968782.1 (TcBIB, *T. castaneum*), XP_970791.1 (*T. castaneum*), XP_970912.1 (*T. castaneum*), XP_001121899.1 (*A. mellifera*), XP_001601231.1 (*N. vitripennis*), XP_624194.1 (*A. mellifera*), XP_001601253.1 (*N. vitripennis*), NP_001106228.1 (AQP-Bom2, *B. mori*), BAH47555.1 (AQP-Gra2, *G. molesta*), BAF62091.1 (PvAQP2, *P. vanderplanki*), XP_001650169.1 (AaAQP5, *A. aegypti*), XP_001850887.1 (*C. quinquefasciatus*), XP_318238.4 (*A. gambiae*), NP_611812.1 (*D. melanogaster*), NP_611813.1 (*D. melanogaster*), NP_611811.3 (*D. melanogaster*), XP_001650168.1 (AaAQP4, *A. aegypti*), XP_554502.2 (*A. gambiae*), NP_611810.1

(*D. melanogaster*), XP_001121043.1 (*A. mellifera*), XP_001603421.1 (*N. vitripennis*), and XP_970728.1 (*T. castaneum*).

d) Structural predictions

Topographical analyses to determine transmembrane regions were carried out with the programs TMHMM (www.cbs.dtu.dk/services/TMHMM/) (Krogh et al., 2001) and SMART (http://smart.embl-heidelberg.de/smart/set_mode.cgi) (Letunic et al., 2009). Phosphorylation sites and kinases were determined using NetPhos 2.0 and NetPhosK 1.0 programs (Blom et al., 1999; Blom et al., 2004), respectively, on ExPASy Proteomic Tools (http://expasy.org/tools). Predictions of tridimensional structure were carried out with the 3D-JIGSAW Protein Comparative Modelling Server (http://bmm.cancerresearchuk.org/~3djigsaw/) (Bates et al., 2001), and analyzed using PyMOL Molecular Graphics System, Version 1.2r3pre, Schrödinger, LLC.

e) Functional expression in *Xenopus laevis* oocytes

The open reading frame (ORF) of BgAQP cDNA was cloned into the pSTBlue-1 vector and subcloned into the *Eco*RV/*Spe*I sites of the pT7Ts expression vector (Deen et al., 1994). Capped RNA (cRNA) was synthesized *in vitro* with T7 RNA Polymerase (Roche) from *Xba*I-linearized pT7Ts vector containing the BgAQP cDNA.

The isolation and microinjection of stage V-VI oocytes of *X. laevis* was carried out as previously described (Deen et al., 1994). For water permeability experiments, oocytes were injected with either 50 nl of RNase-free water (negative control) or 50 nl of water solution containing 10 ng cRNA of BgAQP. For glycerol and urea uptake experiments, oocytes were injected with 25 ng cRNA of BgAQP, human AQP1 (negative control) or human AQP3 (positive control). Human AQP1 and AQP3 were kindly provided by P. Deen (Department of Physiology, Radboud University Nijmegen Medical Centre, Nijmegen, The Netherlands).

f) Swelling assays

Osmotic water permeability (P_f) was measured from the time course of oocyte swelling in a standard assay (Deen et al., 1994). Water- and cRNA-injected *X. laevis* oocytes were transferred from 200 mOsm modified Barth's culture medium (MBS; 0.33 mM $Ca(NO_3)_2$, 0.4 mM $CaCl_2$, 88 mM NaCl, 1 mM KCl, 2.4 mM $NaHCO_3$, 10 mM Hepes, 0.82 mM $MgSO_4$, pH 7.5) to 20 mOsm MBS at room temperature. Oocyte swelling was followed by video microscopy using serial images at 2 sec intervals during the first 20 sec period. The P_f values were calculated taking into account the time-course changes in relative oocyte volume [d $(V/V_o)/dt$], the molar volume of water (V_w = 18 cm^3/ml) and the oocyte surface area (S), using the formula V_o [d $(V/V_o)/dt$]/ [SV_w (Osm_{in}-Osm_{out})]. To examine the inhibitory effect of mercury on P_f, oocytes were pre-incubated for 15 min in MBS containing 1 mM $HgCl_2$ before

and during the swelling assays. To determine the reversibility of the inhibition, the oocytes were rinsed 2 times with fresh MBS and incubated for another 15 min with 5 mM β-mercaptoethanol before being subjected to swelling assays.

g) Radioactive solute uptake assays

To determine the uptake of [^{3}H]glycerol (60 Ci/mmol) and [^{14}C]urea (52 mCi/mmol), groups of 10 *X. laevis* oocytes injected with water or 25 ng cRNA encoding BgAQP, human AQP1 or human AQP3, were incubated in 200 µl of MBS containing 20 µCi of the radiolabeled solute (cold solute was added to give 1 mM final concentration) at room temperature. After 10 min (including zero time for subtraction of the signal from externally bound solute), oocytes were washed rapidly in ice-cold MBS three times, and individual oocytes were dissolved in 10% SDS for 1 h before scintillation counting.

h) RNA Extraction and retrotranscription to cDNA

All RNA extractions were performed using the Gen Elute Mammalian Total RNA kit (Sigma, Madrid, Spain). An amount of 400 ng from each RNA extraction was DNase treated (Promega, Madison, WI, USA) and reverse transcribed with Superscript II reverse transcriptase (Invitrogen, Carlsbad CA, USA) and random hexamers (Promega). RNA quantity and quality was estimated by spectrophotometric absorption at 260 nm in a Nanodrop

Spectrophotometer ND-1000 (NanoDrop Technologies, Wilmington, DE, USA).

i) Determination of mRNA levels with quantitative real-time PCR

Quantitative real time PCR (qRT-PCR) reactions were carried out in triplicate in an iQ5 Real-Time PCR Detection System (Bio-Rad Laboratories), using SYBRGreen (Power SYBR Green PCR Master Mix; Applied Biosystems). A control without template was included in all batches. The efficiency of each primer set was first validated by constructing a standard curve through four serial dilutions. The PCR program began with a single cycle at 95°C for 3 min, 40 cycles at 95°C for 10 sec and 55°C for 30 sec. mRNA levels were calculated relative to BgActin-5c (GenBank accession number AJ862721) expression, using the Bio-Rad iQ5 Standard Edition Optical System Software (version 2.0). Results are given as copies of mRNA per 1,000 copies of BgActin-5c mRNA.

j) Induction of water stress

In order to identify the critical moment in which water stress causes clear phenotypical effects, adult *B. germanica* females were initially subjected to water deprivation from day 0, 1, 3, or 4. All specimens that were water-deprived from day 0 and 1 died after 8 to 11 days, whereas those water-deprived from day 4 did not present any phenotype. Specimens that were water-deprived from day 3

presented ovarian resorption starting on day 5. Thus, we decided to follow this treatment, in comparison with a control group that received water *ad libitum*. Water-deprived and control specimens were studied at 24 h intervals until day 7 of adult life.

k) RNAi experiments

A dsRNA (dsBgAQP) was prepared encompassing a 188 bp region starting at nucleotide 771 of BgAQP sequence. The fragment was amplified by PCR and cloned into the pSTBlue-1 vector. As control dsRNA (dsMock), we used a 307 bp sequence from *Autographa californica* (Speyer) nucleopolyhedrovirus (GenBank accession number K01149, from nucleotide 370 to 676). The preparation of the dsRNAs was performed as previously described (Ciudad et al., 2006). Freshly emerged specimens from last (6th) nymphal instar were injected into the abdomen with 3 µg of dsBgAQP in a volume of 1 µl. Control specimens were injected with the same volume and dose of dsMock. After the imaginal moult, one mature male (6- to 8-day-old) per female was added to the rearing jars, in order to bring about mating.

l) Statistics

Data are expressed as mean ± standard error of the mean (s.e.m.). Statistical analysis of gene expression values was carried out using the REST-2008 program (Relative Expression Software Tool V 2.0.7; Corbett Research) (Pfaffl et al., 2002). This program

calculates changes in gene expression between two groups, control and sample, using the corresponding distributions of *Ct* values as input. Values of P_f, P_{gly} and radioactive solute uptake were statistically analyzed in an unpaired Student's *t*-test.

3.4. Results

a) Cloning and sequence characterization of BgAQP from *Blattella germanica*

The sequence of a partial cDNA encoding a *B. germanica* AQP was cloned from ovarian tissue of 3-day-old adult females by using specific primers based on an expressed sequence tag (EST) deposited in GenBank (accession number FG128078.1). This EST nucleotide sequence was derived from male and female whole organism. Consecutive 5'- and 3'-RACE experiments were carried out in order to obtain the full-length cDNA, which was named BgAQP (GenBank accession number: FR744897). The BgAQP cDNA has 1,838 bp and contains an ORF encoding a polypeptide of 277 amino acids (nucleotide positions 95-925) with an estimated molecular weight of 29,541 Da and an isoelectric point of 5.86 (Figure 3.S1). Hydrophobicity and tridimensional predictions indicate that BgAQP has 6 putative transmembrane domains, five connecting loops, and cytoplasmic N- and C-termini, which are typical AQP features. The second (B) and fifth (E) loops contain the highly conserved NPA motifs (residues 93-95 and 209-211). The

amino acids forming the ar/R constriction region (Phe^{73}, His^{197} and Arg^{212}) and the P1-P5 residues (Thr^{133}, Thr^{213}, Ala^{217}, Tyr^{229} and Trp^{230}), which are conserved in water-selective AQPs, were present in BgAQP. In the amino acid sequence, a consensus motif for *N*-linked glycosylation [NX(S/T)] in loop C (Asn^{35}), as well as seven potential phosphorylation sites (Thr^{48}, Thr^{53}, Ser^{207}, Ser^{220}, Thr^{255}, Thr^{257} and Ser^{260}) and one protein kinase C-specific site (Ser^{216}), were also identified (Figure 3.S1).

b) Phylogenetic analysis of BgAQP

As the fat body and the ovary of *B. germanica* harbour the endosymbiont bacteroid *Blattabacterium cuenoti* (Giorgi and Nordin, 1994), we first evaluated whether the putative AQP cDNA cloned was really originated from the host cockroach ovary. BLAST analyses against the genome of *B. cuenoti* (Lopez-Sanchez et al., 2009), revealed that the bacteroid does not have any gene sequence matching the nucleotide sequence of BgAQP, which indicates that the cloned cDNA came from *B. germanica*. Then, in order to place BgAQP in an evolutionary context within insects, we carried out a phylogenetic analysis of representative insect AQPs available in public databases. The amino acid alignment of these sequences suggested that BgAQP was more related to a putative AQP from the phthirapteran *P. humanus* (XP_002429480) and the AQP homolog from the coleopteran *P. rufa* (AAL09065.1). Subsequently, following maximum-likelihood analyses, we obtained the tree depicted in Figure 3.1. This tree shows the same

general topology published by Campbell et al. (2008) and recently by Mathew et al. (2011), who defined four main clusters of insect AQPs: PRIP (from *Pyrocoelia rufa* Integral Protein), DRIP (from *Drosophila* Integral Protein), BIB (from neurogenic gene *Drosophila* big brain), and a fourth cluster of unclassified AQPs. In our tree, BgAQP falls into the well supported (96% bootstrap value) PRIP cluster, whereas the DRIP cluster appears as the sister group of PRIP, and the BIB cluster appears as the sister group of DRIP+PRIP. Finally, the fourth node of unclassified AQPs appears as the sister group of DRIP+PRIP+BIB.

Figure 3.2 depicts an amino acid alignment of BgAQP with the four aquaporins of the PRIP node that have been functionally characterized: EsAQP1 (Philip et al., 2011), AgAQP1 (Liu et al., 2011), PvAQP1 (Kikawada et al., 2008) and BaAQP1 (Goto et al., 2011). The percentage of identity of BgAQP with PvAQP1, AgAQP1, BaAQP1 and EsAQP1, all four from dipteran species, falls between 38% and 41%. All the amino acid sequences show the typical P1-P5 and ar/R residues conserved in water-selective AQPs, but they lack the Cys upstream of the second NPA motif considered as the mercurial sensitive-site of some vertebrate AQPs.

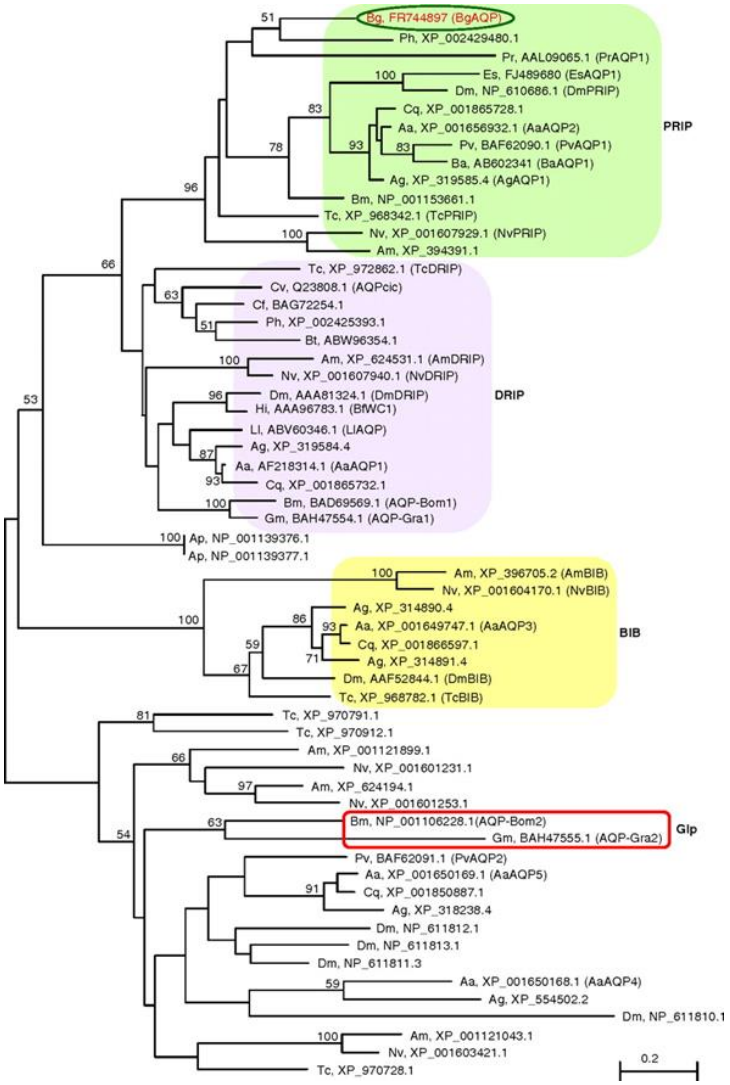

Figure 3.1: Maximum-likelihood phylogenetic tree showing the position of Blattella germanica aquaporin (BgAQP, ringed) with respect to other insect AQPs. Scale bar represents the number of amino acid substitutions per site. Numbers at the nodes are bootstrap values (only bootstrap values >50 are shown). The sequences are indicated by the initials of the scientific name of the species, followed by the accession number and, in parentheses, the acronym commonly used, if any. Complete binomial names of the species are indicated in Materials and methods. The PRIP (*Pyrocoelia rufa* integral protein), DRIP (*Drosophila* integral protein) and BIB (neurogenic gene *Drosophila* big brain) nodes are indicated. BgAQP falls into the PRIP node. Also indicated are the aquaglyceroporins (Glp) AQP-Bom2 from *Bombyx mori* and AQP-Gra2 from *Grapholita molesta*, in the node of non-classified AQPs.

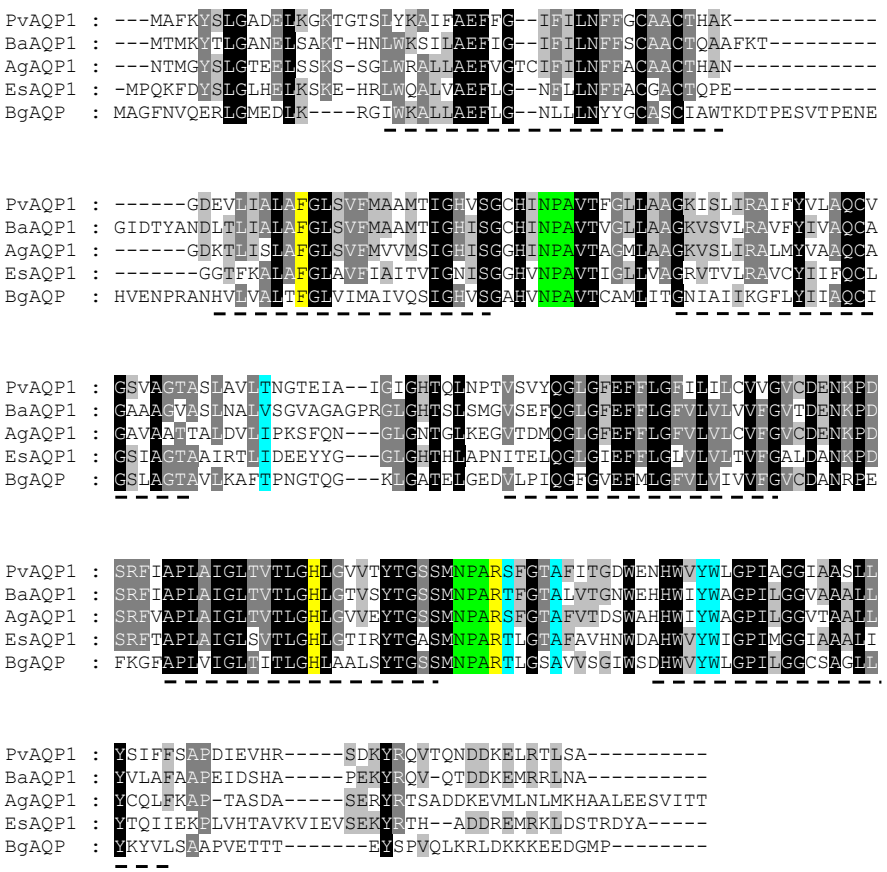

Figure 3.2: Amino acid sequence alignment of BgAQP from *B. germanica* with the four AQPs of the insect PRIP node that have been functionally characterized: BaAQP1 from *Belgica antarctica* (AB602340), which transports water but not glycerol or urea (Goto et al., 2011), PvAQP1 from *Polypedilum vanderplanki* (BAF62090.1), which transports water but not glycerol (urea transport was not studied) (Kikawada et al., 2008), and AgAQP1 from *Anopheles gambiae* (XP_319585.4) and EsAQP1 from *Eurosta solidaginis* (FJ489680), which transport water (Liu et al., 2011; Philip et al., 2011). Fully conserved amino acids are shaded in black, whereas conserved substitutions are shaded in grey. The transmembrane domains of BgAQP are underlined, and the NPA motifs are highlighted in green. The amino acids typically conserved in water-selective AQPs in the ar/R constriction region (de Groot et al., 2003) and in positions P1–P5 (Froger et al., 1998) are shaded in yellow and blue, respectively.

c) Water and solute permeability of BgAQP expressed in *X. laevis* oocytes

To study whether the BgAQP effectively transports water, the cRNA was ectopically expressed in *X. laevis* oocytes. Forty-eight hours after cRNA microinjection, oocytes were transferred to a hypo-osmotic medium and oocyte swelling determined. These experiments indicated that water permeability of oocytes expressing 10 ng BgAQP cRNA was 18-fold higher than that of control (water-injected) oocytes (Figure 3.3A). Despite that BgAQP does not show a Cys residue preceding the second NPA motif, pre-incubation of oocytes with 1 mM $HgCl_2$ reduced significantly ($p < 0.05$) the P_f of BgAQP-expressing oocytes, and this inhibition was partially reversed with the reducing agent β-mercaptoethanol (Figure 3.3A).

To investigate if BgAQP is a water-selective AQP, as other members of the PRIP group of insect AQPs, glycerol and urea permeability of oocytes expressing BgAQP were analyzed by radioactive solute uptake assays. For these experiments, we used oocytes expressing 25 ng BgAQP cRNA, as well as negative and positive control oocytes expressing human AQP1 or AQP3, respectively, to discriminate better if BgAQP was able to transport solutes. The results confirmed that BgAQP-expressing oocytes did not transport glycerol significantly (Figure 3.3B). However, urea was incorporated at slightly but significantly ($p < 0.05$) higher levels in oocytes expressing BgAQP than in water-injected oocytes or in oocytes expressing human AQP1 (negative control). These

data indicated that BgAQP can transport urea, although in much lower amounts than human AQP3 (positive control) (Figure 3.3C).

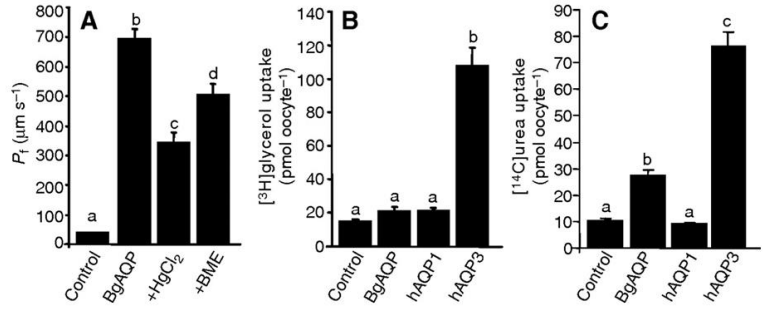

Figure 3.3: Water and solute permeability of BgAQP expressed in *X. laevis* oocytes. (A) Osmotic water permeability (Pf) of oocytes injected with water (control) or expressing 10 ng BgAQP cRNA. Water permeability was inhibited with 1 mmol l–1 HgCl2 and reversed with 5 mmol l–1 β-mercaptoethanol (BME) (N=12 oocytes). (B,C) Radioactive glycerol (B) and urea (C) uptake by control oocytes and oocytes expressing 25 ng cRNA encoding BgAQP, human AQP1 (hAQP1) or human AQP3 (hAQP3) (N=10–12 oocytes). In each histogram, different letters at the top of the columns indicate significant differences (t-test, P<0.001). Data are expressed as the mean ± s.e.m.

d) mRNA expression of BgAQP in the ovary during adult development

First of all, although the BgAQP was isolated from ovarian tissue, we were interested in assessing whether it was ovary-specific. Thus, we analyzed by qRT-PCR the BgAQP mRNA expression in ovary, fat body, muscle, digestive tract, Malpighian tubules and colleterial glands collected from 3-day-old adult females. Results indicated that the highest levels of BgAQP mRNA were observed in ovaries;

lower expression was detected in fat body and muscle tissues, whereas it was almost undetectable in colleterial glands, digestive tract or Malpighian tubules (Figure 3.4A).

Then, we studied the expression pattern of BgAQP in the ovary. Thus, total RNA was isolated from pools of four to six ovary pairs collected from animals at selected ages and stages, and mRNA levels were analyzed by qRT-PCR. Then, we determined the expression of BgAQP in the ovaries during the transition from 6th nymphal instar to adult, and thereafter during the 7 days of the first gonadotrophic cycle of the adult. Results (Figure 3.4B) showed that BgAQP transcript levels are moderate (ca. 35 copies of BgAQP per 1,000 copies of BgActin-5c) during the last two days of the 6th nymphal instar. Then they increase ca. 2-fold in freshly emerged adults, and decrease thereafter (5-20 copies of BgAQP per 1,000 copies of BgActin-5c) between day 1 and day 7, in the stage of late chorion formation (D7lc) (Figure 3.4B).

In order to study whether BgAQP could play a role in the ovary under water stress, we conducted a water-deprivation experiment. Adult females of *B. germanica* were provided with food and water *ad libitum* during the first three days of adult life, and water was then removed. Under these conditions, the specimens underwent basal oocyte resorption from day 5. Using this experimental design, we measured ovarian BgAQP mRNA levels by qRT-PCR on days 4, 5, 6 and 7 of the first gonadotrophic cycle in control and water-stressed adult specimens. Although the results (Figure 3.4C)

showed a slight increase of BgAQP mRNA levels in water-stressed specimens at day 4 and 6, the differences were not statistically significant.

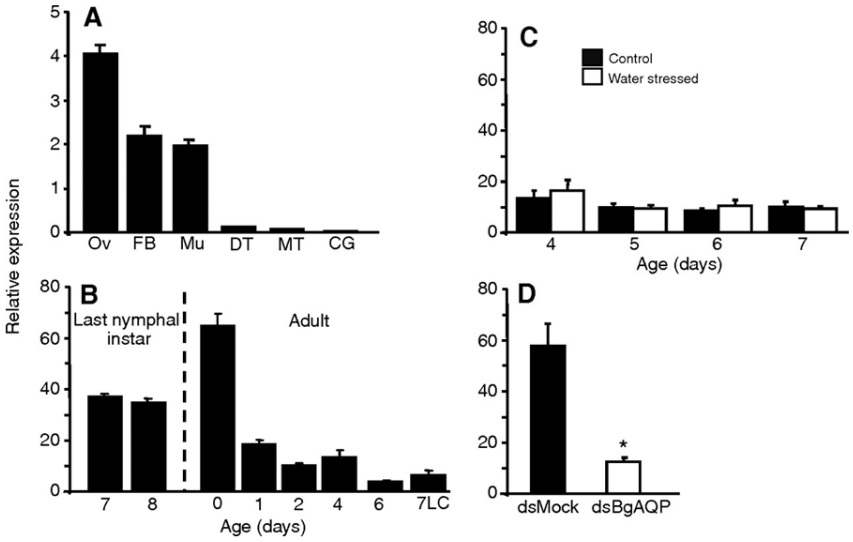

Figure 3.4: Expression of BgAQP. (A) Expression in different tissues from 3 day old females (Ov, ovary; FB, fat body; Mu, muscle; DT, digestive tract; MT, Malpighian tubules; CG, colleterial glands). (B) Expression in the ovary during the last 2 days of 6th nymphal instar (days 7 and 8), and during the first gonadotrophic cycle (days 0 to 7LC; LC, late choriogenesis stage). (C) Expression in the ovary of water-stressed females. Females were water deprived on day 3 of adult age, and ovaries were dissected on days 4, 5, 6 or 7, in order to measure BgAQP mRNA levels. Control females were maintained with water *ad libitum*. (D) Expression in dsMock- and dsBgAQP-treated specimens in RNAi experiments. The asterisk indicates that the difference between the two is statistically significant ($P<0.0001$). Treatments were carried out on freshly emerged 6th (last) instar nymphs, and measurements were taken from freshly emerged adults. Data represent the number of copies per 1000 copies of BgActin-5c, and are expressed as the mean + s.e.m. (N=3).

e) RNAi experiments

To investigate the role of BgAQP, the expression of BgAQP was silenced by RNAi and the phenotype determined. For these experiments, dsBgAQP was injected in freshly emerged 6th instar female nymphs, and controls were injected with dsMock in the same conditions. The objective was to deplete the peak of BgAQP mRNA occurring in ovaries of freshly emerged adults (Figure 3.4B), which might be functionally important, for example to avoid desiccation immediately after molting. Just after the imaginal moult, BgAQP mRNA levels in dsBgAQP-treated specimens were 12.19 ± 1.22 copies per 1,000 copies of BgActin-5c, whereas in dsMock-treated they were 55.34 ± 8.17 copies per 1,000 copies of BgActin-5c (Figure 3.4D), which indicates that BgAQP mRNA levels were reduced ca. 80% by the RNAi. Statistically, according to REST-2008 (Pfaffl et al., 2002), BgAQP was down-regulated in ovaries from dsBgAQP-treated specimens by a mean factor of 0.223 ($p < 0.0001$). The duration of the 6th nymphal instar was 8 days, either in dsBgAQP-treated as in controls, and the imaginal moult proceeded normally. After the moult, we added a mature male per female, and we studied the female first reproductive cycle. The number of days until the formation of the first ootheca was 7 in both, treated and controls, and most of the mated females formed the ootheca correctly (10 out of 11 in dsBgAQP-treated and 7 out of 7 in controls). All ootheca were viable, and the duration of embryogenesis was similar in controls and treated, ca. 18 days. The number of nymphs hatched per ootheca were 40.71 ± 4.07 in

controls (n = 7), and 36.36 ± 9.24 in treated (n = 10), differences that were not statistically significant.

3.5. Discussion

We have isolated and functionally characterized a novel AQP from the ovary of the cockroach *B. germanica*, which has been named BgAQP. Its deduced amino acid sequence shows the characteristic structural features of AQPs. BgAQP has the ar/R constriction and P1-P5 residues typically conserved in water-specific AQPs (Beitz et al., 2006; Froger et al., 1998). Accordingly, BgAQP effectively transported water when expressed in *X. laevis* oocytes, and this transport was inhibited by mercury chloride ($HgCl_2$) and recovered with β-mercaptoethanol, as it occurs for other AQPs (Yukutake et al., 2008). Site-directed mutations on human AQP1 have revealed that the Cys^{189}, located three amino acids upstream of the second NPA in loop E, is the mercury-sensitive site (Preston et al., 1993). However, it has been shown that the absence of Cys^{198} does not prevent inhibition of water flux by mercury (Daniels et al., 1996; Tingaud-Sequeira et al., 2008; Yukutake et al., 2008), which implies that sensitivity of AQPs to mercurial compounds may involve other residues in addition to Cys^{189}. BgAQP lacks a Cys residue near the second NPA box, but it has a Cys residue shortly downstream of the first NPA in loop B (Cys^{98}). This residue could be a good candidate as the site for mercurial inhibition in BgAQP since it locates in a similar spatial position than Cys^{189} in AQP1.

Other insect AQPs lacking a Cys residue on loop E, such as PvAQP1 or EsAQP1, are also mercury-sensitive and similarly to BgAQP they have a candidate Cys in loop B (Duchesne et al., 2003; Kikawada et al., 2008; Philip et al., 2011).

In our study, radioactive solute uptake assays showed that BgAQP is not permeable to glycerol but it is able to transport low amounts of urea. To date, two insect AQPs from lepidopteran larvae show glycerol and urea uptake: AQP-Bom2 and AQP-Gra2, which have been classified as typical aquaglyceroporins (Kataoka et al., 2009a; Kataoka et al., 2009b). BgAQP cannot be classified as an aquaglyceroporin because does not transport glycerol, does not show the residues in the ar/R constriction region conserved in aquaglyceroporins, and is phylogenetically distant from AQP-Bom2 and AQP-Gra2. Our data therefore indicate that BgAQP is the first reported insect AQP from the PRIP group that shows water and urea permeability. This feature has only been described so far for some teleost AQP paralogs related to mammalian AQP8 (Tingaud-Sequeira et al., 2010), which is water and ammonia permeable (Litman et al., 2009). The structural basis of BgAQP for water and urea permeability, while excluding that of glycerol, is yet unknown as it occurs for teleost Aqp8s (Cerdà and Finn, 2010; Tingaud-Sequeira et al., 2010). Nevertheless, the permeability of BgAQP to urea may be physiologically relevant because a metabolic complementation for nitrogen metabolism appears to exist between *B. germanica* and their endosymbiont *B. cuenoti* through the combination of a urea cycle (host) and urease activity (endosymbiont) (Lopez-Sanchez et al., 2009).

The phylogenetic analyses reported by Campbell et al. (2008), followed by Mathew et al. (2011) grouped insect AQPs into four groups: DRIP, PRIP, BIB, and non-classified AQPs, the latter being the sister group of the other three. Parallel studies carried out by Kambara et al. (2009), followed by Goto et al. (2011), resulted in a tree with a topology similar to that reported by Campbell et al. (2008), although the main nodes were not nominated but simply numbered. However, the PRIP and DRIP nodes of Campbell et al. (2008) are recovered in the "Group 1" of Kambara et al. (2009) and Goto et al. (2011). The tree obtained in our study shows the same topology of these studies, and consistently clusters the BgAQP sequence into the PRIP node. This node appears functionally heterogeneous given that it contains a member that transports water and urea, such as BgAQP, and other members that are apparently water-selective, namely EsAQP1 (Philip et al., 2011), AgAQP1 (Liu et al., 2011), PvAQP1 (Kikawada et al., 2008) and BaAQP1 (Goto et al., 2011). However, the ability of PvAQP1 and AgAQP1 to transport urea has not been investigated (Kikawada et al., 2008; Liu et al., 2011), whereas other PRIP members have not been functionally studied at all. Therefore, the possibility that other members of this node can transport urea, as BgAQP does, remains to be determined.

Expression analyses indicated that BgAQP mRNA was accumulated in fat body, muscle and ovarian tissues, although the highest transcript levels were observed in the ovary. Another AQP primarily expressed in the ovary has been described in the

American dog tick, *Dermacentor variabilis* (Say) (Holmes et al., 2008), which has been speculated that may function in lipid metabolism and/or water transport. However, no experimental studies have been carried out with this AQP, beyond the functional expression in *X. laevis* oocytes. In the yellow fever mosquito, *A. aegypti*, 6 AQPs have been characterized, and one of them, namely AaAQP2, is strongly expressed in ovaries (as well as in the Malpighian tubules and the midgut) (Drake et al., 2010). Nevertheless, specific knockdown of AaAQP2 through RNAi, although significantly decreased the corresponding transcript levels, did not give any noticeable phenotype (Drake et al., 2010). In teleosts, a functional AQP1-related water channel has been described in oocytes where it plays a role during oocyte hydration prior to ovulation (Fabra et al., 2005; Zapater et al., 2011). During vitellogenesis, basal oocytes of *B. germanica* increase in size exponentially due to the incorporation of yolk precursors and water (Belles et al., 1987; Ciudad et al., 2006; Martín et al., 1995), and AQPs may be involved in oocyte water balance during this process. Concerning the expression pattern in the ovary, BgAQP mRNA levels show a peak in freshly emerged adult females, which suggest that most of the BgAQP mRNA necessary for the first reproductive cycle is produced just after the imaginal moult, and then their translation is regulated according to the protein needs.

To investigate the functions of BgAQP in the ovary of *B. germanica*, we monitored its expression in water-stressed specimens. The hypothesis was that water deprivation would

modify the expression of BgAQP in the ovary, since one the earliest consequences of water stress in *B. germanica* is the resorption of the oocytes. However, despite the fact that the ovaries from water-stressed specimens started basal oocyte resorption 48 h after water deprivation, no significant differences were observed in the levels of BgAQP mRNA in the ovary between control and water-stressed specimens. AQPs are regulated post-translationally by phosphorylation-dependent gating and especially by trafficking of the protein between the plasma membrane and the intracellular storage vesicle (Törnroth-Horsefield et al., 2010), thus, the effects of water stress on BgAQP may not be evident at the mRNA level.

As a further approach to investigate the role of BgAQP in the ovary, we performed RNAi experiments. *B. germanica* is very sensitive to RNAi (Belles, 2010), and expression of membrane-associated proteins has been successfully silenced (Ciudad et al., 2006). The timing of the treatment was designed to deplete the peak of ovarian BgAQP mRNA that occurs in freshly emerged adults, and it was efficiently depleted (by 80%) by our RNAi experiments. However, no phenotypic differences were observed. These results are reminiscent of those obtained on *A. aegypti* (see above), where RNAi of AaAQP2, a mosquito AQP strongly expressed in the ovary, did not result in phenotypical effects (Drake et al., 2010). The most parsimonious explanation for these results is that there must be other ovarian AQPs in *B. germanica*, not affected by our RNAi experiments that play functions redundant with BgAQP. Indeed, an insect as successful as *B. germanica*, arguably well

adapted to xeric environments (Appel, 1995), is likely to have robust and redundant mechanisms to regulate water balance.

3.6. Acknowledgements

We are grateful to Javier Igea for his help with the phylogenetic analyses. Financial support from the Spanish Ministry of Science and Innovation (projects BFU2008-00484 to M-D. Piulachs, CGL2008-03517/BOS to X. Belles, and AGL2010-15597 to J. Cerdà), Generalitat de Catalunya (2005 SGR 00053), and LINC-Global is gratefully acknowledged. A. Herraiz received a pre-doctoral research grant (JAE-LINCG program) from CSIC. F. Chauvigné was supported by a postdoctoral fellowship from Juan de la Cierva Programme (Spanish Ministry of Science and Innovation). Thanks are also due to David L. Denlinger and Shin G. Goto for providing us with the sequence of BaAQP1 that was used in our phylogenetical analyses.

3.7. References

Appel, A. G. (1995). *Blattella* and related species. In *Understanding and controlling the German cockroach*, (eds. M. K. Rust J. M. Owens and D. A. Reierson), pp. 1-20. New York: Oxford University Press.

Bates, P. A., Kelley, L. A., MacCallum, R. M. and Sternberg, M. J. (2001). Enhancement of protein modeling by human intervention in applying the automatic programs 3D-JIGSAW and 3D-PSSM. *Proteins* **Suppl 5**, 39-46.

Beitz, E., Wu, B., Holm, L. M., Schultz, J. E. and Zeuthen, T. (2006). Point mutations in the aromatic/arginine region in aquaporin 1 allow passage of urea, glycerol, ammonia, and protons. *Proc Natl Acad Sci U S A* **103**, 269-74.

Belles, X. (2010). Beyond *Drosophila*: RNAi in vivo and functional genomics in insects. *Annu Rev Entomol* **55**, 111-28.

Belles, X., Casas, J., Messeguer, A. and Piulachs, M. D. (1987). *In vitro* biosynthesis of JH III by the corpora allata of *Blattella germanica* (L.) adult females. *Insect Biochem.* **17**, 1007-1010.

Blom, N., Gammeltoft, S. and Brunak, S. (1999). Sequence and structure-based prediction of eukaryotic protein phosphorylation sites. *J Mol Biol* **294**, 1351-62.

Blom, N., Sicheritz-Ponten, T., Gupta, R., Gammeltoft, S. and Brunak, S. (2004). Prediction of post-translational glycosylation and phosphorylation of proteins from the amino acid sequence. *Proteomics* **4**, 1633-49.

Büning, J. (1994). The insect ovary. Ultrastructure, previtellogenic growth and evolution. London: Chapman & Hall.

Campbell, E. M., Ball, A., Hoppler, S. and Bowman, A. S. (2008). Invertebrate aquaporins: a review. *J Comp Physiol [B]* **178**, 935-55.

Cerdà, J. and Finn, R. N. (2010). Piscine aquaporins: an overview of recent advances. *J Exp Zool A Ecol Genet Physiol* **313**, 623-50.

Ciudad, L., Piulachs, M. D. and Belles, X. (2006). Systemic RNAi of the cockroach vitellogenin receptor results in a phenotype similar to that of the *Drosophila* yolkless mutant. *FEBS J* **273**, 325-35.

Daniels, M. J., Chaumont, F., Mirkov, T. E. and Chrispeels, M. J. (1996). Characterization of a new vacuolar membrane aquaporin sensitive to mercury at a unique site. *Plant Cell* **8**, 587-99.

de Groot, B. L., Frigato, T., Helms, V. and Grubmuller, H. (2003). The mechanism of proton exclusion in the aquaporin-1 water channel. *J Mol Biol* **333**, 279-93.

Deen, P. M., Verdijk, M. A., Knoers, N. V., Wieringa, B., Monnens, L. A., van Os, C. H. and van Oost, B. A. (1994). Requirement of human renal water channel aquaporin-2 for vasopressin-dependent concentration of urine. *Science* **264**, 92-5.

Drake, L. L., Boudko, D. Y., Marinotti, O., Carpenter, V. K., Dawe, A. L. and Hansen, I. A. (2010). The Aquaporin gene family of the yellow fever mosquito, *Aedes aegypti*. *PLoS One* **5**, e15578.

Duchesne, L., Hubert, J. F., Verbavatz, J. M., Thomas, D. and Pietrantonio, P. V. (2003). Mosquito (*Aedes aegypti*) aquaporin, present in tracheolar cells, transports water, not glycerol, and forms orthogonal arrays in *Xenopus* oocyte membranes. *Eur J Biochem* **270**, 422-9.

Echevarria, M., Ramirez-Lorca, R., Hernandez, C. S., Gutierrez, A., Mendez-Ferrer, S., Gonzalez, E., Toledo-Aral, J. J., Ilundain, A. A. and Whittembury, G. (2001). Identification of a new water channel (Rp-MIP) in the Malpighian tubules of the insect *Rhodnius prolixus*. *Pflugers Arch* **442**, 27-34.

Fabra, M., Raldua, D., Power, D. M., Deen, P. M. and Cerdà, J. (2005). Marine fish egg hydration is aquaporin-mediated. *Science* **307**, 545.

Froger, A., Tallur, B., Thomas, D. and Delamarche, C. (1998). Prediction of functional residues in water channels and related proteins. *Protein Sci* **7**, 1458-68.

Giorgi, F. and Nordin, J. H. (1994). Structure of yolk granules in oocytes and eggs of Blattella germanica and their interaction with vitellophages and endosymbiotic bacteria during granule degradation. *J Insect Physiol* **40**, 1077-1092.

Gomes, D., Agasse, A., Thiebaud, P., Delrot, S., Geros, H. and Chaumont, F. (2009). Aquaporins are multifunctional water and solute transporters highly divergent in living organisms. *Biochim Biophys Acta* **1788**, 1213-28.

Goto, S. G., Philip, B. N., Teets, N. M., Kawarasaki, Y., Lee, R. E., Jr. and Denlinger, D. L. (2011). Functional characterization of an aquaporin in the Antarctic midge *Belgica antarctica*. *J Insect Physiol* **57**, 1106-14.

Hirano, Y., Okimoto, N., Kadohira, I., Suematsu, M., Yasuoka, K. and Yasui, M. (2010). Molecular mechanisms of how mercury inhibits water permeation through aquaporin-1: understanding by molecular dynamics simulation. *Biophys J* **98**, 1512-9.

Holmes, S. P., Li, D., Ceraul, S. M. and Azad, A. F. (2008). An aquaporin-like protein from the ovaries and gut of American dog tick (Acari: Ixodidae). *J Med Entomol* **45**, 68-74.

Jung, J. S., Preston, G. M., Smith, B. L., Guggino, W. B. and Agre, P. (1994). Molecular structure of the water channel through aquaporin CHIP. The hourglass model. *J Biol Chem* **269**, 14648-54.

Kambara, K., Takematsu, Y., Azuma, M. and Kobayashi, J. (2009). cDNA cloning of aquaporin gene expressed in the digestive tract of the Formosan subterranean termite, *Coptotermes formosanus* Shiraki (Isoptera: Rhinotermitidae). *Appl. Entomol. Zool.* **44**, 315-321.

Kataoka, N., Miyake, S. and Azuma, M. (2009a). Aquaporin and aquaglyceroporin in silkworms, differently expressed in the hindgut and midgut of *Bombyx mori*. *Insect Mol Biol* **18**, 303-14.

Kataoka, N., Miyake, S. and Azuma, M. (2009b). Molecular characterization of aquaporin and aquaglyceroporin in the alimentary canal of *Grapholita molesta* (the oriental fruit moth) - comparison with *Bombyx mori* aquaporins. *J. Insect Biotechnol. Sericol.* **78**, 2_81-2_90.

Kaufmann, N., Mathai, J. C., Hill, W. G., Dow, J. A., Zeidel, M. L. and Brodsky, J. L. (2005). Developmental expression and biophysical characterization of a *Drosophila melanogaster* aquaporin. *Am J Physiol Cell Physiol* **289**, C397-407.

Kikawada, T., Saito, A., Kanamori, Y., Fujita, M., Snigorska, K., Watanabe, M. and Okuda, T. (2008). Dehydration-inducible changes in expression of two aquaporins in the sleeping chironomid, *Polypedilum vanderplanki*. *Biochim Biophys Acta* **1778**, 514-20.

King, L. S., Kozono, D. and Agre, P. (2004). From structure to disease: the evolving tale of aquaporin biology. *Nat Rev Mol Cell Biol* **5**, 687-98.

Krogh, A., Larsson, B., von Heijne, G. and Sonnhammer, E. L. (2001). Predicting transmembrane protein topology with a hidden Markov model: application to complete genomes. *J Mol Biol* **305**, 567-80.

Le Caherec, F., Deschamps, S., Delamarche, C., Pellerin, I., Bonnec, G., Guillam, M. T., Thomas, D., Gouranton, J. and Hubert, J. F. (1996). Molecular cloning and characterization of an insect aquaporin functional comparison with aquaporin 1. *Eur J Biochem* **241**, 707-15.

Letunic, I., Doerks, T. and Bork, P. (2009). SMART 6: recent updates and new developments. *Nucleic Acids Res* **37**, D229-32.

Litman, T., Sogaard, R. and Zeuthen, T. (2009). Ammonia and urea permeability of mammalian aquaporins. *Handb Exp Pharmacol*, 327-58.

Liu, K., Tsujimoto, H., Cha, S. J., Agre, P. and Rasgon, J. L. (2011). Aquaporin water channel AgAQP1 in the malaria vector mosquito *Anopheles gambiae* during blood feeding and humidity adaptation. *Proc Natl Acad Sci U S A* **108**, 6062-6.

Lopez-Sanchez, M. J., Neef, A., Pereto, J., Patino-Navarrete, R., Pignatelli, M., Latorre, A. and Moya, A. (2009). Evolutionary convergence and nitrogen metabolism in *Blattabacterium* strain Bge, primary endosymbiont of the cockroach *Blattella germanica*. *PLoS Genet* **5**, e1000721.

Martín, D., Piulachs, M. D. and Belles, X. (1995). Patterns of haemolymph vitellogenin and ovarian vitellin in the German cockroach, and the role of juvenile hormone. *Physiol. Entomol.* **20**, 59-65.

Mathew, L. G., Campbell, E. M., Yool, A. J. and Fabrick, J. A. (2011). Identification and characterization of functional aquaporin water channel protein from alimentary tract of whitefly, *Bemisia tabaci*. *Insect Biochem Mol Biol* **41**, 178-90.

Maurel, C., Verdoucq, L., Luu, D. T. and Santoni, V. (2008). Plant aquaporins: membrane channels with multiple integrated functions. *Annu Rev Plant Biol* **59**, 595-624.

Murata, K., Mitsuoka, K., Hirai, T., Walz, T., Agre, P., Heymann, J. B., Engel, A. and Fujiyoshi, Y. (2000). Structural determinants of water permeation through aquaporin-1. *Nature* **407**, 599-605.

Pfaffl, M. W., Horgan, G. W. and Dempfle, L. (2002). Relative expression software tool (REST) for group-wise comparison and statistical analysis of relative expression results in real-time PCR. *Nucleic Acids Res* **30**, e36.

Philip, B. N., Kiss, A. J. and Lee, R. E., Jr. (2011). The protective role of aquaporins in the freeze-tolerant insect *Eurosta solidaginis*: functional characterization and tissue abundance of EsAQP1. *J Exp Biol* **214**, 848-57.

Preston, G. M., Jung, J. S., Guggino, W. B. and Agre, P. (1993). The mercury-sensitive residue at cysteine 189 in the CHIP28 water channel. *J Biol Chem* **268**, 17-20.

Rojek, A., Praetorius, J., Frokiaer, J., Nielsen, S. and Fenton, R. A. (2008). A current view of the mammalian aquaglyceroporins. *Annu Rev Physiol* **70**, 301-27.

Shakesby, A. J., Wallace, I. S., Isaacs, H. V., Pritchard, J., Roberts, D. M. and Douglas, A. E. (2009). A water-specific aquaporin involved in aphid osmoregulation. *Insect Biochem Mol Biol* **39**, 1-10.

Telfer, W. H. (2009). Egg formation in lepidoptera. *J Insect Sci* **9**, 1-21.

Tingaud-Sequeira, A., Calusinska, M., Finn, R. N., Chauvigné, F., Lozano, J. and Cerdà, J. (2010). The zebrafish genome encodes the largest vertebrate repertoire of functional aquaporins with dual paralogy and substrate specificities similar to mammals. *BMC Evol Biol* **10**, 38.

Tingaud-Sequeira, A., Chauvigné, F., Fabra, M., Lozano, J., Raldua, D. and Cerdà, J. (2008). Structural and functional divergence of two fish aquaporin-1 water channels following teleost-specific gene duplication. *BMC Evol Biol* **8**, 259.

Törnroth-Horsefield, S., Hedfalk, K., Fischer, G., Lindkvist-Petersson, K. and Neutze, R. (2010). Structural insights into eukaryotic aquaporin regulation. *FEBS Lett* **584**, 2580-8.

Yanochko, G. M. and Yool, A. J. (2002). Regulated cationic channel function in *Xenopus* oocytes expressing *Drosophila* big brain. *J Neurosci* **22**, 2530-40.

Yukutake, Y., Tsuji, S., Hirano, Y., Adachi, T., Takahashi, T., Fujihara, K., Agre, P., Yasui, M. and Suematsu, M. (2008). Mercury chloride decreases the water permeability of aquaporin-4-reconstituted proteoliposomes. *Biol Cell* **100**, 355-63.

Zapater, C., Chauvigné, F., Norberg, B., Finn, R. N. and Cerdà, J. (2011). Dual neofunctionalization of a rapidly evolving aquaporin-1 paralog reveals constrained and relaxed traits controlling channel function during meiosis resumption in marine teleosts. *Mol Biol Evol.* **in press**.

Zardoya, R. (2005). Phylogeny and evolution of the major intrinsic protein family. *Biol Cell* **97**, 397-414.

3.8. Supplementary material

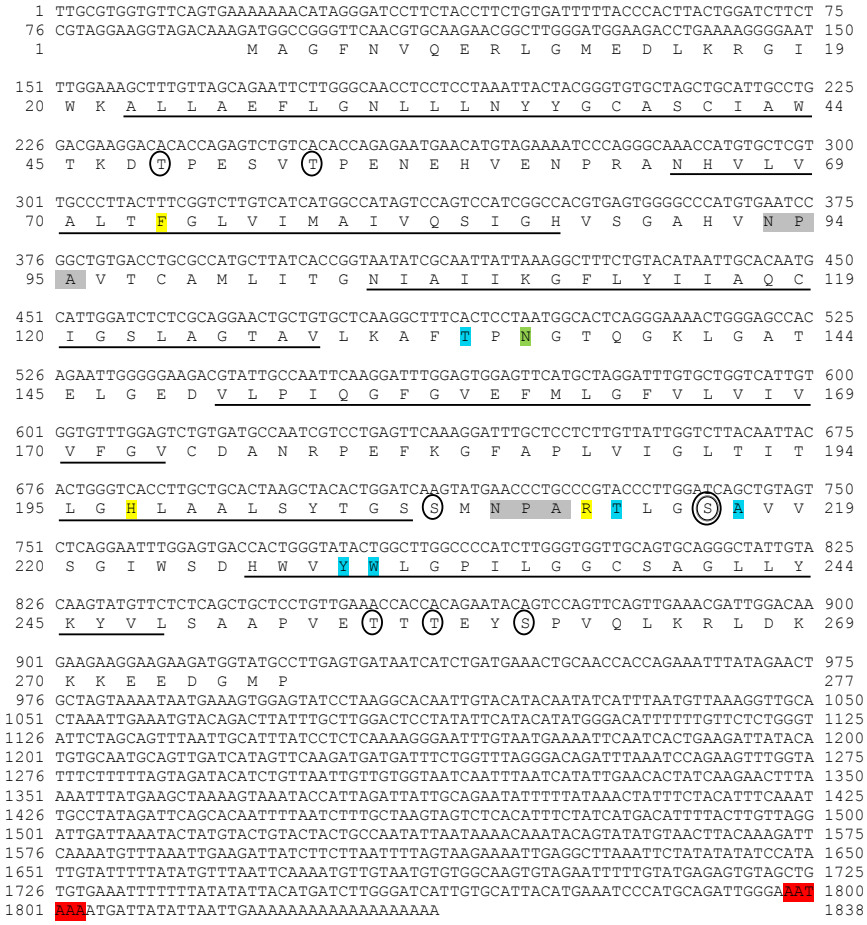

Figure 3.S1: Structural features of BgAQP. Nucleotide sequence and the deduced amino acid sequence. Domains are underlined; NPA motifs are in grey; circles represent putative phosphorylation sites; double circle represents putative PKC regulation site; a putative N-glycosylation site is indicated in green; in yellow are the amino acids forming the ar/R constriction; in blue the P1−P5 water-selective AQP conserved sites; in red the putative polyadenylation signal.

4. MicroRNAs EXPRESSED UNDER HYDRIC STRESS CONDITIONS IN *BLATTELLA GERMANICA* OVARIES

MicroRNAs expressed under hydric stress conditions in *Blattella germanica* ovaries

Alba Herraiz, Aníbal de Horna, Maria-Dolors Piulachs, Xavier Belles.

Institut de Biologia Evolutiva (CSIC-Universitat Pompeu Fabra), and LINCGlobal, Passeig Marítim de la Barceloneta 37-49. 08003 Barcelona, Spain.

4.1. Abstract

MicroRNAs (miRNAs) are small non coding RNAs that regulate gene expression at mRNA level. They are involved in numerous processes like morphogenesis, development, growth and apoptosis, and play key roles in stress responses. Here we explore whether miRNAs may be involved in hydric stress response in the ovary of the cockroach *Blattella germanica*. We have constructed a library of canonical miRNAs present in ovaries from females subjected to 48 h of hydric stress. Illumina sequencing resulted in 16,882,082 reads, which led to 26 canonical miRNAs after the filtering processes. We analysed the differential expression of 13 of them in ovaries of control and water-stressed females, and assessed an overexpression of most of them. Among the miRNAs overexpressed upon hydric stress, we selected miR-34-5p to perform a deeper study. We analysed miR-34-5p function in the ovary and studied a number of putative mRNA targets.

4.2. Introduction

MiRNAs are small endogenous non coding RNAs of about 22 nt in length that regulate gene expression at post-transcriptional level (Ambros, 2004; Bartel, 2004). Biogenesis of miRNAs starts with the transcription of a primary transcript (pri-miRNA), normally by RNApolymerase II (Lee et al., 2004). This product is then processed within the nucleus by the microprocessor complex, which contains the RNase III enzyme Drosha and the double-stranded

RNA-binding protein Pasha (DGCR8 in mammals and in the worm *Caenorhabditis elegans*). The microprocessor complex cleaves the pri-miRNA into a hairpin-structured pre-miRNA of about 70 nt in length that is exported to the cytoplasm by the Ran-GTP-dependent dsRNA-binding receptor Exportin-5 (Exp5). The pre-miRNA is then cleaved in the cytoplasm by the RNase III enzyme Dicer-1, which releases a duplex of about 22 nt composed by two strands, usually one is the mature miRNA and the other is the so-called passenger strand (or miRNA*) (reviewed by Bushati and Cohen, 2007; and Lucas and Raikhel, 2013). The duplex is then loaded into the RNA-induced silencing complex (RISC) through the protein Argonaute 1. The passenger strand is usually degraded and the mature miRNA guides the RISC to the target mRNA leading to translational inhibition or transcript degradation (Bartel, 2004). Because in some cases both strands give active miRNAs (Okamura et al., 2008; Ruby et al., 2007; Yang et al., 2011), miRNAs are nowadays known as miRNA-5p or miRNA-3p depending on its position in the pre-miRNA.

Mature miRNAs can modify their expression upon different biotic and abiotic stresses in invertebrates (Abbott, 2011; Freitak et al., 2012), in mammals (Hu et al., 2012; Lee et al., 2012) and in plants (Guleria et al., 2011; Zhu et al., 2013), thus revealing its important role in homeostasis maintenance in eukaryotic organisms. Among the best studied miRNAs that change their expression levels in stress conditions there is miR-34-5p. Upon diverse genotoxic stresses, miR-34-5p is up-regulated and promotes cell cycle arrest

and cell death by down-regulating target mRNAs involved in these pathways (reviewed by Thomas and Lieberman, 2013).

Our laboratory is interested in the regulation of oogenesis and reproduction in basal insects using the hemimetabolous species *Blattella germanica* as a model. We have seen that water stress in *B. germanica* females impairs reproductive processes by triggering perturbations related to basal follicle maturation, oocyte resorption, as well as delays in oviposition and ootheca formation. We wanted to know whether miRNAs play a role in these water stress-associated effects, and in the work described in the present chapter we intended to identify miRNAs expressed upon hydric stress in *B. germanica* ovary and to analyse their differential expression in control and water-stressed females.

4.3. Material and Methods

a) Insects

Freshly ecdysed *B. germanica* adult females were obtained from a colony reared in the dark at 29 ± 1°C and 60–70% relative humidity and fed with Panlab dog chow and water *ad libitum*. All dissections and tissue sampling were carried out on carbon dioxide-anaesthetized specimens. After dissection, ovaries were frozen on liquid nitrogen and stored at -80ºC until use. Control insects received food and water *ad libitum*.

b) Water stress induction and preparation of miRNA libraries

From the work described in chapter 2 we knew that when drinking water is supressed on the third day of the adult life, the female experiences ovarian resorption starting 48 h after the beginning of the stress. These experimental conditions were repeated for the present chapter: females were water-deprived 3 days after the imaginal moult, and ovaries were collected 48 h later (at day 5 of the adult life). An amount of 10 µg of total RNA was extracted from a pool of 10 ovaries from 5-day-old water-stressed females using miRNeasy Mini Kit (Qiagen, Venlo, Netherlands) according to manufacturer protocols. RNA quantity and quality were estimated by spectrophotometric absorption at 260 nm in a NanoDrop Spectrophotometer ND-1000 (NanoDrop Technologies, Wilmington, DE, USA). For high throughput miRNA sequencing, total RNA was sent to the Centre for Genomic Regulation (CRG) (Barcelona, Spain) for small RNAs isolation and sequencing.

c) Analysis of miRNA library data

Small RNA sequencing was performed with Illumina technology at the CRG. Sequences were received in FASTQ format, with the adaptor sequences trimmed. Filtering process was carried as reported elsewhere (Rubio et al., 2012). Briefly described, the process consisted in the following steps. First, those reads having 80% of the sequence with quality values lower than 20 were

eliminated. Second, low quality regions and regions containing repetitive nucleotides or short motifs were trimmed. Then, sequences with the same length were grouped and collapsed using the suite of programs Fastx-toolkit (http://hannonlab.cshl.edu/fastx_toolkit), and those sequences with 10-28 nucleotides were kept. To eliminate artefacts, sequences were mapped against Pfam database (excluding miRNAs), and against the genome sequences of *Blattabacterium cuenoti*, a bacteroid endosimbiont of *B. germanica* (Lopez-Sanchez et al., 2009), *B. germanica* densovirus (Mukha et al., 2006) and *Escherichia coli*. Positive-matched sequences were eliminated and the remaining sequences were considered putative miRNAs. Canonical miRNAs were identified by Bowtie alignment (Langmead et al., 2009) against mature miRNAs of the mirBASE database (November 2011 version) (Griffiths-Jones, 2004), and selected.

d) miRNA quantification

To quantify miRNAs expression levels, total RNA was extracted from 2 pools of 10 ovary pairs from 5-day-old adult females, one from control females, and the other from stressed ones, in the case of hydric stress experiment; and from isolated ovary pairs from 5, 6 and 7-day-old in the case of miR-34-5p knock-down experiment. The extraction was performed using miRNeasy Mini Kit. RNA quantity and quality were estimated by spectrophotometric absorption at 260 nm in a NanoDrop Spectrophotometer ND-1000. An amount of 400 ng from each RNA extraction was then reverse

transcribed using NCode miRNA First-Strand complementary DNA (cDNA) Synthesis (Life Technologies, Carlsbad, CA, USA). Quantitative real-time PCR (qRT-PCR) reactions were carried out using iQ SYBR Green Supermix (BioRad, Hercules, CA, USA) in an iQ5 Real-Time PCR Detection System (BioRad) using the following protocol: 95ºC for 2 min, 40 cycles of 95ºC for 15 s and 60ºC for 30 s. The following endogenous reference genes were used: ncRNA U6 for the studies of miRNAs expression under hydric stress compared to control conditions, ncRNA U2 for the miR-34-5p expression pattern, and BgActin-5c mRNA for miR-34-5p depletion experiments. All reactions were run in triplicate. Results are given as copies of RNA per 1000 copies of reference gene or using 1 as a reference value. Primer sequences are detailed in Supplementary Table 4.S1. Statistical analysis was performed using the Relative Expression Software Tool (REST) 2008 program (Pfaffl et al., 2002). All protocols were performed according to manufacturer instructions.

e) mRNA quantification

To quantify mRNAs expression, a sample of 400 ng of total RNA from each extraction was DNase treated (Promega, Madison, WI, USA) and reverse transcribed with Transcriptor First Strand cDNA Synthesis Kit (Roche Applied Science, Penzberg, Upper Bavaria, Germany). RNA quantity and quality were estimated by spectrophotometric absorption at 260 nm in a NanoDrop Spectrophotometer ND-1000. qRT-PCR reactions were carried out

using iQ SYBR Green Supermix in an iQ5 Real-Time PCR Detection System using the following protocol: 95°C for 10 min, and 40 cycles at 95°C for 15 s and 60°C for 60 s. BgActin-5c mRNA was used as reference gene. All reactions were run in triplicate. Results are given as copies of RNA per 1000 copies of BgActin-5c or using 1 as a reference value. Primer sequences are detailed in Supplementary Table 4.1. Statistical analysis was performed using the REST 2008. All protocols were performed according to manufacturer instructions.

f) miR-34-5p knock-down and target prediction

To study miR-34-5p function, freshly emerged adult females were treated injecting into the abdomen 1 µl of a solution 25 nM of miR-34-5p miRCURY LNA oligonucleotide (Exiqon, Vedbaek, Denmark) diluted in DEPC-treated water. Control specimens were injected with same volume and concentration of miRCURY LNA microRNA Inhibitor Negative Control A (Exiqon).

To predict miR-34-5p targets, an ovarian cDNA library from *B. germanica* previously obtained in our laboratory (Paula Irles, personal communication) was scanned with the RNAhybrid software (http://bibiserv.techfak.uni-bielefeld.de/rnahybrid/) (Rehmsmeier et al., 2004), filtering by energy cut off (-25) and helix constraint (nucleotides 2-8). Resulting sequences were blasted and functionally annotated with the Blast2GO software (http://www.blast2go.com/b2ghome) (Conesa et al., 2005).

4.4. Results

a) Ovarian miRNA library from water-stressed females

In order to identify which miRNAs are expressed in *B. germanica* ovaries under hydric stress conditions, we constructed a miRNA library, which was sequenced with Illumina technology. Ovaries from 5-day-old females that had been water-deprived for 48 h were used. After high throughput sequencing, 16,822,082 reads were obtained. These led to 1,776,962 unique sequences after the first filtering processes, which corresponded to 82 canonical miRNAs. Subsequently, the percentage of relative abundance of each miRNAs was calculated, and those under 0.1% of relative abundance were removed, thus 26 miRNAs were finally considered (Table 4.1). Of these, miR-1-3p was the most abundant miRNA, representing 64.5% of the total reads. MiR-275-3p and miR-279-3p followed in relative abundance (Figure 4.1, Table 4.1). Surprisingly, we found 4 canonical miRNAs that were not present in a previous ovarian miRNA library built in our laboratory (Cristino et al., 2011): miR-998-3p, miR-190-5p, miR-34-5p, and miR-317-3p. From these, miR-998-3p was the most represented (1.58% relative abundance), followed by miR-190-5p (0.68%). MiR-34-5p, and miR-317-3p presented similar relative abundance (0.18 and 0.17%, respectively).

Table 4.1: miRNAs present in the library obtained from ovaries of 5-day-old stressed females, number of reads of each miRNA, and their relative abundance (%).

Name	Sequence	Reads	Relative abundance (%)
miR-1-3p	**5'TGGAATGTAAAGAAGTATGGAG3'**	1,036,407	64.50
miR-275-3p	**5'TCAGGTACCTGAAGTAGCGCG3'**	122,578	7.63
miR-279-3p	**5'TGACTAGATCCACACTCATCCA3'**	83,636	5.21
miR-276-3p	**5'TAGGAACTTCATACCGTGCTCT3'**	71,070	4.42
miR-184-3p	**5'GACGGAGAACTGATAAGGGC3'**	56,215	3.50
miR-8-3p	**5'TAATACTGTCAGGTAAAGATGTC3'**	47,278	2.94
miR-8-5p	**5'CATCTTACCGGGCAGCATTAGA3'**	43,140	2.68
miR-998-3p	**5'TAGCACCATGGGATTCAGCT3'**	25,420	1.58
miR-31-5p	**5'GGCAAGATGTCGGCATAGCTG3'**	19,804	1.23
miR-92-3p	**5'AATTGCACTTGTCCCGGCCTGA3'**	18,266	1.14
miR-190-5p	**5'AGATATGTTTGATATTCTTGGTTG3'**	10,968	0.68
miR-283-5p	**5'AAATATCAGCTGGTAATTCT3'**	9,954	0.62
miR-2-3p	**5'TATCACAGCCAGCTTTGATGAGC3'**	8,021	0.50
let-7-5p	**5'TGAGGTAGTAGGTTGTATAGT3'**	6,685	0.42
miR-10-5p	**5'ACCCTGTAGATCCGAATTTGT3'**	6,694	0.42
miR-281-5p	**5'AAGAGAGCTATCCGTCGACAG3'**	5,659	0.35
miR-100-5p	**5'AACCCGTAGATCCGAACTTGTG3'**	5,702	0.35
miR-305-5p	**5'ATTGTACTTCATCAGGTGCTCTGG3'**	5,352	0.33
miR-276-5p	**5'AGCGAGGTATAGAGTTCCTACG3'**	4,955	0.31
miR-12-5p	**5'TGAGTATTACATCAGGTACTG3'**	3,608	0.22
bantam-3p	**5'TGAGATCATTGTGAAAGCTGATT3'**	3,291	0.20
miR-317-3p	**5'TGAACACAGCTGGTGGTATCTCA3'**	2,960	0.18
miR-34-5p	**5'TGGCAGTGTGGTTAGCTGGTTG3'**	2,808	0.17
miR-306-5p	**5'TCAGGTACTGAGTGACTCTGA3'**	2,749	0.17
miR-87-3p	**5'GTGAGCAAAGTTTCAGGTGTGT3'**	1,921	0.12
miR-263a-5p	**5'AATGGCACTGGAAGAATTCACGGA3'**	1,644	0.10

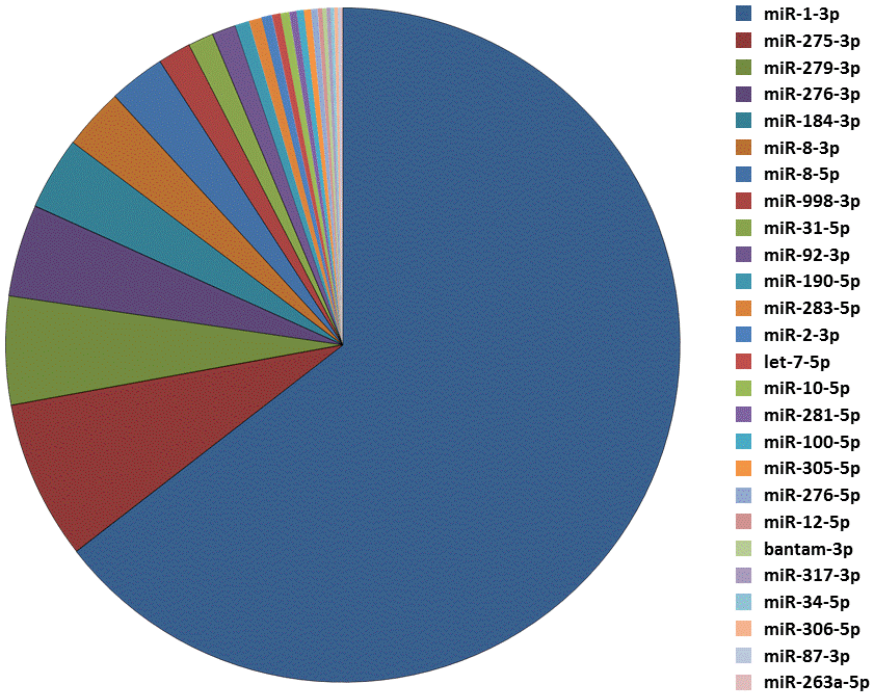

Figure 4.1: Graphical representation of the relative abundance (%) of each miRNA in the library obtained from ovaries of 5-day-old stressed females.

b) Selected miRNAs that are differentially expressed under hydric stress

A group of 13 miRNAs was chosen to analyse by qRT-PCR its expression in control and stressed ovaries from 5-day-old adult females. We included the 5 most abundant miRNAs (miR-1-3p, miR-275-3p, miR-279-3p, miR-276-3p and miR-184-3p) and the new 4 miRNAs that were not present in the previous ovarian miRNA library obtained in our laboratory (Cristino et al., 2011) (miR-998-3p, miR-190-5p, miR-34-5p, and miR-317-3p). We added let-7-5p and miR-100-5p because they have a high

expression level in *B. germanica* ovary (Tanaka and Piulachs, 2012); miR-276-5p was included in our selection in order to know whether both miR-276 strands had differences in expression under stress conditions; finally, we included bantam-3p because it has been described as an anti-apoptotic miRNA in the ovary of *D. melanogaster* (Brennecke et al., 2003; Shcherbata et al., 2007). As expected, most of these miRNAs were up-regulated in the ovary of specimens submitted to hydric stress, and the highest changes were observed in the following miRNAs: miR-1-3p (2.19 fold change), let-7-5p (1.79 fold change), miR-184-3p (1.72 fold change) and miR-34-5p (1.62 fold change). MiR-279-3p, miR-276-3p, miR-998-3p and miR-317-3p did not change their expression upon hydric stress, and only miR-276-5p showed a slight decrease (Figure 4.2). Among the up-regulated miRNAs, we selected miR-34-5p to perform a deeper study, as it has been described to promote cell cycle arrest and cell death upon diverse stress conditions (Kato et al., 2009; Tarasov et al., 2007).

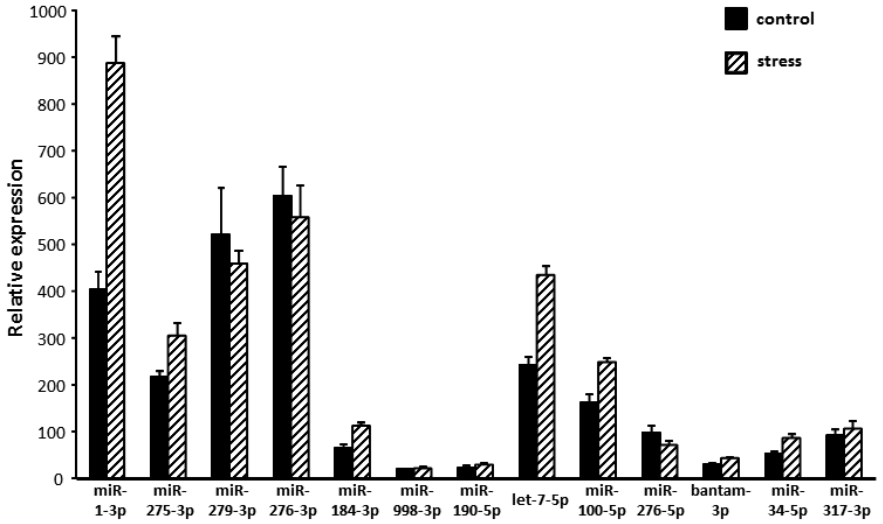

	miR-1-3p	miR-275-3p	miR-279-3p	miR-276-3p	miR-184-3p	miR-998-3p	miR-190-5p	let-7-5p	miR-100-5p	miR-276-5p	bantam-3p	miR-34-5p	miR-317-3p
control	403.4	216.4	521.2	604.4	65.5	19.4	22.9	242.7	163.1	98.5	31.5	53.1	93.9
stress	887.4	305.0	459.4	558.1	112.6	21.5	29.1	434.8	248.5	71.1	43.2	86.3	106.4

Figure 4.2: Relative expression of miRNAs in ovaries from 5-day-old females, controls (closed bars and top row on the legend) and subjected to 48 h of hydric stress (stripped bars and bottom row on the legend). qRT-PCR data are expressed as copies of miRNA per 1000 copies of U6± s.e.m., and represent a pool of 10 ovary pairs.

c) Expression pattern and function of miR-34-5p

Expression of miR-34-5p was measured in the ovary during the first gonadotrophic cycle, in the sixth (last) nymphal instar and in the adult. MiR-34-5p shows a peak of expression 24 h after entering in last nymphal instar. Later, expression decreases until the imaginal moult, when it starts increasing continuously and reaches the highest levels at the end of the gonadotrophic cycle, just before oviposition (Figure 4.3).

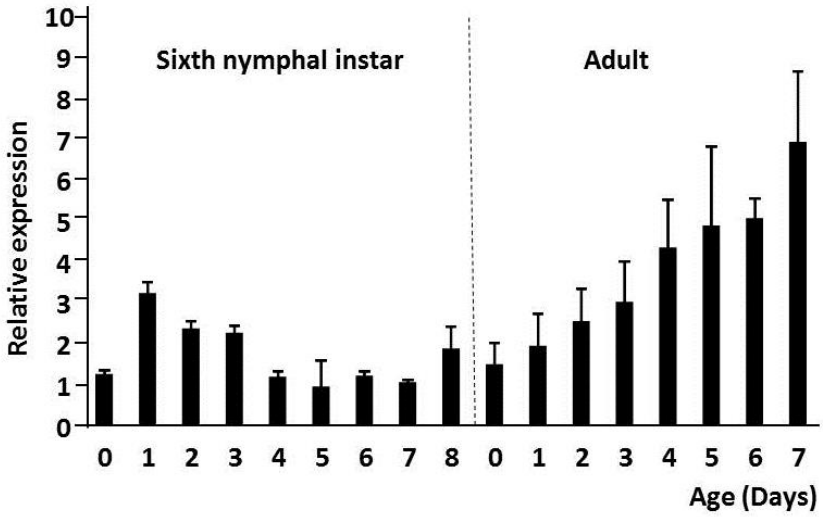

Figure 4.3: MiR-34-5p expression pattern in ovary during the sixth nymphal instar and the adult. qRT-PCR data represent 3 biological replicates and are expressed as copies of miR-34-5p per 1000 copies of U2 ± s.e.m..

To study the function of miR-34-5p in the ovary, we depleted the levels of this miRNA by injecting freshly emerged adult females with 1 μl of anti-miR-34-5p LNA oligonucleotide 25 nM. Control females were injected with the same volume and concentration of a negative LNA control. Ovaries from both groups were dissected 5, 6 and 7 days after the injection, and miR-34-5p expression was measured by qRT-PCR. MiR-34-5p expression was reduced in all three days studied (Figure 4.4), and the reduction was statistically significant on days 6 and 7 ($p<0.001$). Despite this reduction of miR-34-5p expression, ovaries from control and LNA anti-miR-34-5p-treated females were phenotypically indistinguishable (data not shown). To investigate whether miR-34-5p reduction affects reproduction, we left that control and miR-34-5p-depleted females oviposit and we kept the specimens under observation until egg

hatching. Although we observed a slight delay in the oviposition, the number of nymphs hatched per ootheca was very similar, and no statistical differences were observed between both groups (Table 4.2).

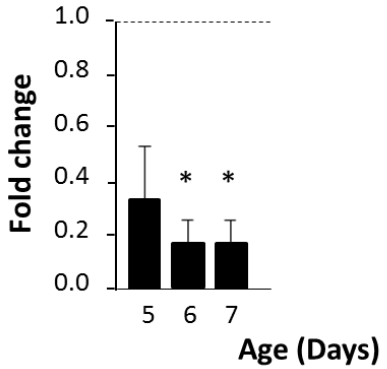

Figure 4.4: MiR-34-5p levels in ovaries from 5, 6 and 7-day-old adult females treated with LNA anti miR-34-5p at 0-day-old adult. qRT-PCR data represent 2-3 biological replicates and are normalized against control ovaries (reference value=1); expression of BgActin-5c was used as a reference and data are expressed as the mean ± s.e.m.. Asterisks mean statistically significant differences ($p<0.001$).

Table 4.2: Effects of miR-34-5p knockdown on reproduction. Percentage of females that oviposited and formed the ootheca in a given day (Day) and number of nymphs (Nymphs) that hatched from control and LNA anti-miR-34-5p-treated females, expressed as mean ± s.e.m.

Treatment	**Day**			**Nymphs**
	8	**9**	**10**	
Negative control (n=6)	33.3%	66.6%	-	44.17 ± 1.49
anti-miR-34-5p (n=9)	22.0%	56.0%	22.0%	42.75 ± 2.87

d) miR-34-5p putative targets

After knockdown experiments, we looked for putative mRNA targets of miR-34-5p as a way to infer the biological role of this particular miRNA. Using the RNAhybrid software, we predicted possible mRNAs targets for this miRNA, filtering by energy cut off (-25) and helix constraint (nucleotides 2-8). For this purpose, we used an ovarian cDNA library from *B. germanica* previously obtained in our laboratory. We obtained 28 sequences from the cDNA library that could be targets of miR-34-5p. Using the Blast2GO software, these sequences were blasted, and those with homology with a known transcript (22 from the 28 blasted) were functionally annotated with the same software, which extracted the Gene Ontology (GO) terms associated to each of the hits (Supplementary Table 4.S2). Sequences were distributed into the three GO categories: *biological process*, *molecular function* and *cellular component*. The most frequent GO term within *biological process* category was *primary metabolic process*, followed by *regulation of cellular process*; within molecular function category the most frequent GO term was *protein binding*; lastly, in the *cellular component* group the most frequent GO term was *cytoplasmic part*, although sequences were more equitably distributed than in the other two categories (Figure 4.5). Among these targets we selected 4 to perform a deeper analysis: the 3'-5' exoribonuclease CSL4-like protein (Csl4), which is included in the exosome, a structure involved in mRNA degradation that has

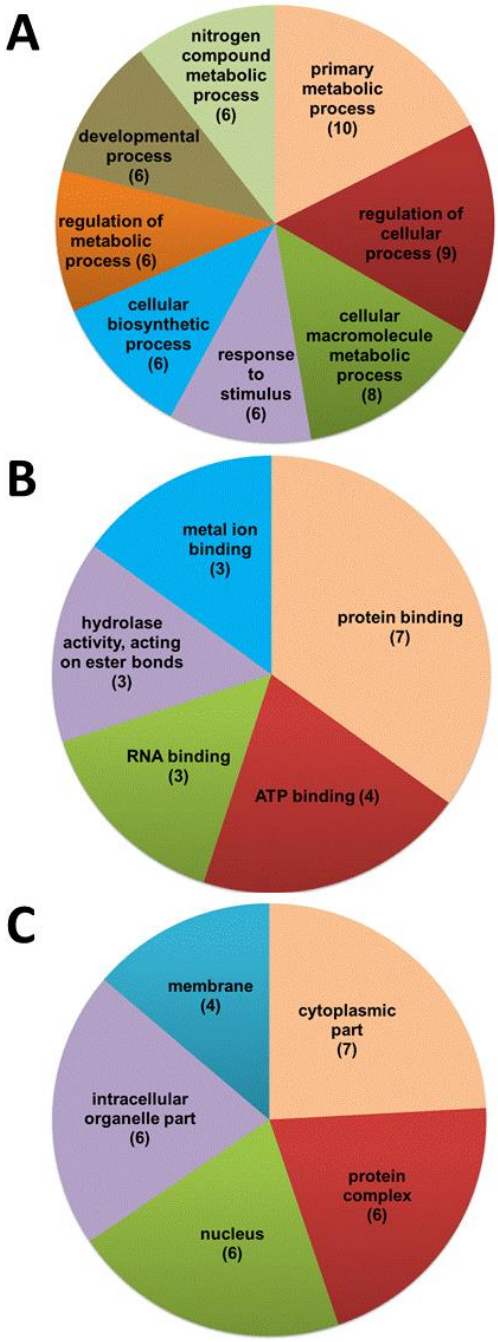

Figure 4.5: GO terms distribution of the miR-34-5p putative targets. **A)** Biological process. **B)** Molecular function. **C)** Cellular component. In all cases GO terms were filtered by sequence number, and the Cutoff was 6 (in A), 3 (in B) and 4 (in C).

been found in several eukaryotes and also in Archaea (Buttner et al., 2005); Limkain-b1 (Lkap), described as human autoantigen localized in peroxisomes (Dunster et al., 2005); Windei, which has been described as a cofactor for an histone methyltransferase in *D. melanogaster* (Koch et al., 2009) and the inhibitor of apoptosis-2 (Iap2), that has been cloned and sequenced in *B. germanica* but its function remains unknown (Mane-Padros et al., 2010). We analysed the expression patterns of these putative targets in adult ovary, and results showed that all four mRNAs have an expression pattern that appears opposite to that of miR-34-5p (Figure 4.6).

In order to know whether miR-34-5p levels affect the expression of these putative targets, we analysed the expression levels of all four mRNAs in control and miR-34-5p knocked down ovaries from 5-, 6- and 7-day-old adult females. Transcript levels of Csl4, Lkap and Iap2 remained invariable (Figure 4.7A,B,C), but Windei was up-regulated upon miR-34-5p depletion on day 5 and 7, the differences being statistically significant ($p<0.05$) in day 5 (Figure 4.7D).

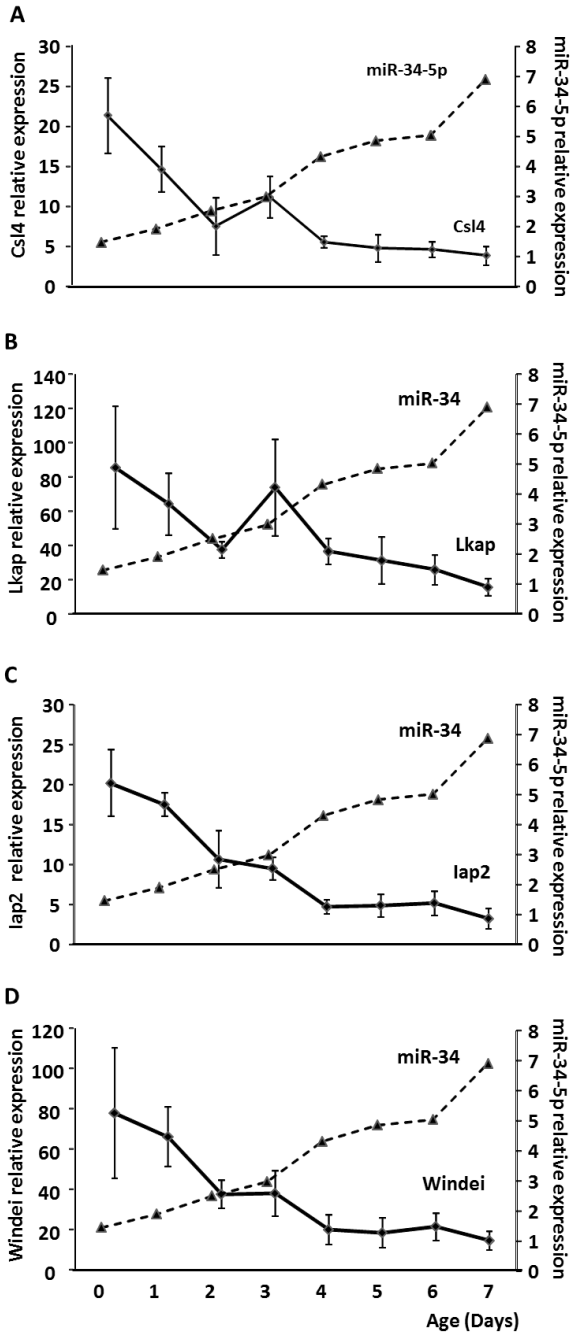

Figure 4.6: Expression patterns of miR-34-5p targets during the first gonadotrophic cycle in adult, expressed as copies per 1000 copies of BgActin-5c ± s.e.m. **A)** Csl-4. **B)** Lkap. **C)** Iap2. **D)** Windei. Dotted lines show the expression pattern of miR-34-5p, expressed as copies per 1000 copies of U2. Measurements represent 3 biological replicates.

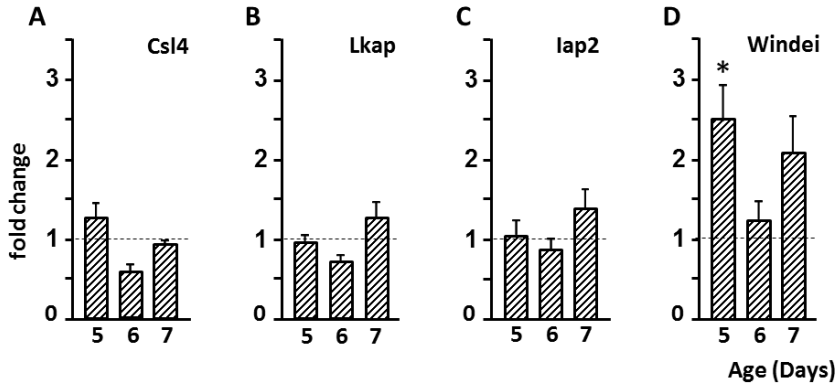

Figure 4.7: Levels of miR-34-5p putative targets after LNA anti miR-34-5-p treatment in ovaries from 5-, 6- and 7-day-old females. A) Csl-4. **B)** Lkap. **C)** Iap2. **D)** Windei. Data are normalized against the expression in control ovaries (reference value=1); expression of BgActin-5c was used as a reference. All measurements represent 3 biological replicates. Data is presented as the mean ± s.e.m.

4.5. Discussion

In the present chapter we describe the sequencing of a library of small RNAs using Illumina technology to investigate which miRNAs are present in *B. germanica* ovary upon hydric stress conditions. MiR-1-3p has appeared as the most abundant known miRNA in the ovary of water stressed 5-day-old adult females. It also appeared as the most abundant canonical miRNA in the ovary of adult *B. germanica* females (pool of all adult days) in a previous study performed in our laboratory (Cristino et al., 2011). MiR-1-3p is specifically expressed in mouse and human heart and skeletal muscle (Sempere et al., 2004), and in *D. melanogaster* it is expressed in muscle cells and is required for larval muscle growing (Sokol and Ambros, 2005). To our knowledge, no functions have been described so far for miR-1-3p in adult ovary, neither in

vertebrates nor in invertebrates. One possible explanation for the high abundance of this miRNA in *B. germanica* ovary could be related with the necessity of microtubules contraction for the oocyte growth, rotation and oviposition. This fact has been elegantly demonstrated in *D. melanogaster* (Viktorinova and Dahmann, 2013), and is presumably applicable to the ovary of other insect species.

Except for the fact that miR-1-3p is also the most abundant miRNA, the relative abundance of miRNAs in the ovarian library of water-stressed specimens differs from that previously described in normal ovarian libraries (Cristino et al., 2011): miR-275-3p and miR-279-3p appear as the most abundant miRNAs after miR-1-3p in the hydric stress library, while let-7-5p and miR-31-5p appeared as the most abundant miRNAs in the previous ovary library, after miR-1-3p. Under stress conditions, miR-184-3p has higher relative abundance, and miR-263a-5p is less represented. There are 4 miRNAs that appear in stress conditions that were not described previously: miR-998-3p, miR-190-5p, miR-34-5p, and miR-317-3p. Some of these differences can be due to the fact that the previous library was performed with a pool of ovaries from all days of the adult stage, while the stress library was performed only with ovaries from 5-day-old females. That could be the case, for example, of let-7-5p, that presents much higher levels on day 3 than on day 5 (Tanaka and Piulachs, 2012). On the other hand, miR-275-3p presents the lowest expression level on day 5 (Tanaka and Piulachs,

2012), so its higher relative abundance in our library is presumably due to the hydric stress.

Expression analysis by qRT-PCR of miRNAs in ovaries from control and water-deprived 5-day-old females revealed that most of the miRNAs were up-regulated upon hydric stress, the highest up-regulation corresponding to miR-1-3p, whose expression increased more than 2 fold. This is not the first time that miR-1-3p shows a role in stress response. It has been described that it increases the expression after H_2O_2 exposure, and regulates apoptosis by targeting Bcl-2 (Li et al., 2012; Tang et al., 2009). MiR-1-3p also contributes to apoptosis in cancer cells (Yoshino et al., 2012), but the mechanisms underlying this response are probably complicated as miR-1-3p has shown to target more than 70 mRNAs in human HeLa cells (Lim et al., 2005). MiR-184-3p, which was also up-regulated in water-stressed ovaries, plays a key role in *D. melanogaster* egg development, and its removal results in several phenotypes, including germarium overgrowth (Iovino et al., 2009). MiR-184-3p has been also described as a pro-apoptotic miRNA in cancer models (Chen and Stallings, 2007; Foley et al., 2010; Yu et al., 2008). MiR-34-5p was also up-regulated upon hydric stress. This miRNA has been shown to induce cell death under different genotoxic stresses (Thomas and Lieberman, 2013).

Taken together, one of the general tendencies suggested by our data is that hydric stress in *B. germanica* ovary induces an overall miRNAs expression change that triggers an apoptotic response.

In the second part of this chapter, we have focused on miR-34-5p. As stated above, this miRNA was up-regulated in response to hydric stress and it has been described to play a role in apoptosis (Thomas and Lieberman, 2013). The expression pattern of miR-34-5p in the ovary showed a progressive increase during the gonadotrophic cycle, reaching maximal values at the end of it. This is the first time that a miRNA pattern like this is found in the ovary of *B. germanica*; usually miRNA expression decreases as the gonadotrophic cycle progresses (Tanaka and Piulachs, 2012). Previous studies in *D. melanogaster* suggested that miR-34-5p can be regulated by hormones like ecdysone and juvenile hormone (Sempere et al., 2003). Interestingly, in *B. germanica*, the expression pattern of miR-34-5p follows that of the juvenile hormone titre in the hemolymph during the gonadotrophic cycle (Treiblmayr et al., 2006).

We performed specific depletion experiments in order to identify the functions of this miRNA in *B. germanica* ovary, but we did not observe phenotypic differences between control and miR-34-5p-depleted females, apart from a slight delay of oviposition. This result is not fully surprising as it has been widely described that, except few significant examples, loss of function of individual miRNAs do not usually lead to highly penetrant phenotypes under standard laboratory conditions (Leung and Sharp, 2010; Mendell and Olson, 2012).

MiRNAs functions can be indirectly assessed by studying its mRNA targets, so we predicted putative targets for miR-34-5p. We found 28 putative targets within our *B. germanica* transcriptomic database, 22 of which had homology with well identified transcripts. Functional annotation (GO terms) of the obtained targets revealed that most of them were related with metabolic processes, protein binding and protein complexes. We analysed the expression pattern in ovary of 4 of these 22 targets (Csl4, Lkap, Iap2 and Windei) and checked their expression upon LNA anti-miR-34-5p treatment. All 4 mRNAs showed an expression pattern opposite to that of miR-34-5p, but only one, Windei, was up-regulated in miR-34-5p-depleted insects, thus suggesting that it is actually a miR-34-5p target. In *D. melanogaster* ovary, Windei is necessary for histone 3 lysine 9 trimethylation (Koch et al., 2009), but its function in *B. germanica* is unknown.

In summary, we have shown that miR-34-5p increases upon hydric stress in *B. germanica* ovary and that it could have a role in egg development, as its expression is higher at the end of the gonadotrophic cycle, and follows the pattern of juvenile hormone concentration in the hemolymph. Because depletion experiments did not give a clear phenotype, further studies will be necessary to unveil miR-34-5p function in *B. germanica* ovary, may be through the study of putative target mRNAs of particular interest, like Windei.

4.6. References

Abbott, A. L. (2011). Uncovering new functions for microRNAs in *Caenorhabditis elegans*. *Curr Biol* **21**, R668-71.

Ambros, V. (2004). The functions of animal microRNAs. *Nature* **431**, 350-5.

Bartel, D. P. (2004). MicroRNAs: genomics, biogenesis, mechanism, and function. *Cell* **116**, 281-97.

Brennecke, J., Hipfner, D. R., Stark, A., Russell, R. B. and Cohen, S. M. (2003). bantam encodes a developmentally regulated microRNA that controls cell proliferation and regulates the proapoptotic gene hid in Drosophila. *Cell* **113**, 25-36.

Bushati, N. and Cohen, S. M. (2007). microRNA functions. *Annu Rev Cell Dev Biol* **23**, 175-205.

Buttner, K., Wenig, K. and Hopfner, K. P. (2005). Structural framework for the mechanism of archaeal exosomes in RNA processing. *Mol Cell* **20**, 461-71.

Conesa, A., Gotz, S., Garcia-Gomez, J. M., Terol, J., Talon, M. and Robles, M. (2005). Blast2GO: a universal tool for annotation, visualization and analysis in functional genomics research. *Bioinformatics* **21**, 3674-6.

Cristino, A. S., Tanaka, E. D., Rubio, M., Piulachs, M. D. and Belles, X. (2011). Deep sequencing of organ- and stage-specific microRNAs in the evolutionarily basal insect *Blattella germanica* (L.) (Dictyoptera, Blattellidae). *PLoS One* **6**, e19350.

Chen, Y. and Stallings, R. L. (2007). Differential patterns of microRNA expression in neuroblastoma are correlated with prognosis, differentiation, and apoptosis. *Cancer Res* **67**, 976-83.

Dunster, K., Lai, F. P. and Sentry, J. W. (2005). Limkain b1, a novel human autoantigen localized to a subset of ABCD3 and PXF marked peroxisomes. *Clin Exp Immunol* **140**, 556-63.

Foley, N. H., Bray, I. M., Tivnan, A., Bryan, K., Murphy, D. M., Buckley, P. G., Ryan, J., O'Meara, A., O'Sullivan, M. and Stallings, R. L. (2010). MicroRNA-184 inhibits neuroblastoma cell survival through targeting the serine/threonine kinase AKT2. *Mol Cancer* **9**, 83.

Freitak, D., Knorr, E., Vogel, H. and Vilcinskas, A. (2012). Gender- and stressor-specific microRNA expression in *Tribolium castaneum*. *Biol Lett* **8**, 860-3.

Griffiths-Jones, S. (2004). The microRNA Registry. *Nucleic Acids Res* **32**, D109-11.

Guleria, P., Mahajan, M., Bhardwaj, J. and Yadav, S. K. (2011). Plant small RNAs: biogenesis, mode of action and their roles in abiotic stresses. *Genomics Proteomics Bioinformatics* **9**, 183-99.

Hu, Y., Matkovich, S. J., Hecker, P. A., Zhang, Y., Edwards, J. R. and Dorn, G. W., 2nd. (2012). Epitranscriptional orchestration of genetic reprogramming is an emergent property of stress-regulated cardiac microRNAs. *Proc Natl Acad Sci U S A* **109**, 19864-9.

Iovino, N., Pane, A. and Gaul, U. (2009). miR-184 has multiple roles in *Drosophila* female germline development. *Dev Cell* **17**, 123-33.

Kato, M., Paranjape, T., Muller, R. U., Nallur, S., Gillespie, E., Keane, K., Esquela-Kerscher, A., Weidhaas, J. B. and Slack, F. J. (2009). The mir-34 microRNA is required for the DNA damage response in vivo in *C. elegans* and in vitro in human breast cancer cells. *Oncogene* **28**, 2419-24.

Koch, C. M., Honemann-Capito, M., Egger-Adam, D. and Wodarz, A. (2009). Windei, the *Drosophila* homolog of mAM/MCAF1, is an essential cofactor of the H3K9 methyl transferase dSETDB1/Eggless in germ line development. *PLoS Genet* **5**, e1000644.

Langmead, B., Trapnell, C., Pop, M. and Salzberg, S. L. (2009). Ultrafast and memory-efficient alignment of short DNA sequences to the human genome. *Genome Biol* **10**, R25.

Lee, Y., Kim, M., Han, J., Yeom, K. H., Lee, S., Baek, S. H. and Kim, V. N. (2004). MicroRNA genes are transcribed by RNA polymerase II. *EMBO J* **23**, 4051-60.

Lee, Y. J., Johnson, K. R. and Hallenbeck, J. M. (2012). Global protein conjugation by ubiquitin-like-modifiers during ischemic stress is regulated by microRNAs and confers robust tolerance to ischemia. *PLoS One* **7**, e47787.

Leung, A. K. and Sharp, P. A. (2010). MicroRNA functions in stress responses. *Mol Cell* **40**, 205-15.

Li, Y., Shelat, H. and Geng, Y. J. (2012). IGF-1 prevents oxidative stress induced-apoptosis in induced pluripotent stem cells which is mediated by microRNA-1. *Biochem Biophys Res Commun* **426**, 615-9.

Lim, L. P., Lau, N. C., Garrett-Engele, P., Grimson, A., Schelter, J. M., Castle, J., Bartel, D. P., Linsley, P. S. and Johnson, J. M. (2005). Microarray analysis shows that some microRNAs downregulate large numbers of target mRNAs. *Nature* **433**, 769-73.

Lopez-Sanchez, M. J., Neef, A., Pereto, J., Patino-Navarrete, R., Pignatelli, M., Latorre, A. and Moya, A. (2009). Evolutionary convergence and nitrogen metabolism in *Blattabacterium* strain Bge, primary endosymbiont of the cockroach *Blattella germanica*. *PLoS genetics.* **5**.

Lucas, K. and Raikhel, A. S. (2013). Insect microRNAs: biogenesis, expression profiling and biological functions. *Insect Biochem Mol Biol* **43**, 24-38.

Mane-Padros, D., Cruz, J., Vilaplana, L., Nieva, C., Urena, E., Belles, X. and Martin, D. (2010). The hormonal pathway controlling cell death during metamorphosis in a hemimetabolous insect. *Dev Biol* **346**, 150-60.

Mendell, J. T. and Olson, E. N. (2012). MicroRNAs in stress signaling and human disease. *Cell* **148**, 1172-87.

Mukha, D. V., Chumachenko, A. G., Dykstra, M. J., Kurtti, T. J. and Schal, C. (2006). Characterization of a new densovirus infecting the German cockroach, *Blattella germanica*. *J Gen Virol* **87**, 1567-75.

Okamura, K., Phillips, M. D., Tyler, D. M., Duan, H., Chou, Y. T. and Lai, E. C. (2008). The regulatory activity of microRNA* species has substantial influence on microRNA and 3' UTR evolution. *Nat Struct Mol Biol* **15**, 354-63.

Pfaffl, M. W., Horgan, G. W. and Dempfle, L. (2002). Relative expression software tool (REST) for group-wise comparison and statistical analysis of relative expression results in real-time PCR. *Nucleic Acids Res* **30**, e36.

Rehmsmeier, M., Steffen, P., Hochsmann, M. and Giegerich, R. (2004). Fast and effective prediction of microRNA/target duplexes. *RNA* **10**, 1507-17.

Rubio, M., de Horna, A. and Belles, X. (2012). MicroRNAs in metamorphic and non-metamorphic transitions in hemimetabolan insect metamorphosis. *BMC Genomics* **13**, 386.

Ruby, J. G., Stark, A., Johnston, W. K., Kellis, M., Bartel, D. P. and Lai, E. C. (2007). Evolution, biogenesis, expression, and target predictions of a substantially expanded set of *Drosophila* microRNAs. *Genome Res* **17**, 1850-64.

Sempere, L. F., Freemantle, S., Pitha-Rowe, I., Moss, E., Dmitrovsky, E. and Ambros, V. (2004). Expression profiling of mammalian microRNAs uncovers a subset of brain-expressed microRNAs with possible roles in murine and human neuronal differentiation. *Genome Biol* **5**, R13.

Sempere, L. F., Sokol, N. S., Dubrovsky, E. B., Berger, E. M. and Ambros, V. (2003). Temporal regulation of microRNA expression in *Drosophila melanogaster* mediated by hormonal signals and broad-Complex gene activity. *Dev Biol* **259**, 9-18.

Shcherbata, H. R., Ward, E. J., Fischer, K. A., Yu, J. Y., Reynolds, S. H., Chen, C. H., Xu, P., Hay, B. A. and Ruohola-Baker, H. (2007). Stage-specific differences in the requirements for germline stem cell maintenance in the *Drosophila* ovary. *Cell Stem Cell* **1**, 698-709.

Sokol, N. S. and Ambros, V. (2005). Mesodermally expressed *Drosophila* microRNA-1 is regulated by Twist and is required in muscles during larval growth. *Genes Dev* **19**, 2343-54.

Tanaka, E. D. and Piulachs, M. D. (2012). Dicer-1 is a key enzyme in the regulation of oogenesis in panoistic ovaries. *Biol Cell* **104**, 452-61.

Tang, Y., Zheng, J., Sun, Y., Wu, Z., Liu, Z. and Huang, G. (2009). MicroRNA-1 regulates cardiomyocyte apoptosis by targeting Bcl-2. *Int Heart J* **50**, 377-87.

Tarasov, V., Jung, P., Verdoodt, B., Lodygin, D., Epanchintsev, A., Menssen, A., Meister, G. and Hermeking, H. (2007). Differential regulation of microRNAs by p53 revealed by massively parallel sequencing: miR-34a is a p53 target that induces apoptosis and G1-arrest. *Cell Cycle* **6**, 1586-93.

Thomas, M. P. and Lieberman, J. (2013). Live or let die: posttranscriptional gene regulation in cell stress and cell death. *Immunol Rev* **253**, 237-52.

Treiblmayr, K., Pascual, N., Piulachs, M. D., Keller, T. and Belles, X. (2006). Juvenile hormone titer versus juvenile hormone synthesis in female nymphs and adults of the German cockroach, *Blattella germanica*. *J Insect Sci* **6**, 1-7.

Viktorinova, I. and Dahmann, C. (2013). Microtubule polarity predicts direction of egg chamber rotation in *Drosophila*. *Curr Biol* **23**, 1472-7.

Yang, J. S., Phillips, M. D., Betel, D., Mu, P., Ventura, A., Siepel, A. C., Chen, K. C. and Lai, E. C. (2011). Widespread regulatory activity of vertebrate microRNA* species. *RNA* **17**, 312-26.

Yoshino, H., Enokida, H., Chiyomaru, T., Tatarano, S., Hidaka, H., Yamasaki, T., Gotannda, T., Tachiwada, T., Nohata, N., Yamane, T. et al. (2012). Tumor suppressive microRNA-1 mediated novel apoptosis pathways through direct inhibition of splicing factor serine/arginine-rich 9 (SRSF9/SRp30c) in bladder cancer. *Biochem Biophys Res Commun* **417**, 588-93.

Yu, J., Ryan, D. G., Getsios, S., Oliveira-Fernandes, M., Fatima, A. and Lavker, R. M. (2008). MicroRNA-184 antagonizes microRNA-205 to maintain SHIP2 levels in epithelia. *Proc Natl Acad Sci U S A* **105**, 19300-5.

Zhu, J., Li, W., Yang, W., Qi, L. and Han, S. (2013). Identification of microRNAs in *Caragana intermedia* by high-throughput sequencing and expression analysis of 12 microRNAs and their targets under salt stress. *Plant Cell Rep*.

4.7. Supplementary information

Supplementary Table 4.S1: **Primers used in the expression studies.**

miRNA or mRNA	Primer name	Primer sequence (5'-3')
miR-1-3p	miR-1-3p	TGGAATGTAAAGAAGTATGGAG
miR-275-3p	miR-275-3p	TCAGGTACCTGAAGTAGCGCG
miR-279-3p	miR-279-3p	TGACTAGATCCACACTCATCCA
miR-276-3p	miR-276-3p	TAGGAACTTCATACCGTGCTCT
miR-184-3p	miR-184-3p	TGGACGGAGAACTGATAAGGGC
miR-998-3p	miR-998-3p	TAGCACCATGGGATTCAGCT
miR-190-5p	miR-190-5p	AGATATGTTTGATATTCTTGGTTG
let-7-5p	let-7-5p	TGAGGTAGTAGGTTGTATAGT
miR-100-5p	miR-100-5p	AACCCGTAGATCCGAACTTGTG
miR-276-5p	miR-276-5p	AGCGAGGTATAGAGTTCCTACG
bantam-3p	bantam-3p	TGAGATCATTGTGAAAGCTGATT
miR-34-5p	miR-34-5p	TGGCAGTGTGGTTAGCTGGTTG
miR-317-3p	miR-317-3p	TGAACACAGCTGGTGGTATCTCA
U2	U2	GCTTGCTCCACCTCTGTCA
U6	U6	CGATACAGAGAAGATTAGCATGG
CSL4-like	csl_RT_Fw	TGAGATGGAGGAACTCGTTTG
CSL4-like	csl_RT_Rv	TGCAGGACTTTTCTTCATTCG
Limkain-b1	lkap_RT_Fw	GTGTTAGTCCCCCGTTAGCA
Limkain-b1	lkap_RT_Rv	GTGCGGTAGAGCCTCCATAA
IAP2	BgIAP2Fw	GCATAGCCAAAGCAGGATTC
IAP2	BgIAP2Rv	GCCATGACCTGATCTCCATAA
Windei	E11009007_RT_Fw	CTGCAAATCATCAGAATCTTCTATAC
Windei	E11009007_RT_Rv	TTGGTGCATAATCAAGAATTCAG
BgActin-5c	BgActinRTFw1	AGCTTCCTGATGGTCAGGTGA
BgActin-5c	Bg Actin R	TGTCGGCAATTCCAGGGTACATGGT

Supplementary Table 4.S2: miR-34-5p putative targets. Blast results and functional annotations (GO IDs and GO terms) are shown. P: biological process; F: molecular function; C: cellular component.

Target name	GO-Group	GO-ID	Term
3'-5' exoribonuclease CSL4-like protein	P	GO:0006397	mRNA processing
	P	GO:0010468	regulation of gene expression
	C	GO:0000177	cytoplasmic exosome (RNase complex)
	F	GO:0000175	3'-5'-exoribonuclease activity
	F	GO:0003723	RNA binding
eukaryotic translation initiation factor 3 subunit e-like	C	GO:0005737	cytoplasm
	P	GO:0006413	translational initiation
	F	GO:0003743	translation initiation factor activity
fanconi anemia group m protein	F	GO:0005524	ATP binding
	F	GO:0008026	ATP-dependent helicase activity
	F	GO:0003676	nucleic acid binding
limkain-b1-like	F	GO:0005488	binding
	P	GO:0010923	negative regulation of phosphatase activity
	C	GO:0005777	peroxisome
atp-dependent helicase brm-like	F	GO:0004386	helicase activity
	F	GO:0003677	DNA binding
	F	GO:0005524	ATP binding
	F	GO:0016740	transferase activity
	C	GO:0005634	nucleus
	P	GO:0006355	regulation of transcription, DNA-dependent
pci domain-containing protein 2	P	GO:2000117	negative regulation of cysteine-type endopeptidase activity
	P	GO:0048536	spleen development
	P	GO:0043488	regulation of mRNA stability
	P	GO:0045893	positive regulation of transcription, DNA-dependent
	P	GO:0043066	negative regulation of apoptotic process
	P	GO:0090267	positive regulation of mitotic cell cycle spindle assembly checkpoint

activating transcription factor 7-interacting protein 1 / windei	F	GO:0016874	ligase activity
probable nucleolar gtp-binding protein 1-like	C	GO:0005730	nucleolus
	F	GO:0005525	GTP binding
	P	GO:0042254	ribosome biogenesis
rb1-inducible coiled-coil protein 1	P	GO:0000045	autophagic vacuole assembly
	P	GO:0007507	heart development
	P	GO:0007254	JNK cascade
	P	GO:0045793	positive regulation of cell size
	P	GO:0001934	positive regulation of protein phosphorylation
	C	GO:0034045	pre-autophagosomal structure membrane
	F	GO:0019901	protein kinase binding
actin-related protein isoform a	C	GO:0030027	lamellipodium
	C	GO:0005884	actin filament
	P	GO:0030713	ovarian follicle cell stalk formation
	P	GO:0030037	actin filament reorganization involved in cell cycle
	P	GO:0045747	positive regulation of Notch signaling pathway
	P	GO:0006911	phagocytosis, engulfment
	P	GO:0030833	regulation of actin filament polymerization
	P	GO:0006886	intracellular protein transport
	P	GO:0007520	myoblast fusion
	P	GO:0007303	cytoplasmic transport, nurse cell to oocyte
	F	GO:0003779	actin binding
	P	GO:0008335	female germline ring canal stabilization
	C	GO:0005885	Arp2/3 protein complex
	P	GO:0007413	axonal fasciculation
	P	GO:0030589	pseudocleavage involved in syncytial blastoderm formation
	P	GO:0022416	chaeta development
	F	GO:0005524	ATP binding
	F	GO:0005200	structural constituent of cytoskeleton

	P	GO:0051491	positive regulation of filopodium assembly
mesencephalic astrocyte-derived neurotrophic factor homolog	P	GO:0007275	multicellular organismal development
	C	GO:0005576	extracellular region
	F	GO:0005509	calcium ion binding
adp-ribosylation factor-like protein 2	C	GO:0005622	intracellular
	F	GO:0005525	GTP binding
	P	GO:0007264	small GTPase mediated signal transduction
	P	GO:0006886	intracellular protein transport
protein croquemort-like	P	GO:0006915	apoptotic process
	P	GO:0007155	cell adhesion
	P	GO:0006952	defense response
	P	GO:0042116	macrophage activation
	P	GO:0006911	phagocytosis, engulfment
	C	GO:0005887	integral to plasma membrane
	F	GO:0005044	scavenger receptor activity
piggybac transposable element-derived protein 4-like	C	GO:0016020	membrane
	C	GO:0005634	nucleus
	F	GO:0005044	scavenger receptor activity
	F	GO:0003700	sequence-specific DNA binding transcription factor activity
jerky protein homolog-like	F	GO:0003677	DNA binding
exosome component 10	F	GO:0003824	catalytic activity
	F	GO:0003676	nucleic acid binding
	P	GO:0000956	nuclear-transcribed mRNA catabolic process
	P	GO:0071027	nuclear RNA surveillance
	F	GO:0000166	nucleotide binding
glutamine synthetase 2	F	GO:0004356	glutamate-ammonia ligase activity
	F	GO:0005524	ATP binding
	P	GO:0006807	nitrogen compound metabolic process
	P	GO:0006542	glutamine biosynthetic process
h+ transporting atp synthase gamma subunit	F	GO:0008553	hydrogen-exporting ATPase activity, phosphorylative mechanism

	F	GO:0046933	hydrogen ion transporting ATP synthase activity, rotational mechanism
	C	GO:0000275	mitochondrial proton-transporting ATP synthase complex, catalytic core F(1)
	P	GO:0015986	ATP synthesis coupled proton transport
	P	GO:0006911	phagocytosis, engulfment
	F	GO:0046961	proton-transporting ATPase activity, rotational mechanism
	C	GO:0005811	lipid particle
	F	GO:0003746	translation elongation factor activity
	F	GO:0008270	zinc ion binding
transcription elongation	P	GO:0006414	translational elongation
factor spt4-like	P	GO:0032786	positive regulation of DNA-dependent transcription, elongation
	C	GO:0005634	nucleus
	F	GO:0048038	quinone binding
	F	GO:0051287	NAD binding
	F	GO:0008137	NADH dehydrogenase (ubiquinone) activity
nadh dehydrogenase			
iron-sulfur protein	C	GO:0005747	mitochondrial respiratory chain complex I
mitochondrial			
	P	GO:0046331	lateral inhibition
	P	GO:0006120	mitochondrial electron transport, NADH to ubiquinone
	F	GO:0004715	non-membrane spanning protein tyrosine kinase activity
	P	GO:0007229	integrin-mediated signaling pathway
integrin-linked protein	P	GO:0006468	protein phosphorylation
kinase-like	F	GO:0005524	ATP binding
	P	GO:0009966	regulation of signal transduction
	F	GO:0004674	protein serine/threonine kinase activity
	C	GO:0005622	intracellular
	P	GO:0043066	negative regulation of apoptotic process
inhibitor of apoptosis 2	P	GO:0043154	negative regulation of cysteine-type endopeptidase activity involved in apoptotic process

P	GO:0070534	protein K63-linked ubiquitination
P	GO:0007423	sensory organ development
F	GO:0008270	zinc ion binding

5. CHORION FORMATION IN PANOISTIC OVARIES REQUIRES WINDEI AND TRIMETHYLATION OF HISTONE 3 LYSINE 9

Chorion formation in panoistic ovaries requires windei and trimethylation of histone 3 lysine 9

Herraiz, A., Belles X., Piulachs MD.

Institute of Evolutionary Biology (CSIC-Universitat Pompeu Fabra), Passeig Maritim de la Barceloneta 37-49, 08003 Barcelona, Spain.

Herraiz A., Belles X, Piulachs MD.
Chorion formation in panoistic ovaries requires windei and trimethylation of histone 3 lysine 9.
Exp Cell Res. 2014 Jan 1; 320(1): 46-53.
DOI: 10.1016/j.yexcr.2013.07.006

5.9. Supplementary material

Supplementary Table 5.S1. List of oligonucleotides used as primers in the experimental work

	Primer name	Primer sequence
BgWde sequencing	BgWde_Fw1	5'ACTACTGGTGGAGGTGAGAA3'
	BgWde_Fw2	5'GGTGATGCTCGTACAAGGAA3'
	BgWde_Fw3	5'CGCTTCTTTGACAAGATGGAA3'
	BgWde_Fw4	5'TTTGGTTTGAGTGATTCTGAGG3'
	BgWde_Fw5	5'ATGCCCTTTGGTTGTAAACG3'
	BgWde_Fw6	5'GGTGCCATTGGAAATGTCTG3'
	BgWde_Fw7	5'AGCAAACAATCTACAACAACCA3'
	BgWde_Fw8	5'TAGGAATCAAGCGCAGGTGA3'
	BgWde_Fw9	5'GTGTTGCCAACAGTATGATA3'
	BgWde_Rv1	5'TTCCTTGTACGAGCATCACC3'
	BgWde_Rv2	5'TTGTACTTTCACTACTGTCCCTTTTT3'
	BgWde_Rv3	5'CCACTTCACTGTCTTTTGGTTG3'
	BgWde_Rv4	5'TGGTTGTTGTAGATTGTTTGCT3'
	BgWde_Rv5	5'CAGACATTTCCAATGGCACC3'
	BgWde_Rv6	5'CGTTTACAACCAAAGGGCAT3'
	BgWde_Rv7	5'TGAAGGCCAACCTCGCATATG3'
	BgWde_Rv8	5´AACAAATAACTTCCGTCGTC3'

dsBgWde synthesis	BgWde_dsRNA_Fw	5'AGCAGCTCAAGGATATGGAA3'
	BgWde_dsRNA_Rv	5'TTGCTGCTGCTGCTGACTAT3'
BgWde qRTPCR	BgWde_RT_Fw	5'CTGCAAATCATCAGAATCTTCTATAC3'
	BgWde_RT_Rv	5'TTGGTGCATAATCAAGAATTCAG3'
Brownie qRTPCR	Brownie_RT_Fw	5'CTCAGCACAAAGCCGTAGCA3'
	Brownie_RT_Rv	5'CGTCGGCGTAAGCTTCGTAG3'
Citrus qRTPCR	Citrus_RT_Fw	5'TCGTGCTTTTCAATGTGCGTA3'
	Citrus_RT_Rv	5'GGGAATCCAGGGTATTTGGAA3'
Fcp 3c qRTPCR	Fcp3c_RT_Fw	5'TAGTCCAGATCCCCCTAAGGG3'
	Fcp3c_RT_Rv	5'CCTTCTGCATGAGCTGATGGA3'
Hippo qRTPCR	Hippo _RT_Fw	5'GGGTCAAATGATAGCTGAAGCAC3'
	Hippo _RT_Rv	5'CGATAACTCTGGTTTTCCCGG3'
Yorkie qRTPCR	Yorkie _RT_Fw	5'CAGTCGTGAAAATTCGGCAGA3'
	Yorkie _RT_Rv	5'GCTCCAACAGATGCTGTACCG3'
Notch qRTPCR	Notch _RT_Fw	5'GCTAAGAGGCTGTTGGATGC3'
	Notch _RT_Rv	5'TGCCAGTGTTGTCCTGAGAG3'
Hindsight qRTPCR	Hnt_RT_Fw	5'CTACGACATCGCAAGAAGCA3'
	Hnt_RT_Rv	5'AAAGGGCAGTGGAGTTGTTG3'
Cut qRTPCR	Cut_RT_Fw	5'AAATATGTGCTCGGCCTGTC3'
	Cut_RT_Rv	5'TGCATCTTGCGGTAACTGTC3'
Orc1 qRTPCR	Orc1_RT_Fw	5'ACAAACCCAGAGCCTCTGTGATT3'
	Orc1_RT_Rv	5'GCACATTCGATGGCTTATCAACT3'
Cyclin E qRTPCR	CycE_RT_Fw	5'TACCTGGGCAAATCCAAGAG3'
	CycE_RT_Rv	5'TTCATCTCGCTCATGACTGG3

5.10. Annex

Windei is under-expressed in hydric stress conditions

As shown in the former chapter of this thesis, Windei is a putative target of miR-34-5p, a miRNA that was overexpressed in ovary 48 h after hydric stress induction. In order to know whether Windei expression was also altered under hydric stress conditions, we analysed it in ovaries of 5-day-old control females and in ovaries of 5-day-old females that were water-deprived 48 h before. Our results showed an under-expression of BgWde mRNA in ovaries of water-stressed females (Figure 5.A1), although the differences were not statistically significant.

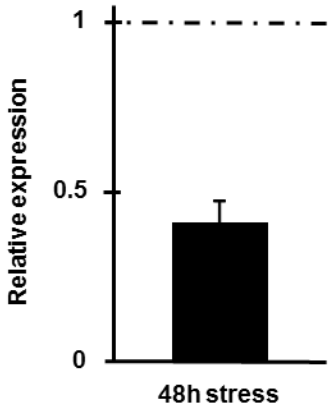

Figure 5.A1: Level of BgWde mRNA in ovaries from 5-day-old females subjected to 48h of hydric stress; qRT-PCR data represent 3 biological replicates and are normalized against control ovaries (reference value=1); expression of actin-5c was used as a reference. Data are expressed as mean ± s.e.m.

The under-expression of BgWde mRNA upon hydric stress is coherent with the up-regulation of miR-34-5p in the same conditions (see chapter 4), as BgWde is a putative target of this microRNA.

As shown in the present chapter, BgWde is necessary for the occurrence of the repressive epigenetic mark H3K9me3, and BgWde RNAi led to the overexpression of most of genes analysed. We can hypothesize that BgWde is under-expressed in hydric stress conditions, which helps to increase the expression of genes involved in the stress response.

6. BgCARMER, A GENE ENCODING AN ARGININE METHYLTRANSFERASE, IS OVEREXPRESSED UNDER HYDRIC STRESS AND IS REQUIRED FOR REPRODUCTION

BgCARMER, a gene encoding an arginine methyltransferase, is overexpressed under hydric stress and is required for reproduction

Alba Herraiz, Xavier Belles, Maria-Dolors Piulachs

Institut de Biologia Evolutiva (CSIC-Universitat Pompeu Fabra), and LINCGlobal, Passeig Marítim de la Barceloneta 37-49. 08003 Barcelona, Spain.

6.1. Abstract

Mammalian CARM1 and its *Drosophila melanogaster* ortholog CARMER are arginine methyltransferases belonging to the PRMT (protein arginine methyltransferase) family. They are recruited to promoters of genes regulated by steroid hormones and help to activate transcription by methylating different protein substrates in arginine residues. Here we report the occurrence of a CARM1/CARMER ortholog present in the ovary of the hemimetabolous insect *Blattella germanica*, which we have named BgCARMER. BgCARMER mRNA levels are increased in ovaries of females subjected to 48 h of hydric stress. Depletion of BgCARMER in ovary led to decreased dimethylation of arginine 17 in histone H3 in follicular cells of ovarian basal follicles and to an altered expression of the ecdysone cascade genes and associated caspases.

6.2. Introduction

Activation of transcription requires the binding of protein complexes that remodel the chromatin structure and recruit and activate RNA polymerase II. Nuclear receptors are transcriptional activators that in the presence of ligand recruit secondary complexes to the target gene promoters to initiate transcription (Glass and Rosenfeld, 2000; McKenna et al., 1999). In mammals, CARM1 (coactivator-associated arginine methyltransferase 1) is recruited to steroid hormone-regulated promoters in response to the

corresponding hormone and contribute to activate transcription (Bauer et al., 2002; Ma et al., 2001; Stallcup et al., 2003). CARM1 belongs to Class I of PRMT (protein arginine methyltransferase) family, thus it is also known as PRMT4. Class I PRMTs catalyse the formation of monomethyl- and asymmetric dimethylarginine, which is involved in transcriptional activation (Bedford and Richard, 2005; Pahlich et al., 2006). CARM1 methylates several proteins involved in gene expression, which can be divided into two groups: proteins involved in chromatin remodelling, like histone H3 (in the arginine residues R2, R17 and R26) and p300/CREB-binding protein and proteins directly involved in transcription, like RNA-binding proteins and splicing factors (Cheng et al., 2007; Chevillard-Briet et al., 2002; Teyssier et al., 2002; Troffer-Charlier et al., 2007). All PRMTs share a common catalytic core region that contains four conserved amino acid motifs (I, postI, II and III) as well as a THW loop (Frankel et al., 2002; Zhang et al., 2000). CARM1 additionally presents specific N- and C-terminal domains needed for enzymatic activity and for binding to transcriptional coactivators (Stallcup et al., 2003; Teyssier et al., 2002).

In *Drosophila melanogaster* cells, a CARM1 ortholog known as CARMER (coactivator arginine methyltransferase for EcR/Usp) binds to ecdysone receptor (EcR), enhancing the ecdysone-mediated transcription of genes involved in cell death. As in CARM1, CARMER is responsible for the asymmetric dimethylation of R17 in histone H3 (H3R17me2a) (Cakouros et al., 2004). Other genes orthologous to CARM1 gene have been found in insects, but only

AgCARM1 from *Anopheles gambiae* has been characterized (Kuhn et al., 2009).

Here we report the occurrence of a CARM1/CARMER ortholog in the ovary of the hemimetabolous insect *Blattella germanica* that we have named BgCARMER. It was overexpressed under hydric stress conditions and its depletion led to reduced H3R17me2a, and prevented reproduction in 70% of the experimental specimens.

6.3. Material and Methods

a) Insect colony and tissue sampling

Sixth instar nymphs or freshly ecdysed adult females of *B. germanica* were obtained from a colony fed on Panlab dog chow and water *ad libitum*, and reared in the dark at 29±1°C and 60–70% relative humidity. All dissections were carried out on carbon dioxide-anaesthetized specimens. After the dissection, ovaries for mRNA expression studies were frozen on liquid nitrogen and stored at -80ºC until use, and ovaries for immunohistochemical studies were immediately processed.

b) Cloning and sequencing

A fragment of 331 bp corresponding to a putative protein arginine n-methyltransferase was obtained from a transcriptome of ovary from 5-day-old adult females subjected to 48 h of hydric stress

previously obtained in our laboratory (unpublished results). To complete the sequence, conventional PCRs were applied to ovarian cDNA, and 3'- and 5′-rapid amplifications of cDNA ends (RACE) were applied to ovarian RNA using FirstChoice RLM-RACE (Ambion, Huntingdon, Cambridgeshire, UK), according to the manufacturer's instructions. The amplified fragments were analysed by agarose gel electrophoresis, cloned into the pSTBlue-1 vector (Novagen, Madison, WI, USA) and sequenced. Primers used are detailed in Supplementary Table 6.S1. Secondary structure predictions were made with SMART software (http://smart.embl-heidelberg.de/) (Letunic et al., 2012).

c) Phylogenetic analyses

Putative CARM1/CARMER mRNA sequences were retrieved from GenBank. Protein sequences were aligned with that obtained for *B. germanica*, using CLUSTALX2. The resulting alignment was analyzed using a maximum-likelihood approach as implemented in PhyML 3.1 (Guindon et al., 2009) with the LG amino acid substitution model, and data was bootstrapped for 100 replicates. The sequences used in the phylogenetic analysis were as follows: EFN75292.1 (*Harpegnathos saltator*), EFZ21951.1 (*Solenopsis invicta*), EGI69535.1 (*Acromyrmex echinatior*), XP_003489685.1 (*Bombus impatiens*), XP_003250875.1 (*Apis mellifera*), XP_003699947.1 (*Megachile rotundata*), EHJ77473.1 (*Danaus plexippus*), BAN21131.1 (*Riptortus pedestris*), XP_004926170.1 (*Bombyx mori*), XP_972906.2 (*Tribolium castaneum*),

XP_002428291.1 (*Pediculus humanus corporis*), NP_649963.1 (*D. melanogaster*), XP_318375.4 (*Anopheles gambiae*), XP_001843300.1 (*Culex quinquefasciatus*), XP_004529208.1 (*Ceratitis capitata*), EFX85598.1 (*Daphnia pulex*), EKC18160.1 (*Crassostrea gigas*), NP_001003645.1 (*Danio rerio*), NP_954592.1 (*Homo sapiens*), NP_067506.2 (*Mus musculus*).

d) Induction of water stress

Control insects received food and water *ad libitum*. Experimental individuals were water-deprived at day 3 of the adult life and received food *ad libitum*. Control and water-deprived individuals were dissected at day 5 of the adult life.

e) RNA extraction and retrotranscription to cDNA

RNA extractions were performed using the GenElute Mammalian Total RNA kit (Sigma, Madrid, Spain). RNA quantity and quality were estimated by spectrophotometric absorption at 260 nm/280nm in a Nanodrop Spectrophotometer ND-1000 (NanoDrop Technologies, Wilmington, DE, USA). A sample of 400 ng of total RNA from each extraction was treated with DNase (Promega, Madison, WI, USA) and reverse transcribed with Transcriptor First Strand cDNA Synthesis Kit (Roche, Sant Cugat del Valles, Barcelona, Spain). In all cases we followed the manufacturer's protocols.

f) Expression studies

The expression of BgCARMER was measured by quantitative real-time PCR (qRT-PCR) in ovary during the first gonadotrophic cycle in the sixth (last) nymphal instar and the adult, and to assess the effect of RNAi (see below). qRT-PCR reactions were carried in an iQ5 Real-Time PCR Detection System (Bio-Rad Laboratories, Madrid, Spain), using IQ SYBR Green Supermix (BioRad). The actin-5c gene of *B. germanica* was used as a reference for expression pattern studies and the eukaryotic initiation factor 4A, BgEIF4-AIIIa, was used in the functional studies because expression of actin-5c was altered by RNAi treatment. The efficiency of primers was first validated by constructing a standard curve through four serial dilutions of cDNA from ovaries. At least two independent qRT-PCR experiments (biological replicates) were performed, and each measurement was done in triplicate (technical replicates). qRT-PCR reactions were performed and analysed as previously described (Herraiz et al., 2011). Fold change expression was calculated using the REST-2008 program (Relative Expression Software Tool V 2.0.7; Corbett Research). Statistical analyses were tested with the same program, which makes no assumptions about the distributions, evaluating the significance of the derived results by Pair-Wise Fixed Reallocation Randomization Test (Pfaffl et al., 2002). PCR primers used in qRT-PCR expression studies were designed using the Primer Express 2.0 software (Applied Biosystems, Foster City, CA, USA), and are indicated in Supplementary Table 6.S1.

Together with actin-5c (GenBank: *AJ862721*), eIF4AIII (GenBank: *HF969254*) and CARMER (under submission in GenBank), we studied the expression of the following genes of *B. germanica*: Fushi tarazu factor 1 (FTZ-F1) (GenBank: *FM163377.1*), HR3 isoform A (HR3) (GenBank: *AM259128.1*) and ecdysone inducible protein 75 isoform A (E75A) (GenBank: *AM238653.1*). We also analysed the expression of caspase 1 and caspase 5, on the basis of sequences communicated by Paula Irles and Maria-Dolors Piulachs (unpublished results).

g) RNAi experiments

A dsRNA was prepared encompassing a 326 bp region starting at nucleotide 517 of the BgCARMER sequence (dsBgCARMER). The fragment was amplified by PCR and cloned into the pSTBlue-1 vector. As control dsRNA, we used a 307 bp sequence from *Autographa californica* nucleopolyhedrovirus (GenBank: *K01149*, nucleotides 370–676) (dsMock), as reported elsewhere (Lozano and Belles, 2011). Preparation of the dsRNAs was performed as previously described (Ciudad et al., 2006). Freshly ecdysed specimens from the last nymphal instar were treated with 2.5 μg of dsBgCARMER, injected into the abdomen in a volume of 1 μl of water-DEPC. Control specimens were treated similarly with 1 μg of dsMock.

h) Immunofluorescence and cell staining

To detect the asymmetric dimethylation of histone H3 at arginine 17 (H3R17me2a) determined by the action of CARMER, ovaries from 5 and 7-day-old adult females were dissected, fixed and processed as previously described (Tanaka and Piulachs, 2012). H3R17me2a was detected using a rabbit polyclonal anti-H3R17me2a antibody (Novus Biologicals NB21-1132, Cambridge, UK) diluted 1:100. As secondary antibody, an Alexa Fluor 647-conjugated donkey anti-rabbit IgG (Invitrogen, Carlsbad CA, USA) diluted 1:400 was used. For F-actin visualization, ovaries were incubated with Phalloidin-TRITC (5µg/ml, Sigma) during 20 min. Ovarioles were mounted in UltraCruz Mounting Medium (Santa Cruz Biotechnology, inc., Delaware CA, USA), which contains DAPI for DNA staining. Samples were observed by epifluorescence microscopy using an AxioCam MRm camera adapted to a Zeiss AxioImager.Z1 microscope (Apo Tome) (Carl Zeiss MicroImaging).

6.4. Results

a) *B. germanica* has a CARMER homolog

The complete sequence of BgCARMER is 2,139 bp long, with an ORF encoding for a protein of 570 amino acids (nucleotide positions 146-1,855) (Supplementary Figure 6.S1), with an estimated molecular mass of 63.9 kDa and an isoelectric point of 5.95. BLAST analysis against NCBI database revealed its

homology with CARM1/CARMER proteins. The overall identity between BgCARMER and DmCarmer is 66%, and between BgCARMER and murine (*M. musculus*) CARM1 is 57%. Higher identity was found with the hemipteran species *R. pedestris* (74% of overall identity). Secondary structure predictions showed that this protein presents two conserved domains: a CARM1 domain (residues 2-110) and a PRMT catalytic domain (residues 124-423). The PRMT catalytic domain contains the four sequence motifs as well as the THW loop that are conserved among all PRMTs (Frankel et al., 2002; Zhang et al., 2000) (Figure 6.1).

b) BgCARMER clusters with heteropteran CARMER in a phylogenetical context

In order to place BgCARMER in an evolutionary context, we performed a phylogenetic analysis of CARM1/CARMER proteins available in public databases. Following maximum-likelihood analyses, we obtained a tree with two separated groups, one containing the sequences from arthropods, and the other containing the sequences from vertebrates together with the mollusc *C. gigas* (Figure 6.2). All sequences from hymenopterans fall into a well-supported cluster (100% bootstrap value). Sequences from dipterans appear into a cluster supported with 99% of bootstrap value that is the sister group of the lepidopteran cluster. The sequence of *B. germanica* appears with that of *R. pedestris*, coherently with the high similarity among both sequences.

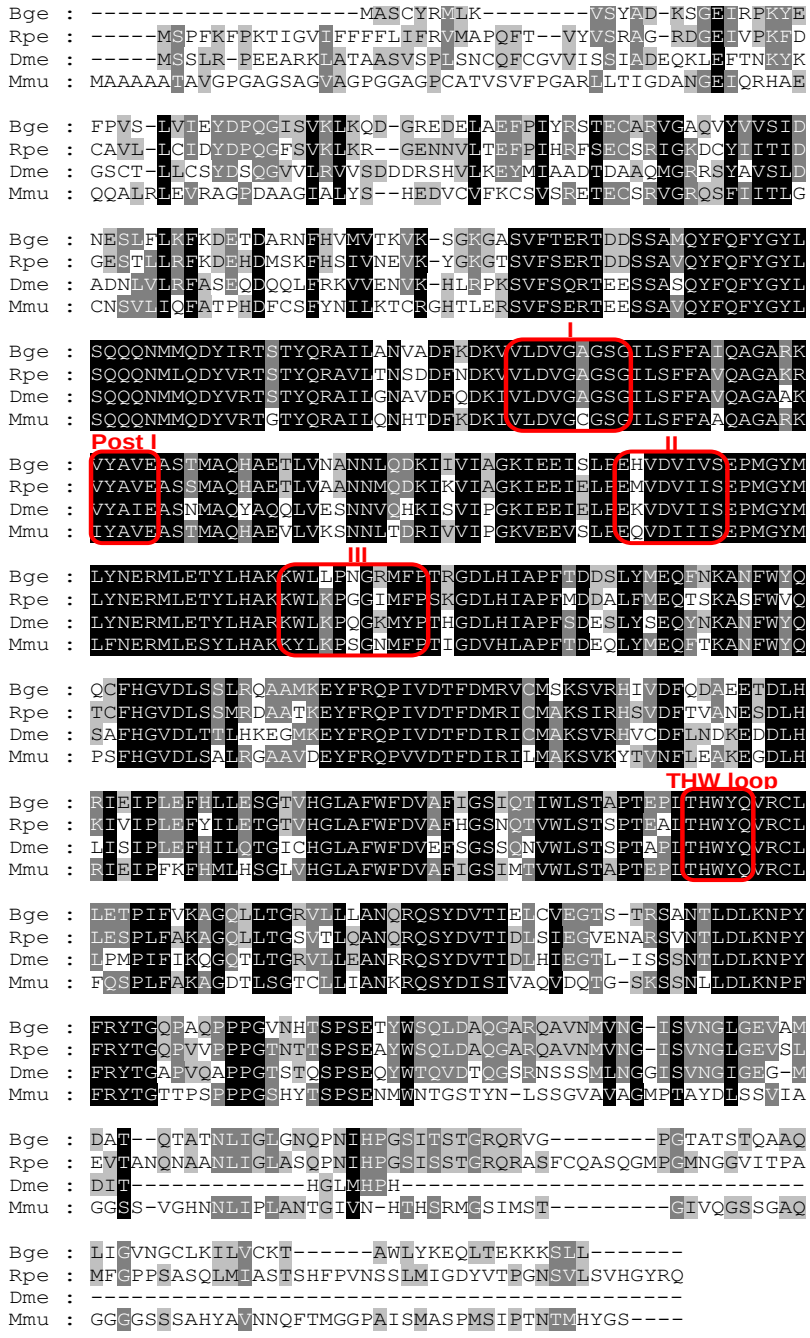

Figure 6.1: Amino acid sequence alignment of BgCARMER (Bge) with its orthologs from *R. pedestris* (Rpe), *D. melanogaster* (Dme), and *M. musculus* (Mmu). The four sequence motifs conserved among PRMTs and the TWH loop are boxed in red.

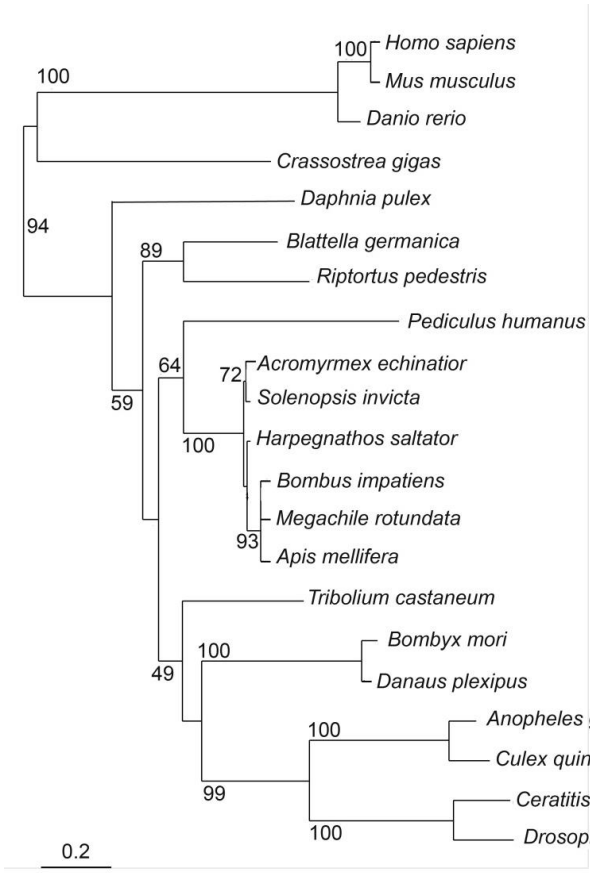

Figure 6.2: Maximum-likelihood phylogenetic tree showing the position of *B. germanica* CARMER with respect to CARM1/CARMER from other organisms. Scale bar represents the number of amino acid substitutions per site. Numbers at the nodes are bootstrap values (only bootstrap values higher than 45 are shown).

c) BgCARMER mRNA levels in ovaries progressively decrease from the last nymphal instar to the adult

The expression pattern of BgCARMER in ovaries during the last nymphal instar and the adult stage was measured by qRT-PCR (Figure 6.3A). As a whole, BgCARMER mRNA levels are higher

in the last nymphal instar than in the adult. The highest expression is found immediately after the moult to the sixth nymphal instar (nymph 6, day 0); on day 1 there is a pronounced decrease, but on day 2 the levels increase again. BgCARMER mRNA levels decrease gradually during the following days until day 6, when we find the lower expression in the sixth nymphal instar. On day 7 the mRNA level starts to increase again, reaching a peak just after the imaginal moult (adult day 0). In the following days the mRNA levels decrease rapidly, being minimal at the end of the cycle, when the oocytes are ready to be oviposited.

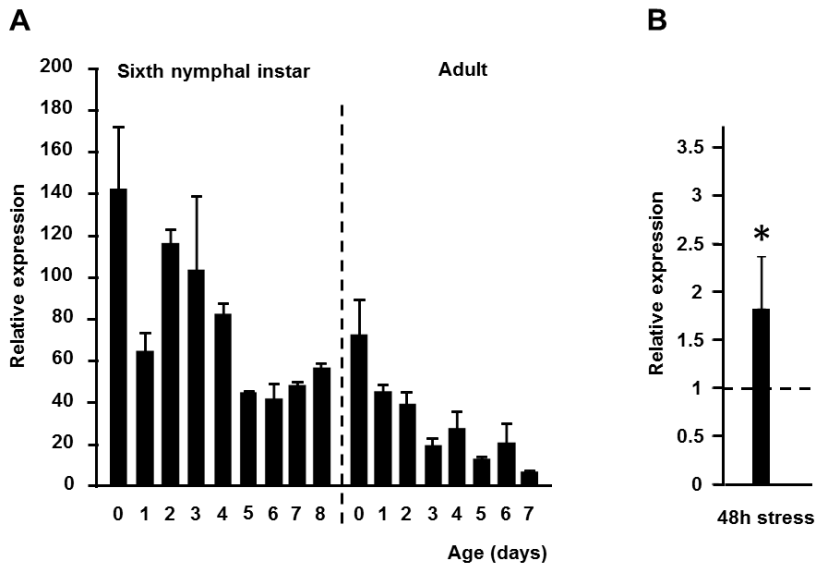

Figure 6.3: Expression of BgCARMER mRNA on *Blattella germanica* ovaries. A) Expression pattern during the sixth nymphal instar and the first reproductive cycle in the adult; qRT-PCR was performed using the expression of actin-5c as a reference; data represent 2-3 biological replicates and are expressed as copies of BgCARMER mRNA per 1000 copies of actin-5c mRNA. Dashed line is showing the moult to adult. **B)** Level of BgCARMER mRNA in ovaries from 5-day-old females subjected to 48h of hydric stress; qRT-PCR data represent 6 biological replicates and are normalized against control ovaries (reference value=1); expression of actin-5c was used as a reference. In all cases data are expressed as mean ± s.e.m.

BgCARMER was found in a transcriptome from ovaries belonging to females subjected to 48 h of hydric stress. To analyse whether it has a role in the ovary under such stress we performed an experiment repeating the conditions used in the construction of that transcriptome. Adult females were water-deprived at day 3 of the adult life, and dissected 48 h later. Control females were water-provided *ad libitum* and also dissected at day 5 of the adult life. BgCARMER mRNA levels were measured in ovaries from 5 day-old control and water-stressed females, revealing that BgCARMER is upregulated 48 h after the stress induction by a mean factor of 1.828 ($p<0.001$) (Figure 6.3B).

d) RNAi depletes BgCARMER expression in ovary

In order to investigate the role of BgCARMER in the ovary, we conducted an RNAi assay. Freshly ecdysed last instar female nymphs were injected into the abdomen with either 2.5 μg of dsBgCARMER or 2.5 μg of dsMock. Ovaries were dissected and BgCARMER mRNA levels were measured at different adult ages (Figure 6.4). BgCARMER mRNA levels were reduced in ovaries from freshly ecdysed adults by a mean factor of 0.6. In ovaries from 5- and 7-day-old adult females BgCARMER expression was reduced by a mean factor of 0.35 and 0.18, respectively, being these reductions statistically significant ($p<0.05$).

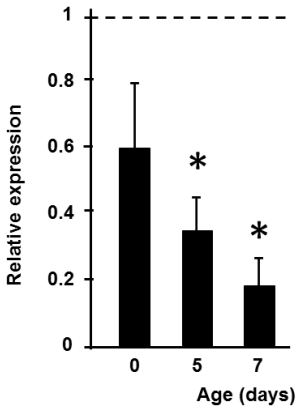

Figure 6.4: Levels of BgCARMER mRNA in ovaries from dsBgCARMER-treated females. Expression was measured in ovaries from 0-, 5-, and 7-day-old adult females; qRT-PCR data represent 2-3 biological replicates and are normalized against the control ovaries (reference value=1); expression of eIF4AIII was used as a reference. Data are expressed as mean ± s.e.m.

e) BgCARMER depletion reduces H3R17me2a in follicular cells

One of the known substrates of CARM1 and CARMER is H3R17, which is dimethylated asymmetrically (Cakouros et al., 2008; Wu and Xu, 2012). We thus wondered whether BgCARMER might be also responsible for this histone post-translational modification in *B. germanica* follicular cells. Ovaries from 5-day-old and 7-day-old females either dsMock-treated or dsBgCARMER-treated were immunolabelled with an antibody against H3R17me2a. In basal follicles of 5-day-old dsMock-treated females we found about one third of the total follicular cells labelled and they appeared clearly concentrated in the apical pole. At day 7 we still detected about one third of the cells labelled, but that accumulation in the apical pole

had disappeared (Figure 6.5A, C, E). In basal follicles of dsBgCARMER-treated females the number of follicle cells labelled in the whole follicle was strongly reduced at both ages, and we did not observe the typical accumulation of labelled cells in the apical pole in 5-day-old females (Figure 6.5B, D, F).

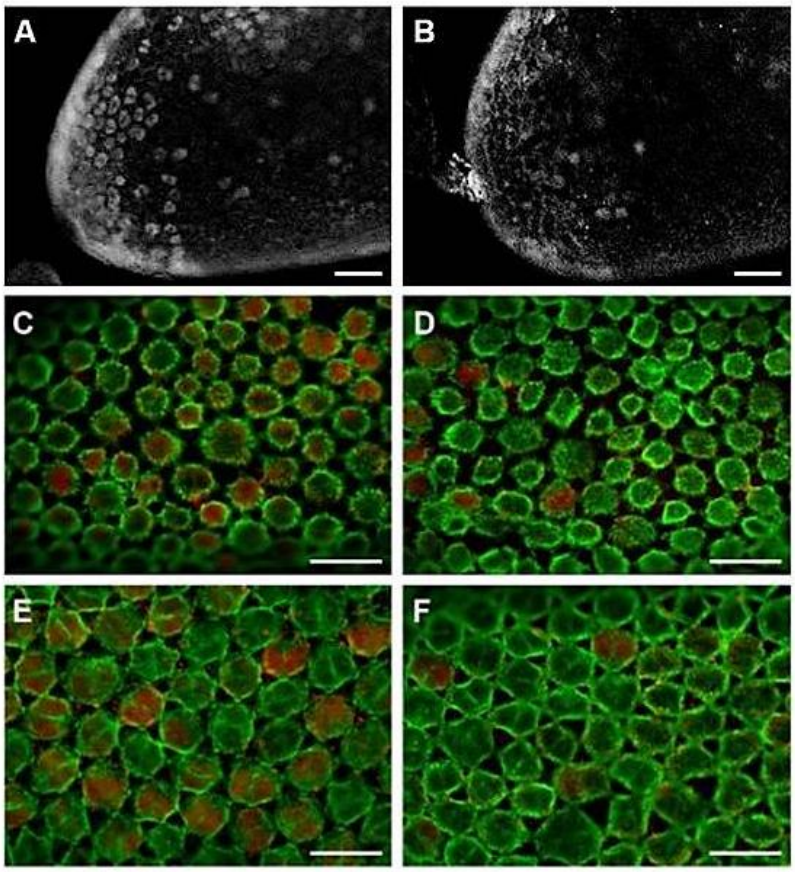

Figure 6.5: Effects of BgCARMER RNAi on H3R17me2a. A) Apical pole of the basal follicle from a 5-day-old dsMock-treated female. **B)** Apical pole of the basal follicle from a 5-day-old dsBgCARMER-treated female. **C)** Follicular epithelium of the basal follicle from 5-day-old dsMock-treated female. **D)** Follicular epithelium of the basal follicle from 5-day-old dsBgCARMER-treated female. **E)** Follicular epithelium of the basal follicle from 7-day-old dsMock-treated female. **F)** Follicular epithelium of the basal follicle from 7-day-old dsBgCARMER-treated female. H3R17me2a was revealed by immunofluorescence (light grey in A and B, red in C-F); actins (green in C-F) were stained with Phalloidin-TRITC. Scale bar: 50 µm.

f) BgCARMER depletion impairs ecdysis, oviposition, and ootheca carrying

From the total dsBgCARMER-treated females (n=52), a small percentage (7.7%) died during the moulting process, incapable of shed off the exuvia. Successfully ecdysed females were mated and monitored until nymphs from the first reproductive cycle hatched in dsMock females. From dsBgCARMER-treated surviving females (n=48), only 31.25% delivered offspring. The remaining specimens either dropped the ootheca before egg hatching (31.25%) or did not oviposit at all (37.5%).

Observing the basal follicles of dsBgCARMER- and dsMock-treated females, we did not find clear differences between both groups that might explain in the above reproductive defects. Ovarian follicles from dsBgCARMER-treated females developed normally and formed the chorion layers at the end of the cycle, just as ovarian follicles from control females.

g) BgCARMER depletion affects the expression of ecdysone-cascade genes and associated caspases

Given that in *D. melanogaster* CARMER enhances the transcription of genes induced by ecdysone (Cakouros et al., 2004), we wondered whether BgCARMER is also involved in the transcription of ecdysone-induced genes. In *B. germanica*, the level of 20-hydroxyecdysone (20E) in ovary peaks at the end of the first

gonadotrophic cycle (Pascual et al., 1992), and triggers the expression of a cascade of transcription factors, and among them the three nuclear receptors E75A, HR3 and FTZ-F1 (Cruz, 2005; Mane-Padros et al., 2008). Thus, we analysed their expression in ovaries from 7-day-old dsMock- and dsBgCARMER-treated females. E75A mRNA levels increased by a mean factor of 5.12, and FTZ-F1 and HR3 mRNA levels were reduced by a mean factor of 0.36 and 0.43 respectively, although none of these changes in the expression levels were statistically significant due to the high standard deviation of the measurements (Figure 6.6A).

CARMER is needed for the expression of caspases induced by ecdysone during *D. melanogaster* metamorphosis (Cakouros et al., 2004), and also in *B. germanica*, programmed cell death is controlled by ecdysteroids as shown in the case of prothoracic gland degeneration during metamorphosis (Mane-Padros et al., 2010). With this antecedent in mind, we analysed the expression level of the effector caspase 1 and the initiator caspase 5, in 7-day-old females that were dsMock- or dsBgCARMER-treated. Both caspases were under-expressed, caspase 1 by a mean factor of 0.46, and caspase 5 by a mean factor of 0.85, although none of those changes was statistically significant (Figure 6.6B).

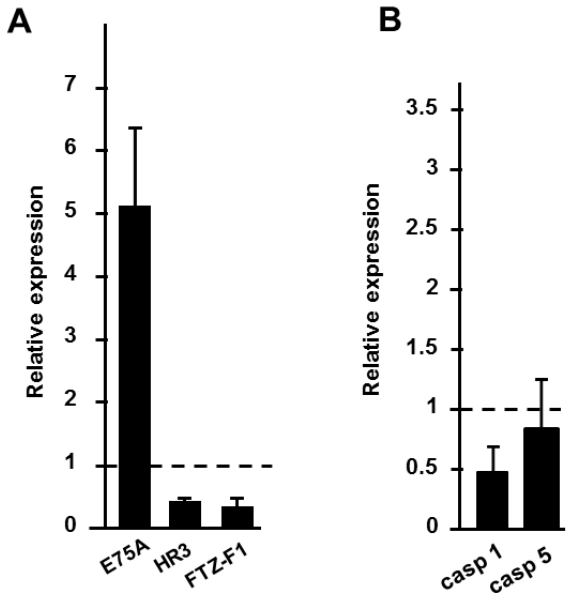

Figure 6.6: Effects of BgCARMER RNAi on expression of other genes. A) mRNA levels of, E75A, HR3 and FTZ-F1 (E75A, HR3 and FTZ-F1, respectively) in ovaries from 7-day-old dsBgCARMER-treated females. **B)** mRNA levels of caspase 1 and caspase 5 (casp 1 and casp 5, respectively) in ovaries from 7-day-old dsBgCARMER-treated females. qRT-PCR data represent 3 biological replicates and are normalized against control ovaries (reference value=1); expression of eIF4AIII was used as a reference. In all cases data are expressed as mean ± s.e.m.

6.5. Discussion

We have characterized an ortholog of the genes encoding mammalian CARM1 (coactivator-associated arginine methyltransferase 1) and *D. melanogaster* CARMER (coactivator Arg methyltransferase for EcR/Usp) that is present in *B. germanica* ovaries. CARM1/CARMER proteins belong to the PRMT (protein arginine methyltransferases) family, thus they are also known as PRMT4. We have named the gene BgCARMER to follow the

nomenclature used in *D. melanogaster*. All members of PRMT family share a well conserved catalytic core region that contains 4 conserved amino acid motifs as well as a THW loop (Frankel et al., 2002; Zhang et al., 2000), which are also present in BgCARMER. Besides, secondary structure predictions indicated that BgCARMER holds the CARM1 characteristic N-terminal domain (Teyssier et al., 2002), confirming that it is a ortholog of CARM1.

Phylogenetic analyses showed that BgCARMER is well conserved across animal evolution, not only among insects but in all organisms studied, which suggests that its function is also conserved and important. Our results are coherent with a previous study on PRMTs phylogeny, which showed that CARM1/CARMER are well conserved among metazoans; indeed it is the second PRMT best conserved after PRMT1 (Wang and Li, 2011). Both proteins cooperate in activating transcription (Lee et al., 2002).

CARM1 and its ortholog CARMER induce H3R17me2a (Cakouros et al., 2008; Wu and Xu, 2012). To investigate whether BgCARMER exert also this function, we analysed the occurrence of H3R17me2a in the follicular epithelium of ovaries from dsMock- and dsBgCARMER-treated females. In general terms, we found less cells labelled with H3R17me2a antibody in the follicular epithelium of ovaries from dsBgCARMER-treated females. Thus, we can conclude that the protein encoded by BgCARMER is needed for this methylation, as occurs with their orthologs in other species. Of

particular interest is the observation that H3R17me2a is predominant in the apical pole of follicles of 5-day-old control females, and this abundance is lost in follicles of dsBgCARMER-treated females of the same age. Previous researches in our laboratory indicate that the follicular cells of the apical pole change its cellular program at day 5. This change is needed for the future formation of crucial structures in the egg, like the sponge-like body, a respiratory device essential for egg viability that is built up thanks to the gene *Brownie* (Irles et al., 2009). Based on our results showing that H3R17me2a is strongly reduced in apical cells of basal follicles of dsBgCARMER-treated females, together with the fact that ca.70 % of dsBgCARMER-treated females were unable to give offspring, we hypothesize that H3R17me2a is involved in the aforementioned change of follicular cells program.

In *D. melanogaster*, CARMER binds to the EcR/Usp receptor and is required for the transduction of the ecdysone signalling (Cakouros et al., 2004). In our experiments, BgCARMER mRNA depletion provoked the death of 7.7% of females during the ecdysis process, which is coherent with this function, given that deficiencies in the transduction of the ecdysone signal often led to unproper ecdysis (see, for example, Cruz et al., 2006). We presume that BgCARMER expression was still high at the end of the nymphal stage because levels were higher in 0-day-old adults than in 5-day-old and 7-day-old adults. This could explain the low penetrance of mortality during ecdysis.

Moreover, BgCARMER mRNA depletion prevented reproduction in ca. 70% of the females. The results about ecdysis and reproduction again suggest that BgCARMER is involved in the transduction of the ecdysone signalling in *B. germanica* in reproductive processes. To further explore this hypothesis we measured the mRNA expression in the ovaries of 3 representative genes of the 20E signalling cascade: E75A, HR3 and FTZ-F1. In the same line, we also measured the expression levels of an initiator and an effector caspase (caspase 5 and caspase 1, respectively), because 20E induces the transcription of cell death genes in insects (reviewed by Buszczak and Segraves, 2000) and in *D. melanogaster* CARMER is necessary for this ecdysone-induced transcription (Cakouros et al., 2004). In *B. germanica*, high levels of 20E induce E75 and HR3 expression. HR3 is necessary for the activation of FTZ-F1, which is involved in caspase expression (Mane-Padros et al., 2010). Double negative feedback occurs between E75 and HR3: E75 represses the activation of HR3, and HR3 indirectly (through HR4) represses E75 activation (Martin, 2010). Our results show that in dsBgCARMER-treated females the levels of HR3, FTZ-F1, caspase 1 and caspase 5 are lower than in control females, which suggest that BgCARMER is needed for the transduction of the 20E signalling, as occurs in *D. melanogaster*. The high levels of E75A observed in dsBgCARMER-treated specimens could be explained as a late result of the reduction of the indirect repression exerted by HR3. Expression of caspase 1 seems more clearly dependent on BgCARMER action than expression of caspase 5, as it experienced a higher reduction upon BgCARMER mRNA depletion. We assume

that *B. germanica* caspase 1 is an effector caspase and *B. germanica* caspase 5 is an initiator caspase based on their homology with lepidopteran caspases 1 and 5, which cluster with the *D. melanogaster* effector caspases DRICE and DCP-1, and the initiator caspase DRONC, respectively (Courtiade et al., 2011).

BgCARMER mRNA was overexpressed 48 h after water deprivation, which suggests that it plays a role in the response to hydric stress. Previous work (unpublished, see chapter 2) showed that *B. germanica* ovarian basal follicles undergo degeneration upon hydric stress conditions, while activated caspases are present in dying follicles. BgCARMER overexpression in ovaries of water-stressed females may be responsible for an increase in effector caspases, which, in turn, would lead to the resorption processes undertaken by the ovarian basal follicles. To our knowledge, this is the first time that a CARM1/CARMER ortholog overexpression is reported upon stress conditions, although studies conducted in humans have shown that CARM1 expression increased in different cancers, a situation where homeostasis is also finally lost (Cheng et al., 2013; Kim et al., 2010; Osada et al., 2013).

6.6. References

Bauer, U. M., Daujat, S., Nielsen, S. J., Nightingale, K. and Kouzarides, T. (2002). Methylation at arginine 17 of histone H3 is linked to gene activation. *EMBO Rep* **3**, 39-44.

Bedford, M. T. and Richard, S. (2005). Arginine methylation an emerging regulator of protein function. *Mol Cell* **18**, 263-72.

Buszczak, M. and Segraves, W. A. (2000). Insect metamorphosis: out with the old, in with the new. *Curr Biol* **10**, R830-3.

Cakouros, D., Daish, T. J., Mills, K. and Kumar, S. (2004). An arginine-histone methyltransferase, CARMER, coordinates ecdysone-mediated apoptosis in *Drosophila* cells. *J Biol Chem* **279**, 18467-71.

Cakouros, D., Mills, K., Denton, D., Paterson, A., Daish, T. and Kumar, S. (2008). dLKR/SDH regulates hormone-mediated histone arginine methylation and transcription of cell death genes. *J Cell Biol* **182**, 481-95.

Courtiade, J., Pauchet, Y., Vogel, H. and Heckel, D. G. (2011). A comprehensive characterization of the caspase gene family in insects from the order Lepidoptera. *BMC Genomics* **12**, 357.

Cruz, J. (2005). Receptores nucleares implicados en la regulación endocrina en *Blattella germanica* (L) (Dictyoptera, Blattellidae). Caracterización de los genes BgEcR-A, BgHR3 y BgFTZ-F1. PhD Thesis. In *Departamento de Fisiologia. Facultad de Biología*. Barcelona: Universidad de Barcelona.

Cruz, J., Mane-Padros, D., Belles, X. and Martin, D. (2006). Functions of the ecdysone receptor isoform-A in the hemimetabolous insect Blattella germanica revealed by systemic RNAi in vivo. *Dev Biol* **297**, 158-71.

Cheng, D., Cote, J., Shaaban, S. and Bedford, M. T. (2007). The arginine methyltransferase CARM1 regulates the coupling of transcription and mRNA processing. *Mol Cell* **25**, 71-83.

Cheng, H., Qin, Y., Fan, H., Su, P., Zhang, X., Zhang, H. and Zhou, G. (2013). Overexpression of CARM1 in breast cancer is correlated with poorly characterized clinicopathologic parameters and molecular subtypes. *Diagn Pathol* **8**, 129.

Chevillard-Briet, M., Trouche, D. and Vandel, L. (2002). Control of CBP co-activating activity by arginine methylation. *EMBO J* **21**, 5457-66.

Frankel, A., Yadav, N., Lee, J., Branscombe, T. L., Clarke, S. and Bedford, M. T. (2002). The novel human protein arginine N-methyltransferase PRMT6 is a nuclear enzyme displaying unique substrate specificity. *J Biol Chem* **277**, 3537-43.

Glass, C. K. and Rosenfeld, M. G. (2000). The coregulator exchange in transcriptional functions of nuclear receptors. *Genes Dev* **14**, 121-41.

Guindon, S., Delsuc, F., Dufayard, J. F. and Gascuel, O. (2009). Estimating maximum likelihood phylogenies with PhyML. *Methods Mol Biol* **537**, 113-37.

Herraiz, A., Chauvigne, F., Cerda, J., Belles, X. and Piulachs, M. D. (2011). Identification and functional characterization of an ovarian aquaporin from the cockroach *Blattella germanica* L. (Dictyoptera, Blattellidae). *J Exp Biol* **214**, 3630-8.

Irles, P., Belles, X. and Piulachs, M. D. (2009). Brownie, a gene involved in building complex respiratory devices in insect eggshells. *PLoS One* **4**, e8353.

Kim, Y. R., Lee, B. K., Park, R. Y., Nguyen, N. T., Bae, J. A., Kwon, D. D. and Jung, C. (2010). Differential CARM1 expression in prostate and colorectal cancers. *BMC Cancer* **10**, 197.

Kuhn, P., Xu, Q., Cline, E., Zhang, D., Ge, Y. and Xu, W. (2009). Delineating *Anopheles gambiae* coactivator associated arginine methyltransferase 1 automethylation using top-down high resolution tandem mass spectrometry. *Protein Sci* **18**, 1272-80.

Lee, Y. H., Koh, S. S., Zhang, X., Cheng, X. and Stallcup, M. R. (2002). Synergy among nuclear receptor coactivators: selective requirement for protein methyltransferase and acetyltransferase activities. *Mol Cell Biol* **22**, 3621-32.

Letunic, I., Doerks, T. and Bork, P. (2012). SMART 7: recent updates to the protein domain annotation resource. *Nucleic Acids Res* **40**, D302-5.

Ma, H., Baumann, C. T., Li, H., Strahl, B. D., Rice, R., Jelinek, M. A., Aswad, D. W., Allis, C. D., Hager, G. L. and Stallcup, M. R. (2001). Hormone-dependent, CARM1-directed, arginine-specific methylation of histone H3 on a steroid-regulated promoter. *Curr Biol* **11**, 1981-5.

Mane-Padros, D., Cruz, J., Vilaplana, L., Nieva, C., Urena, E., Belles, X. and Martin, D. (2010). The hormonal pathway controlling cell death during metamorphosis in a hemimetabolous insect. *Dev Biol* **346**, 150-60.

Mane-Padros, D., Cruz, J., Vilaplana, L., Pascual, N., Belles, X. and Martin, D. (2008). The nuclear hormone receptor BgE75 links molting and developmental progression in the direct-developing insect *Blattella germanica*. *Dev Biol* **315**, 147-60.

Martin, D. (2010). Functions of Nuclear receptors in Insect Development. In *Nuclear Receptors*, (eds. C. M. Bunce and M. J. Campbell), pp 31-61. Amsterdam: Springer Netherlands.

McKenna, N. J., Xu, J., Nawaz, Z., Tsai, S. Y., Tsai, M. J. and O'Malley, B. W. (1999). Nuclear receptor coactivators: multiple enzymes, multiple complexes, multiple functions. *J Steroid Biochem Mol Biol* **69**, 3-12.

Osada, S., Suzuki, S., Yoshimi, C., Matsumoto, M., Shirai, T., Takahashi, S. and Imagawa, M. (2013). Elevated expression of coactivator-associated arginine methyltransferase 1 is associated with early hepatocarcinogenesis. *Oncol Rep* **30**, 1669-74.

Pahlich, S., Zakaryan, R. P. and Gehring, H. (2006). Protein arginine methylation: Cellular functions and methods of analysis. *Biochim Biophys Acta* **1764**, 1890-903.

Pascual, N., Cerdá, X., Benito, B., Tomás, J., Piulachs, M. D. and Belles, X. (1992). Ovarian ecdysteroid levels and basal oöcyte development during maturation in the cockroach *Blattella germanica* (L.). *J Insect Physiol* **38**, 339-348.

Pfaffl, M. W., Horgan, G. W. and Dempfle, L. (2002). Relative expression software tool (REST) for group-wise comparison and statistical analysis of relative expression results in real-time PCR. *Nucleic Acids Res* **30**, e36.

Stallcup, M. R., Kim, J. H., Teyssier, C., Lee, Y. H., Ma, H. and Chen, D. (2003). The roles of protein-protein interactions and protein methylation in transcriptional activation by nuclear receptors and their coactivators. *J Steroid Biochem Mol Biol* **85**, 139-45.

Teyssier, C., Chen, D. and Stallcup, M. R. (2002). Requirement for multiple domains of the protein arginine methyltransferase CARM1 in its transcriptional coactivator function. *J Biol Chem* **277**, 46066-72.

Troffer-Charlier, N., Cura, V., Hassenboehler, P., Moras, D. and Cavarelli, J. (2007). Functional insights from structures of coactivator-associated arginine methyltransferase 1 domains. *EMBO J* **26**, 4391-401.

Wang, Y. C. and Li, C. (2011). Evolutionarily conserved protein arginine methyltransferases in non-mammalian animal systems. *FEBS J* **279**, 932-45.

Wu, J. and Xu, W. (2012). Histone H3R17me2a mark recruits human RNA polymerase-associated factor 1 complex to activate transcription. *Proc Natl Acad Sci U S A* **109**, 5675-80.

Zhang, X., Zhou, L. and Cheng, X. (2000). Crystal structure of the conserved core of protein arginine methyltransferase PRMT3. *EMBO J* **19**, 3509-19.

6.7. Supplementary information

Supplementary Table 6.S1. List of oligonucleotides used as primers in the experimental work.

	Primer name	Primer sequence
BgCARMER sequencing	BgCARMER_Fw1	5'ATCTGAGCCAATGGGCTACA3'
	BgCARMER_Fw2	5'GCTATGCGTCGAAGGAACAA3'
	BgCARMER_Fw3	5'CACCTTGGACCTGAAGAATC3'
	BgCARMER_Fw4	5'CAGCTTATTGGAGTGAATGG3'
	BgCARMER_Rv	5'CCNGTRTATCKRAAGTA3'
dsBgCARMER synthesis	BgCARMER_dsRNA_Fw	5'CGGTTACTTGTCACAACAGCA3'
	BgCARMER_dsRNA_Rv	5'TGTAGCCCATTGGCTCAGAT 3'
BgCARMER qRT-PCR	BgCARMERRT_Fw	5'AATCCGGTAAGGGTGCTTCCT3'
	BgCARMERRT_Rv	5'TGGAAATATTGCATGGCAGA3'
FTZ-F1 qRT-PCR	FTZ-F1_RT_Fw	5'TTGTCACATCGACAAGACGCA3'
	FTZ-F1_RT_Rv	5'GTACATCGGGCCGAATTTGTTTCT3'
HR3-A qRT-PCR	HR3-A_RT_Fw	5'GATGAGCTGCTCTTAAAGGCGAT3'
	HR3-A_RT_Rv	5'AGGTGACCGAACTCCACATCTC3'
E75-A qRT-PCR	E75-A_RT_Fw	5'GTGCTATTGAGTGTGCGACATGAT3'
	E75-A_RT_Rv	5'TCATGATCCCTGGAGTGGTAGAT3'
Caspase 1 qRT-PCR	Casp1_RT_Fw	5'AAGCGGAAGGATTCATACCA3'
	Casp1 _RT_Rv	5'GATGACTGCCTTGCCTCTTC3'
Caspase 5 qRT-PCR	Casp5_RT_Fw	5'ACACCTTGTGGACTCCTTGC3'
	Casp1_RT_Rv	5'TACGTTGCGTGGATTCTGTC3'

```
   1 TCGCGGATCCGAACACTGCGTTTGCTGGCTTTGATGCAATCTGCCATGCAATATTTCCAG  60
  61 AACACTGCGTTTGCTGGCTTTGATGAAAATTTTTTTTTCTGAGACGATCTGAATGTGAAC 120
 121 TATTCTCTTGGTAGAGCGTTATAAAatggcgtcttgttaccgcatgctaaaggtatcgta 180
   1                        M  A  S  C  Y  R  M  L  K  V  S  Y  12
 181 cgcagataaaagtggcgaaattcgtcctaaatatgagttccccgtaagtttagtcatcga 240
  13  A  D  K  S  G  E  I  R  P  K  Y  E  F  P  V  S  L  V  I  E  32
 241 gtatgatcctcagggaatcagcgtcaaattgaagcaagatggtcgtgaagatgaacttgc 300
  33  Y  D  P  Q  G  I  S  V  K  L  K  Q  D  G  R  E  D  E  L  A  52
 301 cgagttccccatataccggtcaacggaatgcgcaagagttggtgcacaagtttatgtagt 360
  53  E  F  P  I  Y  R  S  T  E  C  A  R  V  G  A  Q  V  Y  V  V  72
 361 atccatagataatgagtccttattcttgaagtttaaagatgaaaccgatgcaagaaattt 420
  73  S  I  D  N  E  S  L  F  L  K  F  K  D  E  T  D  A  R  N  F  92
 421 tcatgtgatggtgaccaaagtaaaatccggtaagggtgcttctgtgttcacggagagaac 480
  93  H  V  M  V  T  K  V  K  S  G  K  G  A  S  V  F  T  E  R  T 112
 481 ggacgactcgtctgccatgcaatatttccarttttacggttacttgtcacaacagcaaaa 540
 113  D  D  S  S  A  M  Q  Y  F  Q  F  Y  G  Y  L  S  Q  Q  Q  N 132
 541 tatgatgcaagattacattcgtacaagcacataccagcgtgctatattagctaatgttgc 600
 133  M  M  Q  D  Y  I  R  T  S  T  Y  Q  R  A  I  L  A  N  V  A 152
 601 tgattttaaggacaaagtcgtactagatgttggtgcaggatcaggcattctatccttttt 660
 153  D  F  K  D  K  V  V  L  D  V  G  A  G  S  G  I  L  S  F  F 172
 661 tgctattcaagcgggtgctagaaaggtgtatgccgtagaagctagcacaatggctcagca 720
 173  A  I  Q  A  G  A  R  K  V  Y  A  V  E  A  S  T  M  A  Q  H 192
 721 tgcagaaacactagtgaatgcaaataatttgcaagacaaaattattgtaattgctgggaa 780
 193  A  E  T  L  V  N  A  N  N  L  Q  D  K  I  I  V  I  A  G  K 212
 781 gatagaggaaatttcactccccgaacatgtggatgttatagtatctgagccaatgggcta 840
 213  I  E  E  I  S  L  P  E  H  V  D  V  I  V  S  E  P  M  G  Y 232
 841 catgctttataacgaacggatgttggaaacgtatctacatgcaaagaagtggcttcttcc 900
 233  M  L  Y  N  E  R  M  L  E  T  Y  L  H  A  K  K  W  L  L  P 252
 901 aaatggccggatgttccccacaagaggggatttgcatattgctccattcactgacgatag 960
 253  N  G  R  M  F  P  T  R  G  D  L  H  I  A  P  F  T  D  D  S 272
 961 cttatacatggaacaattcaataaagctaacttttggtaccagcagtgttttcatggggt 1020
 273  L  Y  M  E  Q  F  N  K  A  N  F  W  Y  Q  Q  C  F  H  G  V 292
1021 tgatttaagcagtcttcggcaggcagccatgaaagaatattttcgacaacccattgttga 1080
 293  D  L  S  S  L  R  Q  A  A  M  K  E  Y  F  R  Q  P  I  V  D 312
1081 cactttcgatatgagagtgtgcatgtccaaatctgtacgacatattgtcgactttcagga 1140
 313  T  F  D  M  R  V  C  M  S  K  S  V  R  H  I  V  D  F  Q  D 332
1141 tgccgaggaaactgatttacaccgaatcgagatcccattagaatttcatctcttggaatc 1200
 333  A  E  E  T  D  L  H  R  I  E  I  P  L  E  F  H  L  L  E  S 352
1201 tggaacggttcatggtctggctttctggttcgatgttgcatttataggctccattcaaac 1260
 353  G  T  V  H  G  L  A  F  W  F  D  V  A  F  I  G  S  I  Q  T 372
1261 gatatggttgtcgacggctccaacagaacctttaacacattggtaccaggtccggtgcct 1320
 373  I  W  L  S  T  A  P  T  E  P  L  T  H  W  Y  Q  V  R  C  L 392
1321 tcttgaaactccgatttttgtgaaagctggtcaactgcttaccggaagggtgcttctcct 1380
 393  L  E  T  P  I  F  V  K  A  G  Q  L  L  T  G  R  V  L  L  L 412
1381 tgctaaccagcggcaaagctacgacgtcactattgagctatgcgtcgaaggaacaagcac 1440
 413  A  N  Q  R  Q  S  Y  D  V  T  I  E  L  C  V  E  G  T  S  T 432
1441 gcgctctgcaaacaccttggacctgaagaatccatacttccgrtacacsggwcagcctgc 1500
 433  R  S  A  N  T  L  D  L  K  N  P  Y  F  R  Y  T  G  Q  P  A 452
1501 tcaacccctccaggagtaaaccatacgtcgccgagtgaaacgtactggagccagcttga 1560
 453  Q  P  P  P  G  V  N  H  T  S  P  S  E  T  Y  W  S  Q  L  D 472
1561 tgctcagggagcgcgacaagccgtgaacatggtgaatggaatttcggtcaacggcctagg 1620
 473  A  Q  G  A  R  Q  A  V  N  M  V  N  G  I  S  V  N  G  L  G 492
1621 agaagtggctatggatgcgacgcagacagctacaaatctcatcggactgggaaaccagcc 1680
 493  E  V  A  M  D  A  T  Q  T  A  T  N  L  I  G  L  G  N  Q  P 512
1681 gaacatccatcccggttccattacaagcacgggacgccaaagagtgggacctggaacggc 1740
 513  N  I  H  P  G  S  I  T  S  T  G  R  Q  R  V  G  P  G  T  A 532
1741 aacttctacccaggcggcgcagcttattggagtgaatggttgtttgaagatattagtatg 1800
 533  T  S  T  Q  A  A  Q  L  I  G  V  N  G  C  L  K  I  L  V  C 552
1801 taagactgcgtggttgtacaaagaacagttgactgaaaaaaaaaaatcactgctatgaAA 1860
 553  K  T  A  W  L  Y  K  E  Q  L  T  E  K  K  K  S  L  L  *   570
1861 AAAAAAAAACCTATAGTGAGTCGTATTAATTCGGATCCGCGACACCTTGGACCTGAAGAA 1920
1921 TCACCTTGGACCTGAAGAATCCATACTTCCGGTACACGGGTCAGCCTGCTCAACCCCCTC 1980
1981 CAGGAGTAAACCATACGTCGCCGAGTGAAACGTACTGGAGCCAGCTTGATGCTCAGGGAG 2040
2041 CGCGACAAGGTGAGTATGGTTATGGTTACTATTCTTCCAATTATACATTCAATTAATGCT 2100
2101 TTTGTTTAAAAAAAAAAAAAAAAAAAAAAAAAAAAAAAA 2139
```

Figure 6.S1: Nucleotide and amino acid sequence of BgCARMER

7. DISCUSSION AND FINAL REMARKS

7.1. Discussion

Water balance and desiccation tolerance in insects is not a new research field; these aspects have been widely studied, especially in natural populations that undergo resting periods to survive when environment is hostile (reviewed by Benoit, 2010). However, in recent years, there has been an increasing interest in the study of hydric stress in insects in the context of Global Change, as variations in precipitation and water availability can profoundly affect insect distribution, fitness and survival (Chown et al., 2011).

The study of hydric stress in insects can be addressed through many different approaches. Several previous studies conducted in laboratory animals were based in the measurement of physiological and metabolic parameters, like water loss, cuticular permeability and ion content of the haemolymph (Folk and Bradley, 2003; Wall, 1970; Woods and Harrison, 2001). Some studies conducted in natural populations also investigated behavioural and ecological differences that could explain the differential tolerance to desiccation between closely related species, for instance different moisture preferences in two sympatric species of termites (Hu et al., 2012) or different troglobitic adaptations in 3 species of cave crickets (Yoder et al., 2011).

Molecular approaches to the subject have been mainly used in species known to face desiccation, either as a cryoprotective strategy or because their living in a highly dry environment. Most of

these works showed that there is an up-regulation of heat shock proteins and metabolic genes during desiccation (Cornette et al., 2010; Rajpurohit et al., 2013; Thorne et al., 2011). However, recent transcriptome-based studies in two polar species, the Antarctic midge *Belgica antarctica* and the Arctic springtail *Megaphorura arctica*, showed small overlap in gene expression, suggesting different transcriptomic responses to similar desiccation conditions, which makes the search for general molecular markers of hydric stress a challenging issue (Teets et al., 2012).

Our work aimed at establishing the grounds for further research of the early effects of water deprivation in a model insect, having in mind the long-term objective of finding general molecular markers of hydric stress in insects. To this end, we selected the ovary of a well-known cockroach model to undertake this research because it is known that insect females from most species readily sacrifice unfertilized eggs when environmental conditions are hostile (Papaj, 2000; Rosenheim et al., 2000).

Prior to undertake molecular analyses, we assessed the phenotypic effects caused by hydric stress in the ovaries. We found that when *B. germanica* adult females face water deprivation at the onset of vitellogenesis, they sacrifice the basal ovarian follicles, which either do not mature or degenerate, and finally die. Caspases appear to play a role in this response, as high concentration of activated caspases was observed in follicular cells of apparently normal basal follicles 24 h after water deprivation, as well as in degenerating

follicles 48 h after water deprivation and later on. Several biotic and abiotic stresses provoke ovarian degeneration in different insect species (Barrett et al., 2008; Bodin et al., 2009; Guo et al., 2011; Kotaki, 2003); thus we presumed that hydric stress would also cause this effect in insects like it does in *B. germanica*.

After assessing that hydric stress provokes fatal effects in ovaries, we wondered on molecular mechanisms underlying these effects, thus we started to look for molecular markers. When tackling the study of molecular markers of hydric stress it seems logical to consider aquaporins (AQPs), as they are membrane proteins directly involved in water balance that play key roles in dehydration in insects (Campbell et al., 2008; Chown et al., 2011). A number of previous studies showed changes in mRNA and protein expression of insect AQPs during desiccation (Clark et al., 2009; Kikawada et al., 2008; Philip et al., 2008). We identified an AQP in the ovary of *B. germanica*, demonstrated that it is functional, and analysed its mRNA expression during hydric stress, which remained unaltered. This result, together with that obtained by Goto et al. (2011), who did not find expression changes of an AQP in *B. antarctica* during dehydration or rehydration, led us conclude that AQPs expression cannot be reliable molecular markers of hydric stress.

The study of miRNAs appeared to be more promising, as most of them showed a change of expression under hydric stress. MiRNAs fine-tune gene expression at post-transcriptional level, by interacting with target mRNAs (Belles et al., 2012). Thus, they may

rapidly respond to environmental changes. The analysis of miRNAs in water-stressed specimens can be addressed through different strategies; one approach is to study the expression of miRNAs upon hydric stress induction; the other is based on selecting a few miRNA candidates and studying them functionally, in order to infer its possible role in the hydric stress response. Our study included both approaches. First, we obtained a miRNA library to know which miRNAs were present in stressed ovaries, and from this library, we identified 26 canonical miRNAs in ovaries of 5-day-old females subjected to 48 h of hydric stress. Then, we selected 13 of them to analyse its differential expression under hydric stress conditions and most of them showed expression changes associated with the stress. As expected, miRNAs described as pro-apoptotic, like miR-1-3p, miR-184-3p, miR-34-5p, and let-7-5p (Foley et al., 2010; Li et al., 2012; Qin et al., 2012; Tarasov et al., 2007), were up-regulated. Finally, we selected one of those overexpressed miRNAs known to be involved in cell death, miR-34-5p, to study it functionally.

We knocked down miR-34-5p to investigate its function in the ovary and its possible role in the hydric stress response, but we did not find clear phenotypic effects. Although disappointing at first, this result was not completely surprising as miRNAs have subtle effects and is usual that knock down of a single miRNA do not lead to strong phenotypes (Leung and Sharp, 2010). Subsequently, we predicted putative miR-34-5p mRNA targets as a way to infer the physiological function of this particular miRNA. We found that one

of the predicted targets, BgWindei, was overexpressed in miR-34-5p knocked-down samples, which suggests that it is a functional miR-34-5p target. Therefore, we considered it for a deeper analysis.

We studied BgWindei function in the ovary, and analysed its expression under hydric stress conditions. BgWindei was under-expressed 48 h after hydric stress induction, although differences with respect to controls were not statistically significant. This result is consistent with the overexpression of miR-34-5p in the same conditions, and provides another observation supporting the hypothesis that miR-34-5p regulates BgWindei. Our functional studies revealed that BgWindei is needed for the trimethylation of lysine 9 in histone H3 (H3K9me3), as described in its *Drosophila melanogaster* ortholog (Koch et al., 2009). This epigenetic mark is related to transcriptional repression (Martin and Zhang, 2005) and, indeed, we observed an overall mRNA overexpression after silencing BgWindei, except in the case of chorion-related genes. We propose that a down-regulation of BgWindei under hydric stress conditions contributes to activate the transcription of genes related with the stress response, although the complete picture will be presumably complex, as we have seen the up-regulation of genes known to be both pro-apoptotic, like hippo (Harvey et al., 2003), and anti-apoptotic, like yorkie or cut (Zhai et al., 2012; Zhang and Cohen, 2013).

In the context of a general project of our laboratory, we obtained two transcriptomes from ovaries of 5-day-old females, one from

control females and the other from females subjected to 48 h of hydric stress. The comparison of both transcriptomes led us to choose another candidate, BgCARMER, which appeared over-expressed in the transcriptome from water-stressed specimens. The results obtained with BgWindei led us to the study epigenetic-related genes as candidate markers of hydric stress. Interestingly, BgCARMER is an ortholog of mammalian CARM1 and *D. melanogaster* CARMER, which are arginine methyltransferases involved in transcriptional activation (Cakouros et al., 2004; Wu and Xu, 2012), thus we decided to study this candidate more thoroughly. We analysed BgCARMER function in ovary, and confirmed that it was overexpressed 48 h after hydric stress induction, being this result statistically significant. Based on our result showing that silencing of BgCARMER provoked the down-regulation of caspase 1 and, to a lesser extent, caspase 5, we propose that the up-regulation of BgCARMER is one of the first steps of the apoptotic response triggered by hydric stress.

7.2. References

Barrett, E. L., Preziosi, R. F., Moore, A. J. and Moore, P. J. (2008). Effects of mating delay and nutritional signals on resource recycling in a cyclically breeding cockroach. *J Insect Physiol* **54**, 25-31.

Belles, X., Cristino, A. S., Tanaka, E. D., Rubio, M. and Piulachs, M. D. (2012). Insect MicroRNAs: From Molecular Mechanisms to Biological Roles. In *Insect Molecular Biology and*

Biochemistry (ed. L. Gilbert), pp 30-56. Amsterdam: Elsevier-Academic Press.

Benoit, J. B. (2010). Water management by dormant insects: comparisons between dehydration resistance during summer aestivation and winter diapause. *Prog Mol Subcell Biol* **49**, 209-29.

Bodin, A., Jaloux, B., Delbecque, J. P., Vannier, F., Monge, J. P. and Mondy, N. (2009). Reproduction in a variable environment: How does *Eupelmus vuilleti*, a parasitoid wasp, adjust oogenesis to host availability? *J Insect Physiol* **55**, 643-8.

Cakouros, D., Daish, T. J., Mills, K. and Kumar, S. (2004). An arginine-histone methyltransferase, CARMER, coordinates ecdysone-mediated apoptosis in *Drosophila* cells. *J Biol Chem* **279**, 18467-71.

Campbell, E. M., Ball, A., Hoppler, S. and Bowman, A. S. (2008). Invertebrate aquaporins: a review. *J Comp Physiol B* **178**, 935-55.

Clark, M. S., Thorne, M. A., Purac, J., Burns, G., Hillyard, G., Popovic, Z. D., Grubor-Lajsic, G. and Worland, M. R. (2009). Surviving the cold: molecular analyses of insect cryoprotective dehydration in the Arctic springtail *Megaphorura arctica* (Tullberg). *BMC Genomics* **10**, 328.

Cornette, R., Kanamori, Y., Watanabe, M., Nakahara, Y., Gusev, O., Mitsumasu, K., Kadono-Okuda, K., Shimomura, M., Mita, K., Kikawada, T. et al. (2010). Identification of anhydrobiosis-related genes from an expressed sequence tag database in the cryptobiotic midge *Polypedilum vanderplanki* (Diptera; Chironomidae). *J Biol Chem* **285**, 35889-99.

Chown, S. L., Sorensen, J. G. and Terblanche, J. S. (2011). Water loss in insects: an environmental change perspective. *J Insect Physiol* **57**, 1070-84.

Foley, N. H., Bray, I. M., Tivnan, A., Bryan, K., Murphy, D. M., Buckley, P. G., Ryan, J., O'Meara, A., O'Sullivan, M. and Stallings, R. L. (2010). MicroRNA-184 inhibits neuroblastoma cell

survival through targeting the serine/threonine kinase AKT2. *Mol Cancer* **9**, 83.

Folk, D. G. and Bradley, T. J. (2003). Evolved patterns and rates of water loss and ion regulation in laboratory-selected populations of *Drosophila melanogaster*. *J Exp Biol* **206**, 2779-86.

Goto, S. G., Philip, B. N., Teets, N. M., Kawarasaki, Y., Lee, R. E., Jr. and Denlinger, D. L. (2011). Functional characterization of an aquaporin in the Antarctic midge *Belgica antarctica*. *J Insect Physiol* **57**, 1106-14.

Guo, J. Y., Dong, S. Z., Ye, G. Y., Li, K., Zhu, J. Y., Fang, Q. and Hu, C. (2011). Oosorption in the endoparasitoid, *Pteromalus puparum*. *J Insect Sci* **11**, 90.

Harvey, K. F., Pfleger, C. M. and Hariharan, I. K. (2003). The Drosophila Mst ortholog, hippo, restricts growth and cell proliferation and promotes apoptosis. *Cell* **114**, 457-67.

Hu, J., Neoh, K. B., Appel, A. G. and Lee, C. Y. (2012). Subterranean termite open-air foraging and tolerance to desiccation: Comparative water relation of two sympatric *Macrotermes spp.* (Blattodea: Termitidae). *Comp Biochem Physiol A Mol Integr Physiol* **161**, 201-7.

Kikawada, T., Saito, A., Kanamori, Y., Fujita, M., Snigorska, K., Watanabe, M. and Okuda, T. (2008). Dehydration-inducible changes in expression of two aquaporins in the sleeping chironomid, *Polypedilum vanderplanki*. *Biochim Biophys Acta* **1778**, 514-20.

Koch, C. M., Honemann-Capito, M., Egger-Adam, D. and Wodarz, A. (2009). Windei, the *Drosophila* homolog of mAM/MCAF1, is an essential cofactor of the H3K9 methyl transferase dSETDB1/Eggless in germ line development. *PLoS Genet* **5**, e1000644.

Kotaki, T. (2003). Oosorption in the stink bug, Plautia crossota stali: induction and vitellogenin dynamics. *J Insect Physiol* **49**, 105-13.

Leung, A. K. and Sharp, P. A. (2010). MicroRNA functions in stress responses. *Mol Cell* **40**, 205-15.

Li, Y., Shelat, H. and Geng, Y. J. (2012). IGF-1 prevents oxidative stress induced-apoptosis in induced pluripotent stem cells which is mediated by microRNA-1. *Biochem Biophys Res Commun* **426**, 615-9.

Martin, C. and Zhang, Y. (2005). The diverse functions of histone lysine methylation. *Nat Rev Mol Cell Biol* **6**, 838-49.

Papaj, D. R. (2000). Ovarian dynamics and host use. *Annu Rev Entomol* **45**, 423-48.

Philip, B. N., Yi, S. X., Elnitsky, M. A. and Lee, R. E., Jr. (2008). Aquaporins play a role in desiccation and freeze tolerance in larvae of the goldenrod gall fly, *Eurosta solidaginis*. *J Exp Biol* **211**, 1114-9.

Qin, B., Xiao, B., Liang, D., Li, Y., Jiang, T. and Yang, H. (2012). MicroRNA let-7c inhibits Bcl-xl expression and regulates ox-LDL-induced endothelial apoptosis. *BMB Rep* **45**, 464-9.

Rajpurohit, S., Oliveira, C. C., Etges, W. J. and Gibbs, A. G. (2013). Functional genomic and phenotypic responses to desiccation in natural populations of a desert drosophilid. *Mol Ecol* **22**, 2698-715.

Rosenheim, J. A., Heimpel, G. E. and Mangel, M. (2000). Egg maturation, egg resorption and the costliness of transient egg limitation in insects. *Proc Biol Sci* **267**, 1565-73.

Tarasov, V., Jung, P., Verdoodt, B., Lodygin, D., Epanchintsev, A., Menssen, A., Meister, G. and Hermeking, H. (2007). Differential regulation of microRNAs by p53 revealed by massively parallel sequencing: miR-34a is a p53 target that induces apoptosis and G1-arrest. *Cell Cycle* **6**, 1586-93.

Teets, N. M., Peyton, J. T., Colinet, H., Renault, D., Kelley, J. L., Kawarasaki, Y., Lee, R. E., Jr. and Denlinger, D. L. (2012).

Gene expression changes governing extreme dehydration tolerance in an Antarctic insect. *Proc Natl Acad Sci U S A* **109**, 20744-9.

Thorne, M. A., Worland, M. R., Feret, R., Deery, M. J., Lilley, K. S. and Clark, M. S. (2011). Proteomics of cryoprotective dehydration in *Megaphorura arctica* Tullberg 1876 (Onychiuridae: Collembola). *Insect Mol Biol* **20**, 303-10.

Wall, B. J. (1970). Effects of dehydration and rehydration on *Periplaneta americana*. *J Insect Physiol* **16**, 1027-42.

Woods, H. A. and Harrison, J. F. (2001). The beneficial acclimation hypothesis versus acclimation of specific traits: physiological change in water-stressed Manduca sexta caterpillars. *Physiol Biochem Zool* **74**, 32-44.

Wu, J. and Xu, W. (2012). Histone H3R17me2a mark recruits human RNA polymerase-associated factor 1 complex to activate transcription. *Proc Natl Acad Sci U S A* **109**, 5675-80.

Yoder, J. A., Benoit, J. B., LaCagnin, M. J. and Hobbs, H. H., 3rd. (2011). Increased cave dwelling reduces the ability of cave crickets to resist dehydration. *J Comp Physiol B* **181**, 595-601.

Zhai, Z., Ha, N., Papagiannouli, F., Hamacher-Brady, A., Brady, N., Sorge, S., Bezdan, D. and Lohmann, I. (2012). Antagonistic regulation of apoptosis and differentiation by the Cut transcription factor represents a tumor-suppressing mechanism in *Drosophila*. *PLoS Genet* **8**, e1002582.

Zhang, W. and Cohen, S. M. (2013). The Hippo pathway acts via p53 and microRNAs to control proliferation and proapoptotic gene expression during tissue growth. *Biol Open* **2**, 822-8.

8. CONCLUSIONS

CONCLUSIONS

1. In *Blattella germanica* adult females, hydric stress induces the resorption of ovarian basal follicles, in a process that involves the activation of caspases, thus preventing reproduction.
2. *B. germanica* ovary expresses an aquaporin (BgAQP) that transports water and small amounts of urea, but not glycerol. BgAQP mRNA levels in the ovary are unaffected by hydric stress.
3. In *B. germanica* ovary, hydric stress triggers changes of microRNAs expression. Among them, miR-1-3p, miR-184-3p, let-7-5p, and miR-34-5p are overexpressed.
4. Windei is a putative target of miR-34-5p present in *B. germanica* ovary. Windei is necessary for the trimethylation of lysine 9 in histone H3 in follicular cells, as well as for choriogenesis. Windei mRNA levels in the ovary are down regulated under hydric stress.
5. CARMER encodes an arginine methyltransferase highly conserved through evolution. CARMER is necessary for the asymmetric dimethylation of the arginine 17 in histone H3 in follicular cells of *B. germanica*. CARMER mRNA levels in the ovary are up-regulated under hydric stress.